

Amund Andreassen

Process Concepts for Dehydration of Captured CO₂

Master's thesis in Chemical Engineering and Biotechnology

Supervisor: Magne Hillestad

Co-supervisor: Eivind Johannesen

June 2023



Norwegian University of
Science and Technology

Amund Andreassen

Process Concepts for Dehydration of Captured CO₂

Master's thesis in Chemical Engineering and Biotechnology
Supervisor: Magne Hillestad
Co-supervisor: Eivind Johannesen
June 2023

Norwegian University of Science and Technology



Abstract

In carbon capture and storage, CO₂ is rarely captured in a pure form. Depending on the choice of transport method, additional processing steps to remove impurities such as water are needed.

This thesis has used a CO₂ stream captured through amine scrubbing as a basis, and the goal is to dehydrate this stream and make it ready for transportation in three different states: transport of liquid by ship, dense phase transport by pipeline, and supercritical state transport by pipeline.

This thesis will focus on five dehydration techniques that may be viable for this application; molecular sieves, TEG absorption by conventional absorption column and by membrane contactor, and pressure-temperature swing, with and without the use of a turbo-expander.

For transport of liquid CO₂, TEG absorption with a membrane contactor is recommended as it has the lowest capital and operational cost. Dehydration with molecular sieves and by a dehydration column will also dehydrate the CO₂ sufficiently for this transport. Pressure-temperature swing does not reach the desired water concentration and is not recommended for this application.

For pipeline transport, it is allowed more water in the stream, and all tested methods produce sufficiently dry CO₂ for this.

For transport in dense phase and as supercritical fluid, both methods with TEG absorption are recommended, as these had the lowest costs. Molecular sieve adsorption is another viable option, but with higher costs. Pressure-temperature swing is the most expensive method to dehydrate the CO₂ and is therefore not recommended.

Sammendrag

I karbonfangst vil det veldig sjelden fanges helt ren CO_2 , og det vil typisk være noen urenheter i gasstrømmen, deriblant vann. Dette kan skape problemer for prosessutstyr og transport, og det er derfor ønskelig å senke konsentrasjonen av disse til akseptable nivåer.

Denne oppgaven tar for seg fem forskjellige prosesser for vannfjerning av allerede fanget CO_2 fra forbrenningsreaksjoner, og tar utgangspunkt i CO_2 som er fanget ved hjelp av aminvasking. Målet er å produsere et sluttprodukt som er av en slik sammensetning og under betingelser som gjør den egnet for tre forskjellige typer transport: Skipstransport i væskefase og rørtransport i "tettfase" og som superkritisk fluid.

Tørkeprosessene som er vurdert i denne oppgaven er adsorpsjon ved bruk av molekylsiler, TEG-adsorpsjon gjennom adsorpsjonskolonne og membrankontaktor, samt trykk-temperatursving ved bruk av Joule Thomson-ventil og ved bruk av en turboekspander.

Fra resultatene av dette arbeidet anbefales membrankontaktor for dehydrering til skipstransport, siden den har lavest kapitalkostnad og driftskostnad. Molekylsiler og adsorpsjonskolonner har tilstrekkelig vannfjerning og kan benyttes. Trykk-temperatursving klarer ikke å oppnå den ønskede vannkonsentrasjonen, og er derfor ikke anbefalt.

For rørtransport kan alle metodene benyttes som følge av litt friere krav til vannkonsentrasjon. Til transport i tettfase og superkritisk tilstand har TEG-adsorpsjonsmetodene lavest kapital- og driftskostnad, og anbefales. Bruk av molekylsiler fører til litt høyere kostnader, og trykk-temperatursving er det dyreste alternativet.

Table of Contents

Abstract	i
Sammendrag	ii
1 Introduction	1
2 Background material	2
2.1 Background of Carbon Capture and Storage and CO ₂ dehydration	2
2.2 Amine Scrubbing	3
2.3 Gas specification	5
2.3.1 Chemical impurities in captured CO ₂	5
2.3.2 Transport method	7
2.3.3 Target product	8
3 Dehydration Process Concepts	9
3.1 Molecular sieves, Case A	9
3.2 TEG absorption	12
3.2.1 Absorption column, Case B1	12
3.2.2 Membrane contactor, Case B2	13
3.3 Pressure-Temperature Swing	15
3.3.1 Joule Thomson valve, Case C1	15
3.3.2 Turbo-expansion, Case C2	15
3.4 Post-treatment	16
3.5 Required chemicals	17
4 Simulations	19
4.1 Simulation basis	19
4.2 Pre-Treatment	23
4.3 Post-treatment	25
4.4 Cooling system	25
4.5 Case A - Molecular sieve adsorption	26
4.6 Case B1 - TEG absorption column	27

4.7	Case B2 - TEG absorption with membrane contactor	28
4.8	Case C1 - Pressure temperature swing with Joule Thomson valve	29
4.9	Case C2 - Pressure temperature swing with turbo-expander	30
5	Sizing and cost estimate of equipment	31
5.1	Heat exchangers	31
5.2	Molecular sieve packed beds	32
5.3	Membrane contactor	33
5.4	Separator columns	33
5.5	Pressure altering equipment	34
5.6	CEPCI	35
5.7	Overall Cost	36
5.7.1	Parameters for cost estimation	36
5.7.2	Inside battery limits plant cost	36
6	Results	38
6.1	Summary of results	38
6.2	End Product	39
6.2.1	Purity of end product	41
6.3	Produced water	42
6.4	Heat exchangers	43
6.5	Compressors, pumps, turbo-expanders	43
6.6	Separators	44
6.7	Energy integration	46
6.8	Heat exchanger networks	46
6.9	The membrane contactor model	50
6.10	Makeup glycol	50
6.11	Energy sources	51
6.12	Pipeline transport	51
6.13	Economy	52
6.13.1	Cost trends	52
6.14	Absorption column vs. membrane contactor	53

7 Conclusion & Further Work	54
7.1 Conclusion	54
7.2 Further work	55
Bibliography	56
Appendix	59
A Cost and utilities	59
B Composite curves and heat exchangers	70
C Stream compositions	84

1 Introduction

One of the most direct ways to reduce emissions of the climate gas CO_2 is through carbon capture and storage, *CCS*. The CO_2 is captured, typically from flue gas from energy-demanding industry. After the CO_2 is captured, it is then transported to a suitable location for permanent storage. Different carbon capture methods will have varying amounts of impurities in their end product, and in many cases, it may be necessary to remove these. It is especially important to limit the water content of the CO_2 , since it can create hydrates and react to create corrosive compounds in the fluid, which are known to cause equipment and flow assurance issues.

This master's thesis will focus on 3 different methods for dehydration of a CO_2 stream, namely molecular sieve absorption, TEG absorption, and pressure-temperature swing, in order to prepare it for 3 different transport methods. It will be set up similarly to a case study, and the processes will be simulated and cost estimated in hopes of finding the ideal dehydration process. In addition to this, a preliminary economical study will be conducted.

This master's thesis is inspired by the *Northern Lights* project, a part of Norway's first large-scale CCS project where the intention is to transport the CO_2 in a liquid state by ship, which requires close to water-free CO_2 . This thesis will be based on simulations of different dehydration methods, with the goal of ending up with a recommendation for which method is best suited for a set of realistic transport alternatives.

The thesis will first explain the importance of removing impurities from the CO_2 , with a main focus on water. After that, the process concepts will be described and simulated from a given gas composition. To compare the economic aspects of the methods, an economic analysis of the simulation results will be conducted. Finally, a conclusion with recommendations for each transport method will be provided.

2 Background material

2.1 Background of Carbon Capture and Storage and CO₂ dehydration

Climate gases, also known as greenhouse gases, are gases that contribute to keeping the heat radiation from Earth within the atmosphere. One of the gases that have this effect is CO₂, and the emissions of this gas has increased ever since the industrial revolution. [Jones et al. 2023]

Emissions of CO₂ come from many sources, and the largest contributor is combustion of hydrocarbons from fossil fuels. [Olivier et al. 2013] The carbon in these fuels would otherwise be buried underground and remain inert, so the net carbon increase in the atmosphere and the greenhouse effect will continue to increase as more CO₂ from fossil fuel combustion is released than what is removed.

The amount of CO₂ in the atmosphere take a long time to decrease, and it is difficult to speed this process up or capture already emitted CO₂. By capturing the CO₂ before it is emitted, and transporting it directly to permanent storage, this issue is avoided, while it is still possible to benefit from the energy-rich fuels. [Equinor 2019]

Carbon capture and storage, CCS, is a broad term describing the capture of CO₂ either before or after the energy is extracted from the fuel. The CO₂ is separated from other compounds, then stored permanently. Since CO₂ is a gas at ambient temperature and atmospheric pressure, it will require either high pressure, cooling, or a combination of these two to remain in a spatially efficient manner. Subsurface storage is generally accepted as a robust solution that has sufficient capacity to be practical for storing large quantities of CO₂. [Roberts and Mander 2011]

The *Northern Lights* project plans to transport captured CO₂ from the Oslofjord area in Norway in a liquid state, by ship to a terminal at the western part of Norway, before being transported by pipeline to an offshore storage location 1000 – 3300m below the seabed. Equinor 2019

In an attempt to reduce the CO₂ emissions, several countries have implemented a tax for emitted CO₂, to motivate emission-reducing measures done in the industry. In 1991 the Norwegian government introduced a CO₂ tax, and in 2022 it was equated to 78.33 USD/ton CO₂. [Utslipp til luft 2022]

2.2 Amine Scrubbing

Absorption is a process where a substance acts as a solute, and is incorporated into a solvent. The solvent will typically be a liquid, and for CO_2 absorption, CO_2 is the solute. Over time the CO_2 will be homogeneously dispersed into the solvent. For absorption, the two definitions *lean* and *rich* solvent are important. Lean solvent has a low concentration of solvent and therefore good capacity to absorb solute. After it has absorbed a solute, the solvent will have a high concentration of the solute. When the solvent has a high solute concentration, its capacity for absorption is reduced, and it is referred to as a rich solvent.

Amine absorption and desorption, also known as amine scrubbing can be simplified into 4 stages.

1. Interphase: The flue gas stream, containing CO_2 , is introduced to lean amine. This is typically done in an absorber, where the liquid lean amine enters the absorber from the top, and CO_2 containing gas enters from the bottom. This creates a large area of interphase between the flue gas and the amine
2. Absorption. Here the CO_2 is introduced to the liquid amine, and there is a chemical reaction which binds the CO_2 to the liquid amine, while other components remain in the gas stream.
3. Separation of gas and liquid phase. The gas is allowed to escape at the top of the absorber, while liquid is drained of at the bottom of the absorber.
4. Regeneration. Here, the rich amine is heated up so that the chemical bonds between CO_2 and amine are broken and the CO_2 is desorbed, releasing the CO_2 in a gaseous state, and the CO_2 -free lean amine is ready to be reused. The gas leaves the desorber at the top, while the lean amine is collected at the bottom.

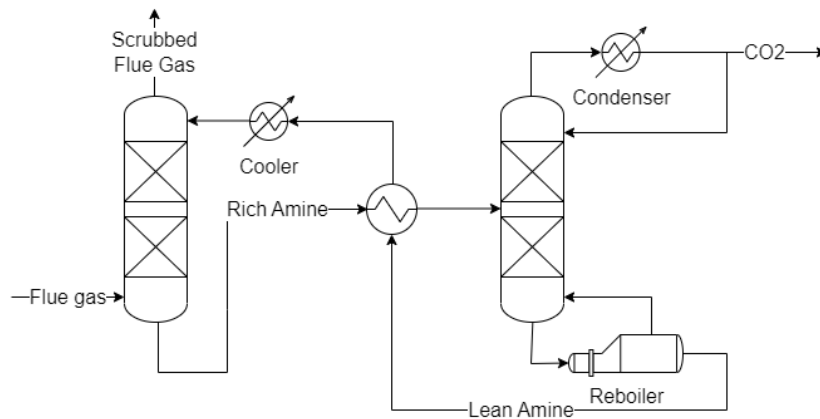
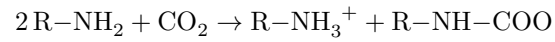


Figure 1: Conceptual figure of amine scrubbing of CO_2 rich gas.

Amine scrubbing can be performed with several different types of amine, and the industrially most used amines are: Diethanolamine (DEA), monoethanolamine (MEA), methyldiethanolamine (MDEA). These all have similar reactions with CO₂, and the reactions can be described by the following main reactions:

The main reaction for the absorption is:



And the main regeneration reaction is:



Despite these being the main reactions, there will also be a variety of other reactions, both chemical and mechanical, occurring which cause the finished CO₂ stream to have some impurities. Depending on the required specification for the end product, the remaining impurities may need to be removed.

2.3 Gas specification

2.3.1 Chemical impurities in captured CO₂

There are several chemicals in the captured CO₂ that may be undesired for further transport and storage. Some of the most important chemicals to consider are listed below.

Water

The main concern related to water in the product streams is the potential formation of solid hydrates. Hydrates are solid crystalline compounds formed by gas and water under high pressure and low temperature. The formation of solids can be detrimental for process equipment, and especially pipelines are at risk of clogging. Clogging will not only stop the transport of fluids, but also causes a pressure increase before the clogged area, which in a worst-case scenario may result in ruptures and leakages. Such incidents are especially expensive to fix if they occur in remote subsurface locations.

There exist counter-measures to hydrate formation, and the two most used in the petroleum industry are the introduction of glycols as an "anti-freeze" compound, and pigging where a mechanical device is sent through the pipe to remove the solids. However, the best solution is to prevent the issue before it happens.

In combination with CO₂, water may react and form carbonic acid, by the following reaction:



This is a diprotic acid and may cause corrosion of equipment. Especially in higher concentrations or in combination with other acids, this will cause undesired wear on process equipment. There are also several other compounds that react with water and create acids. By reducing the amount of water in the stream, the risk of corrosion will therefore be reduced.

Other chemicals

The other chemicals that have a tabulated upper limit in the *Northern Lights* project specification are oxygen, sulfur, nitrogen oxides, amines, ammonia, hydrogen, aldehydes, and heavy metals. These are mostly undesired because of properties that cause increased wear on equipment by corrosion.

Oxygen Oxygen is one of the substances that are required for close to any living organism, and it contributes to the formation of microbial communities within the pipelines. [Zhu et al. 2003] Such formation may clog the pipelines, or produce corrosive compounds that are kept in one spot, creating weak spots in the pipe and after time potentially leakages.

Sulfur Sulfur in the form of sulfur dioxide and hydrogen sulfide can be hazardous to equipment. Hydrogen sulfide may react with oxygen, forming sulfur dioxide and water, by the following reaction:



Sulfur dioxide and water can react to create the strongly corrosive acid sulfuric acid by the reaction presented below:



Nitrous oxides Nitrous oxides may react with water and create nitric acid, in a similar manner to sulfuric oxide. However, nitrogen gas is not considered to be an issue as it does not oxidize and remains inert under the expected process conditions.

the oxidation of this is an endothermic reaction that is typically formed in combustion reactions.

Amines Amines themselves do not typically cause corrosion, but upon degradation, there will be produced corrosive components that increase the corrosive properties of CO₂ on stainless steel. [Fytianos et al. 2016]

Ammonia Ammonia may react with CO₂, creating solid ammonium carbamate. [Forse and Milner 2021] If accumulated this will cause clogging and complications for the transport.

Hydrogen In addition to being a sign of incomplete (and thus less efficient) combustion, hydrogen may be absorbed into metallic surfaces and weaken the corrosion resistance of the material. [Li et al. 2021]

Aldehydes Aldehydes will easily form hydrates with water, which is expected to promote further formation of gas hydrates. [Makwashi et al. 2018]

Heavy metals Most heavy metals are removed due to environmental considerations and regulations. Mercury is not reactive to steel structures, but in contact with aluminum, it will react in an exothermic reaction called amalgamation. This weakens the structural integrity of the aluminum and may cause cracking.

2.3.2 Transport method

This project will consider 3 different methods of transporting the CO₂.

The first method is inspired by the *Northern Lights* project, which intends to transport CO₂ in a liquid by ship from the eastern part of Norway to a receiving terminal in western Norway before it is transported by pipeline to sub-sea storage. [Equinor 2019]

For this, the project has set 30 ppm molar concentration as a maximum water composition for the CO₂. The CO₂ is to be transported at a pressure of 13-15 bar, with corresponding equilibrium temperatures (−31.9°C and −27.7 °C, respectively). The operating conditions for the dehydrated CO₂ for ship transport is in this report simulated to be a pressure of at least 15bar, and a temperature of −30°C

The second method is transport of CO₂ in *dense phase*. Dense phase is CO₂ that has a pressure in the range 100 – 150 bar, and a temperature in the range 15-30°C. [Patchigolla and Oaakey 2013] In this phase, CO₂ has a density similar to a liquid, but a viscosity similar to that of a gas. [Patchigolla and Oaakey 2013] This is expected to be the most common transportation state of CO₂ as the technology becomes more widespread, as described by Munkejord et al. 2016. In this project, dense phase CO₂ will be simulated at a pressure of 150bar and 20°C.

The third method that will be evaluated is transportation in supercritical state. In this phase, the CO₂ is kept at a temperature and pressure above the critical point for the gas, which is 31.1°C and 73.8bar. [X. Zhang et al. 2014] Under these conditions, there is no distinct difference between liquid and gas for the CO₂. For simulations of supercritical CO₂, a temperature of 40°C and a pressure of 150bar is selected.

Transport of CO₂ as both dense phase and supercritical fluid is best suited for pipeline, and the reasoning behind selecting the high pressures is to reduce the requirement for re-compression during transport. As the temperature is higher for these transportation methods, it is expected to be acceptable to have a higher water content in the CO₂ without having the risk of hydrate formation.

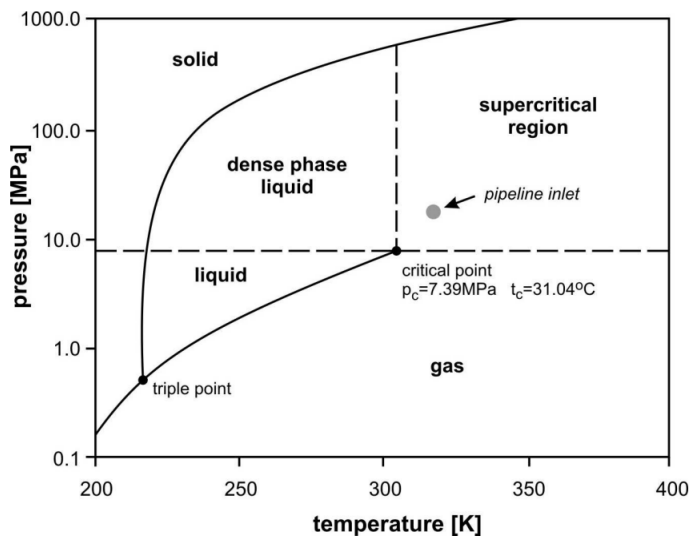


Figure 2: Phase Diagram for CO₂. This figure it fetched from Witkowski et al. 2014.

2.3.3 Target product

Due to the aforementioned reasons, most industries that handle CO₂ for storage will have specified limits for how much of these impurities are allowed. Depending on the transport method, these limits vary.

The table below shows the specifications that are set for the *Northern Lights* projects.

Figure 3: Specification of composition for dehydrated CO₂ in the *Northern Lights* project. Table from [Equinor 2019]

Component	Concentration, ppm (mol)
Water, H ₂ O	≤ 30
Oxygen, O ₂	≤ 10
Sulphur oxides, SO _x	≤ 10
Nitric oxide/Nitrogen dioxide, NO _x	≤ 10
Hydrogen sulfide, H ₂ S	≤ 9
Carbon monoxide, CO	≤ 100
Amine	≤ 10
Ammonia, NH ₃	≤ 10
Hydrogen, H ₂	≤ 50
Formaldehyde	≤ 20
Acetaldehyde	≤ 20
Mercury, Hg	≤ 0.03
Cadmium, Cd Thallium, Tl	≤ 0.03 (sum)

The *Northern lights* specification will be used as a guideline for compositions of the dehydrated CO₂ with the exceptions of water content for pipeline transport that have been previously mentioned.

3 Dehydration Process Concepts

There are various methods to use for dehydration, and this section will present the concepts considered in this report.

Before the various methods are applied, a pre-treatment of the CO₂ stream is performed. This pre-treatment consists of compression and subsequent cooling of the gas. By increasing the pressure and subsequently cooling the stream, two important things happen. The solubility of water and other impurities in CO₂ will decrease, making it possible to separate out water in liquid form from the gas in unheated flash tanks, more commonly known as "knock-out" drums. This water will have some CO₂ dissolved in it, and as the pressure increases, a gradually higher concentration of CO₂ will be present in the produced water. In order to differentiate between pure water, H₂O, and the liquid removed from the CO₂ stream, this liquid will hereafter be called *produced water*. In addition to removing impurities, this will allow for single-phase, adiabatic compression and the compressors are easier to design. The design of compressors is not relevant for this report, but is a consideration for the actual design and will affect the associated cost.

This report will compare 5 ways of dehydrating the CO₂:

- Adsorption with molecular sieves, presented as Case A.
- TEG absorption with the use of a conventional absorption column, presented as Case B1.
- TEG absorption with the use of a membrane contactor, presented as Case B2.
- Pressure-temperature swing with the use of a Joule Thomson valve, presented as Case C1.
- Pressure-temperature swing with the use of a turbo-expander, presented as Case C2.

3.1 Molecular sieves, Case A

The first method for dehydration of CO₂ by the use of molecular sieves, which will also be referred to as Case A.

Adsorption can be briefly explained as the process in which a substance, typically a fluid, adheres to the surface of an adsorbent. The adsorbent is typically a solid with a large surface area. This can occur either as *physical adsorption*, in which the adhesion is mainly caused by weak van der Waals force, or by chemisorption where a chemical reaction holds the two together or a combination of these two. [Dabrowski 2001]

The main difference between absorption and adsorption is that in absorption the solute will be dispersed into the solvent, while in adsorption the adsorbate is only attached to the surface of the adsorbent.

Molecular sieves are small particles, typically spherical with a diameter in the range of 2 – 6 μm, with uniformly sized pores. [Swain 2003] Here, the selection of pore size is the main determining factor for separation. For this separation, it is desired to capture the H₂O molecules in the pores, while the CO₂ flows past. The molecular sieves are usually, made from zeolites consisting of silicon dioxide and hydrated aluminum in addition to a group 1 cation, typically Na⁺ or K⁺, and a group 2 cation, typically Ca²⁺

4 types of zeolites are most commonly used by industry: 3A, 4A, 5A, and 13X. The letter represents the shape of the pores, and the number represents the size. Type A sieves have a cubic shape and the pores are on the side of the cube- Type X sieves have the shape of a cube minus one corner, and the pore is the in the "place of the missing corner". The structures of type A and type X molecular sieves are shown below.



Figure 4: Figure showing the structure of molecular sieve type A. Figure from [Rathish et al. 2013]



Figure 5: Figure showing the structure of molecular sieve type X . Figure from [Rathish et al. 2013]

Despite having different shapes, all molecular sieves are used in the same way. A fluid is passed through a packed column of molecular sieves, where the smaller impurities are caught in the pores, while larger particles pass through. The molecular sieves will reach their adsorption capacity over time, and periodic regeneration or replacement of the sieves is required. To regenerate the molecular sieves, a hot and dry sweep gas is passed through the packed bed and evaporates the water. A bed temperature of 220 – 220°C will effectively evaporate the water without harming the molecular sieves.

In order to have a continuous process, a typical industrial setup will have a minimum of 2 packed beds, making it possible to regenerate one bed while the other is in operation.

This is a well-tested method that is already in use for the dehydration of natural gas. Farag et al. 2011 Secker and Bergene 2011

For gas dehydration, 3A and 4A are typically used, and these have pore sizes of 3.3Å and 3.9Å, respectively. 4A molecular sieves have an approximately 10% higher equilibrium absorption capacity compared to 3A. Secker and Bergene 2011

Water has a nominal molecular size of 2.6Å, and CO₂ has a nominal size of 3.3. Due to this, CO₂ may be absorbed by the larger 4A molecular sieves, which makes 3A appear to be the most suited

alternative, despite a lower absorption capacity.

3A molecular sieves are the same type that is implemented in *Equinor's* Hammerfest facility. After installation, there was an issue of a shorter lifetime than expected for these molecular sieves. This is believed to have been caused by the formation of carbonic acid, which in turn reacted with the alkaline zeolites. For a practical implementation of molecular sieves, this issue must be addressed, and further considerations may prove a different type of molecular sieves to be favored by the industry. However, for a comparison of the dehydration methods, this is not expected to make a too significant difference so 3A molecular sieves are chosen regardless.

3A molecular sieves have a loading capacity of 19 – 20 % weigh by weight of molecular sieves. [Lin et al. 2014] The operational time of the molecular sieves is typically between 8 and 24 hours. [Okoli 2017][Mokhatab et al. 2018]

3.2 TEG absorption

Dehydration with the use of triethylene glycol, TEG, is a common and well-tested method for dehydration of gases. Other glycols, such as monoethylene glycol(MEG) and diethylene glycol share similar water affinity to TEG, but the petroleum favors use of TEG as it has a higher degradation temperature, making it possible to regenerate the glycol to a lower water concentration by distillation. [Ikhlaq 1992]

3.2.1 Absorption column, Case B1

Conventionally, most absorption processes are performed with packed absorption columns. Nivargi et al. 2005 Here, gas is introduced at the bottom of the column, and liquid glycol from the top. TEG has a stronger affinity to water than CO_2 has. This makes the water molecules diffuse into the liquid phase and get absorbed in the TEG. The two phases will then be removed from the absorption column. The rich TEG will be taken out at the bottom, while the CO_2 stream is taken out at the top. The TEG is then regenerated by distillation, releasing the water from the rich TEG, converting it into lean TEG that is recirculated and reused. The water will contain some CO_2 , and the TEG will not be completely regenerated by this method. The regeneration may be improved by having a series of flash drums and a stripper at conditions that effectively separate the CO_2 and decrease the water composition of the lean TEG. By doing this, almost pure water may be purged from the system, and a smaller recycle stream, mainly consisting of CO_2 , is achieved.

The use of packing in columns significantly increases the surface area of the column, facilitating a more efficient mass transfer of the water from the gaseous CO_2 stream into the liquid glycol. Previously, it was more common to use trayed columns due to ease of maintenance, but packed columns have become more common in more recent years. By using packed columns, the same separation requires smaller columns, which reduce the capital cost and will for most instances remove challenges related to very tall columns.

Packing can be done with several different materials, and the packing material is inert. However, it is still important to make some considerations when deciding the material, since water in liquid form reacts with the CO_2 , and creates an acidic environment. Stainless steel packing has sufficient corrosion resistance and is a suitable material for this application. Structured packing is preferred as the design gas velocity is higher than the velocity in trayed columns, while allowing for easier maintenance than random packing. Additionally, lower capital cost than trayed columns and a more robust design than random packing makes this a good alternative.

3.2.2 Membrane contactor, Case B2

An alternative to the traditional absorption columns is membrane contactors, which is a relatively new technology for dehydration of CO_2 . This method uses a membrane contactor instead of an absorption column to create an interphase between the liquid TEG and gaseous CO_2 . These contactors employ a thin, permeable sheet that facilitates mass transfer of water through its porous structure, without allowing TEG to leak into the gas phase. The membranes are typically made from a polymer material and have small pores where the water molecules can pass through. The driving force behind membrane-based separation is concentration and pressure differences, where the water moves from high concentration and pressure to lower. The affinity between water and the two phases also plays a role in determining the transfer rate.

Due to the size difference between water and CO_2 molecules, it might intuitively be expected that the separation is based on the size differences and that the pores are in a size range of $2.9\text{to}3.3\text{\AA}$. However, selecting such a small pore size would give a high resistance and require high pressure difference to achieve sufficient driving forces for efficient separation. The increased pressure difference would result in more wear on the membrane, and limit the material selection. In addition, clogging would occur more often with smaller pores, increasing the need for maintenance. Because of this, using a membrane contactor is a better option than a traditional membrane. The pores are non-selective, and by adjusting the pressure differences between the two sides of the membrane, gas will fill the pores of the membrane. Due to similar pressure on both sides of the membrane, the gas will not bubble into the liquid, nor will the liquid fill up the pores and flow into the gas. Since this allows for larger pore sizes, the risk of clogging is reduced, and the operating pressure difference will be lower, both factors that contribute to a longer lifespan for the membrane contactor. It also allows for a large selection of membrane materials, easing the material selection.

For subsea natural gas dehydration, Teflon AF2400 membranes proved to have appropriate selectivity and a long operational lifespan when used for separating water from natural gas. This was tested with a feed stream consisting of mostly methane. [Ahmadi et al. 2021] Methane is a slightly larger molecule than CO_2 at a size of 3.9\AA , and has a lower dipole polarizability than CO_2 of $2.593 \times 10^{-24} \text{cm}^3$ and $13.8 \times 10^{-24} \text{cm}^3$, respectively, which makes the separation a bit easier than separation from CO_2 . [Secker and Bergene 2011] However, the Teflon AF2400 membrane is still expected to yield good separation.

The main advantage of membrane contactors is significantly lower spacial requirements compared to absorption columns, and therefore the configuration of the membrane should be selected in a manner that promotes a high interface per volume. A configuration that allows for counter-current flow should be chosen to maximize the driving force of concentration differences. To meet both requirements, a spiral wound counter-current membrane contactor is a good choice. The smaller form factor of the membrane contactor will also give a lower capital cost per unit.

The main downsides of using membrane contactors are that the technology is young and relatively untested for large-scale application, the membrane contactor modules have a limited lifespan, and are more pressure sensitive than conventional absorption columns. If the liquid pressure is too high (compared to the gas), a phenomenon called wetting will occur. This involves leakage of TEG into the pores, which will impair the module's loading capacity, and there will be losses if TEG into the product stream. [H. Zhang et al. 2021] If the liquid pressure is too low, a phenomenon called bubbling will occur, which is when the gas bubbles into the TEG, also impairing the separation and losing CO₂ into the TEG stream. This sets requirements for monitoring the pressure and TEG concentration in the gas stream. In theory, it should be possible to have no loss of TEG into the CO₂ stream, but in practice, there may be some minor losses. [Ahmadi et al. 2021] The limited lifespan is to some extent compensated for by the ease of replacing inefficient or broken modules.

The following equation describes the transport phenomenon in the membrane contactor. [Basile and Ghasemzadeh 2019]

$$\frac{1}{K_o} = \frac{m}{k_g d_o / d_i} + \frac{m}{k_m d_{lm} / d_i} + \frac{1}{Ek_l} \quad (4)$$

Here, K_o is the overall mass transfer rate, m is the distribution coefficient between gas and liquid phase and E is an enhancement factor, accounting for how chemical reactions affect the transfer rate. k_m , k_L and k_g is mass transfer coefficients for the membrane, liquid and gas mass transfer rates. d_i , d_o and d_{lm} is inner, outer and log mean diameter of the membrane tube, respectively.

3.3 Pressure-Temperature Swing

The solubility of water in CO₂ is dependent on both temperature and pressure, and by decreasing the temperature, water will be less soluble. In order to achieve the desired separation by solubility, the temperature will need to be below the freezing point of water.

The formation of solids may cause issues for the process equipment, and monoethylene glycol, MEG, will therefore be used as an anti-freeze compound. Having a regeneration of MEG will reduce the operating cost, but makes the process more complicated. For the regeneration of MEG, distillation may be a viable option. This will however not yield a completely water-free MEG.

For the pressure-temperature swing methods, the stream is compressed to a high pressure prior to being cooled down. By rapidly reducing the pressure, the stream will cool itself further by a mechanism called the *Joule-Thomson effect*.

3.3.1 Joule Thomson valve, Case C1

The method of having a Joule-Thomson valve is rather uncomplicated. The gas stream is compressed in the compressor train, and MEG is added. The stream then passes through a decompression valve, reducing the pressure to desired level. For non-ideal fluids, an adiabatic expansion will change the temperature of the fluid. This may either increase or decrease the temperature, depending on the specific Joule Thomson-coefficient for the fluid. The Joule-Thomson constant describes the relation between temperature and pressure differences in an isenthalpic system, as shown in the equation below.

$$\mu_{JT} = \left(\frac{\partial T}{\partial P}\right)_H \quad (5)$$

Here, μ_{JT} is the Joule-Thomson coefficient, ∂T and ∂P are the change of temperature and pressure respectively. $()_H$ indicates that the system is isenthalpic.

For fluids with a positive Joule-Thomson coefficient, a pressure drop will also lead to a temperature drop. As the stream does not have a pure composition, and there will be a phase change occurring the temperature change will not be corresponding to the Joule-Thomson coefficient for CO₂.

By having the expansion through a valve, the process equipment will be uncomplicated and easy to maintain.

3.3.2 Turbo-expansion, Case C2

A way to decrease the temperature more than with an expansion valve is to utilize a turbo-expander. The turbo-expander is a turbine driven by expanding gas. The turbine converts some of the energy of expansion to mechanical energy, thus removing some heat from the stream. This mechanical energy can relatively easily be used for other parts of the process with low energy losses. In compression processes, this can easily be done by simply having a shaft connection between the expander and a compressor or pump.

The turbo-expanders will have to be designed to handle multiphase flows at low temperatures, making them more complicated to construct than a single-phase expander. However, this is still possible and has seen some use in cryogenic cooling of natural gas. [Giakoumis et al. 2020]

3.4 Post-treatment

After a suitable composition is acquired, it will also be necessary to have the CO_2 at appropriate pressures and temperatures for transport. During transport, the fluid will experience a pressure decrease due to several factors, such as frictional losses and elevation changes. The temperature will exchange a certain amount of heat with the surroundings, depending on the insulation used. Due to this, it may be necessary to have re-compression and heating or cooling to keep the fluid in the desired state, in the case of long-distance transport.

For transport by ship, the CO_2 must first be cooled down to a temperature of -30°C . Such temperatures cannot be provided by cooling water, so a different cooling system is required. For this work, a refrigeration system with ammonia is chosen. This system is based on compression, cooling, and expansion of ammonia in a closed loop, connected to a heat exchanger with the dehydrated CO_2 .

The pressure is first increased in an adiabatic compressor, which will heat up the gas as well. Upon cooling down the ammonia, it will condense into a liquid. By passing this liquid through an expansion valve, the liquid will evaporate as the pressure decreases. The evaporation is endothermic and takes energy from the CO_2 in a heat exchanger, thus cooling the CO_2 .

For transport by pipeline, cooling water and multiple compression stages are sufficient to achieve the desired temperature and pressure.

3.5 Required chemicals

The most important properties of the chemicals required for the dehydration processes will be presented below.

TEG

The triethylene glycol used for absorption has the chemical formula $C_6H_{14}O_4$, and is a viscous liquid at room temperature. It has hygroscopic properties that make it suitable for its use in dehydration, which is also why it has been used for a long time in the petroleum industry for dehydration of natural gas. TEG is thermally stable up to $204^{\circ}C$. Above this temperature, there is a risk of degradation.[François 2020]

In order to minimize this degradation, it is advisable to keep the temperature lower than this. TEG has somewhat corrosive properties, but this is not considered to be an issue as long as stainless steel equipment is used. Direct contact with TEG is hazardous and large emissions should be avoided.

MEG

MEG is a glycol with hygroscopic properties and is also well known within the petroleum industry. It has the chemical formula $C_2H_6O_2$ and is mainly used to prevent water from forming hydrates. By mixing water with MEG, it will remain a liquid for temperatures down to $\sim -50^{\circ}C$, depending on the ratio, as shown in figure 6 below.

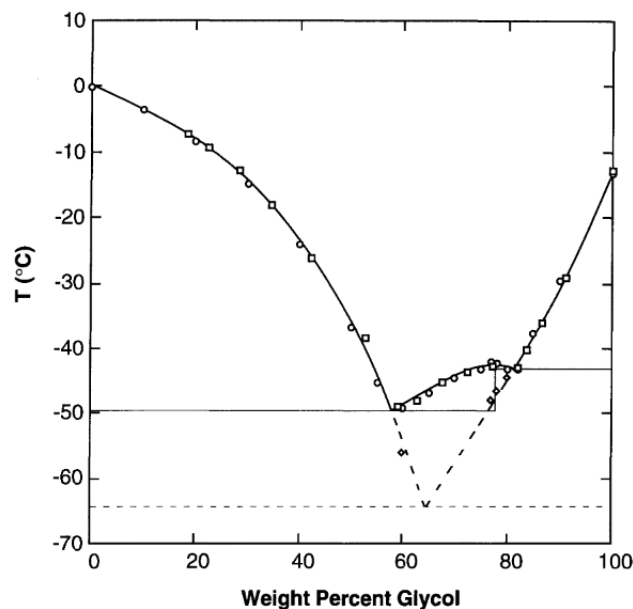


Figure 2. Solid-liquid phase diagram for ethylene glycol + water. \circ : stable freezing points, Lab 1; \square : stable freezing points, Lab 2; \diamond : metastable freezing points, Lab 1; — : average stable freezing curve; - - : metastable freezing curve.

Figure 6: Graphical representation of the freezing point of different concentrations of MEG in water. Figure from Cordray et al. 1996.

The lowered freezing point of water and MEG has been utilized for flow assurance, especially for transport of natural gas. The MEG can be injected into pipelines, and after it has served its purpose, the MEG can be regenerated by flashing off most of the water before reuse. When regenerating MEG, it is important to consider the degradation temperature, which is 135°C. At higher temperatures, there is a risk of MEG degrading. [François 2020]

A mixture of MEG and water can also be used as an inhibitor for corrosion and microbial growth. Exposure to MEG causes irritation, and large emissions should be avoided. In the case of CO₂ storage, this is however not expected to pose a significant risk, and the main reason to remove it from the CO₂ stream before storage is to regenerate and reuse it, instead of wasting a resource.

Ammonia

Ammonia is a chemical that has been used as a refrigeration medium for a long time, especially for industrial-scale systems. At atmospheric pressure, it has a boiling point of -33.3°C , which is sufficient for most cooling applications. Upon vaporization, it requires $\Delta H_{vap} = 23.37\text{kJ/mol}$, which is about 12.6% to that of water, which is a good reason why it is mostly used when spacial requirements are not a big concern.

The main reason why ammonia is chosen is that the gas is classified as having a neutral global warming potential because it will not contribute to the greenhouse effect, and is not ozone layer depleting. The latter is important, as chlorofluorocarbons which for a long time was the preferred refrigeration media is a large contributor to ozone depletion and has been banned for such uses since 2010. [Protocol et al. 1987] Ammonia does not have any corrosion issues with stainless steel or aluminum, making it the most common materials for cooling systems available. [Pearson 2008]

4 Simulations

4.1 Simulation basis

The basis for this master’s thesis is simulations done in the *Aspen Hysys v12.1*, a widely used process simulation tool. The stream data for all simulations is found in Appendix C.

Feed stream

The feed stream is based on the product stream from a simulation of a carbon capture process from a flue gas, with the use of amine scrubbing.

The stream volume is set to equate to approximately 1.5 million metric tons of CO_2 per year, with a mass flow of 185607 kg/hour. This volume is inspired by the target set in *Northern Lights* project, which is a maximum of 1.5 million tons of CO_2 stored per year, and based on 8000 operational hours per year. In order to have the most equal comparison for all streams, an identical feed stream is used for all the processes. The composition and operational parameters of the feed stream used in this thesis are presented in the table below:

Component/Parameter & unit	Value
Temperature [°C]	30
Pressure [bar]	1.8
Mass flow [kg/hour] Total	187500
Mass flow [kg/hour] CO_2	185599.76
Mass flow [kg/hour] H_2O	1856.454
Mass flow [kg/hour] N_2	37.5462
Mass flow [kg/hour] O_2	5.5453
Mass flow [kg/hour] MEA	0.69296

Table 1: Description of the feed stream used for simulations.

Fluid packages

Aspen Hysys has the option to select "fluid packages", which mainly determine the equation of state, EOS, that are used for calculations in various instances. For the simulations used in this thesis, two different fluid packages are used, depending on which components are present.

Peng Robinson

The Peng Robinson fluid package uses the Peng Robinson equation of state to describe the relation between pressure P , temperature T , and molar volume of gas V_m for each component. This is the most used equation of state within the petroleum industry, and AspenTech advises using this for calculations on natural gas. [Ashour et al. 2011] As CO_2 behaves similarly to natural gas, this is considered the best fluid package to use, unless otherwise specified. Peng Robinson EOS is described below:

$$P = \frac{RT}{V_m - b} - \frac{a\alpha}{V_m^2 + 2bV_m - b^2} \quad (6)$$
$$a = \frac{0.45724R^2T_c^2}{P_c}$$

$$b = \frac{0.07780RT_c}{P_c}$$

$$\alpha = (1 + (0.37464 + 1.54226\omega - 0.26992\omega^2)(1 - \sqrt{T_r}))^2$$

$$T_r = \frac{T}{T_c}$$

Here, ω is the acentric factor, P_c is the critical pressure, and T_c is the critical temperature, all for the relevant component.

Glycol Package

The glycol package is a fluid package that uses the Soave Redlich Kwong equation of state with some additional calculations for glycol. This is generally considered to be the most accurate package for streams containing glycol. [Ashour et al. 2011] It is therefore used for all streams/equipment where either MEG or TEG is present.

Soave Redlich Kwong EOS is shown below:

$$P = \frac{RT}{V_m - b} + \frac{a\alpha}{V_m(V_m + b)} \quad (7)$$

$$a = \frac{0.42747R^2T_c^2}{P_c}$$

$$b = \frac{0.08664RT_c}{P_c}$$

$$\alpha = (1 + (0.48508 + 1.55171\omega - 0.15613\omega)(1 - \sqrt{T_r}))^2$$

Like in Peng Robinson EOS, ω is the acentric factor, P_c is the critical pressure, T_c is the critical temperature and V_m is the molar volume for the relevant component.

Membrane contactor model

The membrane contactor model is an unofficial extension for Aspen Hysys and is created by Mahdi Ahmadi to simulate membrane contactors. It was made for use in calculations for subsea natural gas dehydration with the use of TEG as an absorbent. The model was made in parallel with an experimental study in order to compare real and simulated results.

The model simulates the performance of a membrane contactor, giving operating conditions, stream compositions, and the membrane area of a membrane contactor for a given case. Due to some technical difficulties, the membrane contactor was only simulated with the following components: CO_2 , TEG, and Water. As these are the main components in the membrane contactor, this is considered to be a sufficiently good model. The model takes in data from Aspen Hysys and transfers them to a Python script where the calculations are done. It then returns the calculated values back to the Aspen Hysys simulation.

General setup

All the simulations are set up in a similar manner which has been done to organize the stream in a comparable and intuitive manner. They all have the following steps, but the details of the steps vary, and a generalized flowchart like the one below may be used to describe parts of the process.

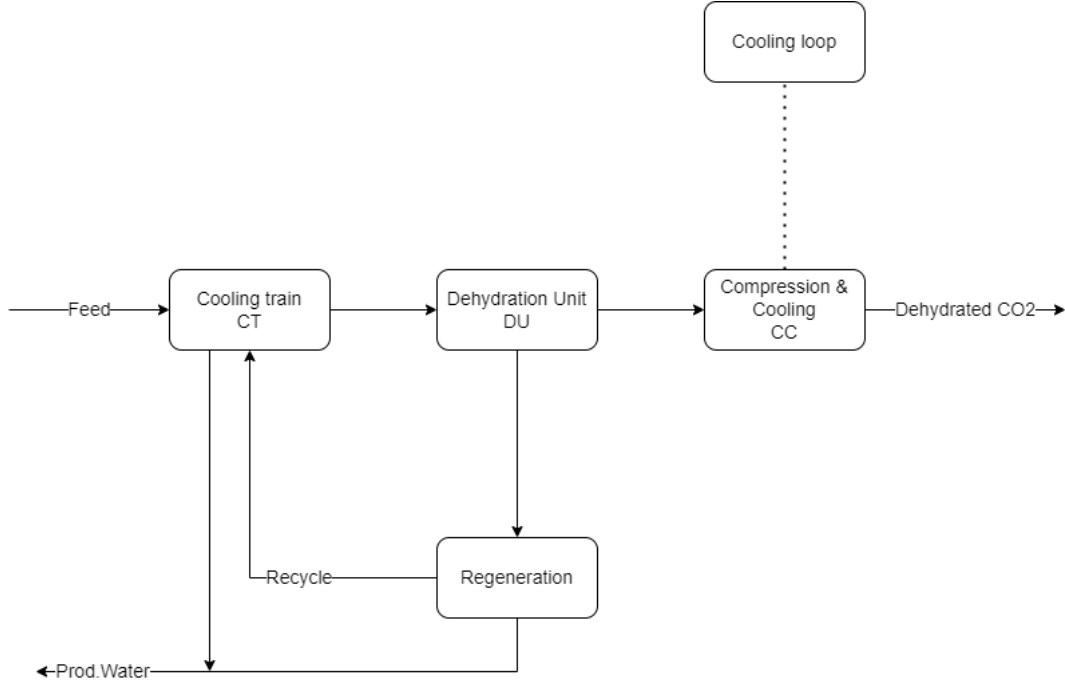


Figure 7: Generalized flowchart for the dehydration process. The feed stream first enters a compressor train, where the gas is first compressed and then cooled down. Condensate is taken out as "Produced water". The stream then enters the dehydration unit, where more water is removed. It will then be a regeneration process for the molecular sieves, TEG or MEG. Some gas will be recycled back to the compressor train, and the dehydrated gas will go through a compression and cooling step to achieve the desired operating conditions for transport. For liquid transport, an external cooling loop provides a lower temperature than what is achievable with cooling water. If the dehydrated CO_2 is transported by pipeline, cooling water will suffice.

1. Compression train: The stream is first passed through a compression train with coolers and knock-out drums. Streams and equipment are marked CT.
2. Dehydration. This is the point where the various dehydration methods take place. Streams and equipment are marked DH.
3. Compression and cooling: This is the post-treatment to get the correct pressure and temperature for further transport. Streams and equipment are marked CC
4. Cooling loop: For ship transport, there is also a cooling loop. These streams only interact with the CO_2 stream through a heat exchangers, and there is no mass transfer between the cooling loop and the rest of the process. These are marked CL.
5. Regeneration: Regeneration is important for all processes, despite being set up in different ways. From here there will also be a recycle stream going back to the compression train to prevent losses. Equipment and streams related to this are marked R.

General design

Most equipment has been designed with the same main ideas:

- Cooling water: This is supplied at 10°C, and is heated up to 20°C, in situations where streams are cooled down to 20°C or warmer. In situations with a lower end temperature, the cooling water is heated up to 15°C.
- ΔT_{min} is the minimum temperature difference in heat exchangers and is set to be 10°C. When feasible, this is used. However, there are some situations where this is not practical, and then the ΔT_{min} may be a bit lower.
- All compressors, pumps, and turbo-expanders are adiabatic, and have an efficiency of 75%. Heating is performed with high-pressure steam at 250°C.
- Compressors and pumps will at max increase the temperature to 125°C. This is to prevent unnecessary wear on compression equipment.

4.2 Pre-Treatment

The following figures show the difference in the beginning for the different processes. The recycle stream in case A will already be pressurized, and it would therefore be a waste of energy to mix it with the feed stream at a lower pressure, as it would just be re-compressed. For Case B1, Case C1, and Case C2, the recycle will be at the same pressure as the feed stream. Instead of having a separate compression for this stream, it is therefore mixed with the feed stream before any operations are done to the captured CO₂.

For Case B2, there is no recycle stream, but rather a bypass stream going into the regeneration process. Here, the pressure is lower than the feed stream, so it makes sense to take out this stream at a later stage of the compressor train. These steps are identical for all the transportation methods with the same dehydration process.

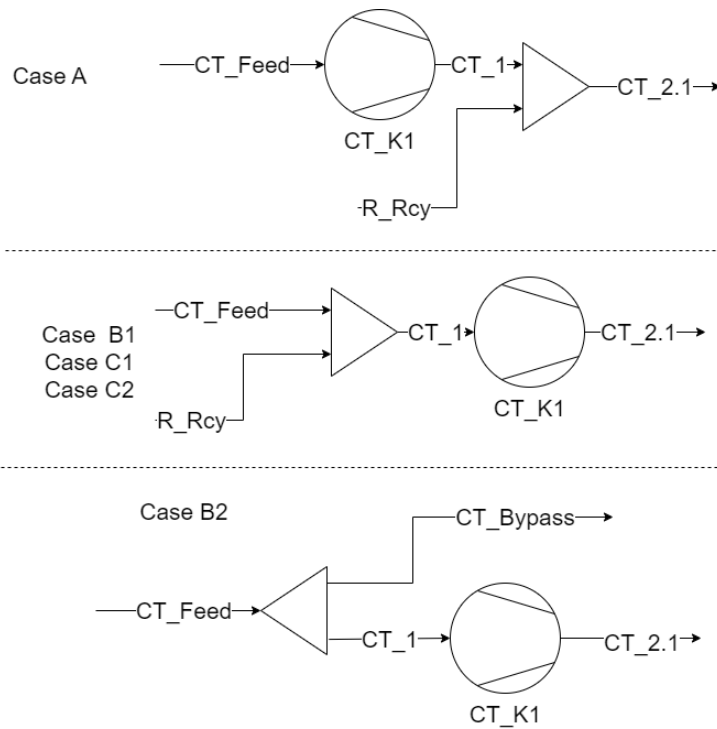


Figure 8: Cooling loop for ship transport of dehydrated CO₂.

After the first compression and mix/split of streams, the main stream passes through a cooler before entering a knock-out drum, where water is removed. This compression, cooling, and knock-out drum is repeated two more times before stream CT_7 is ready for the next part of the process. This configuration is set up in the same way for all cases.

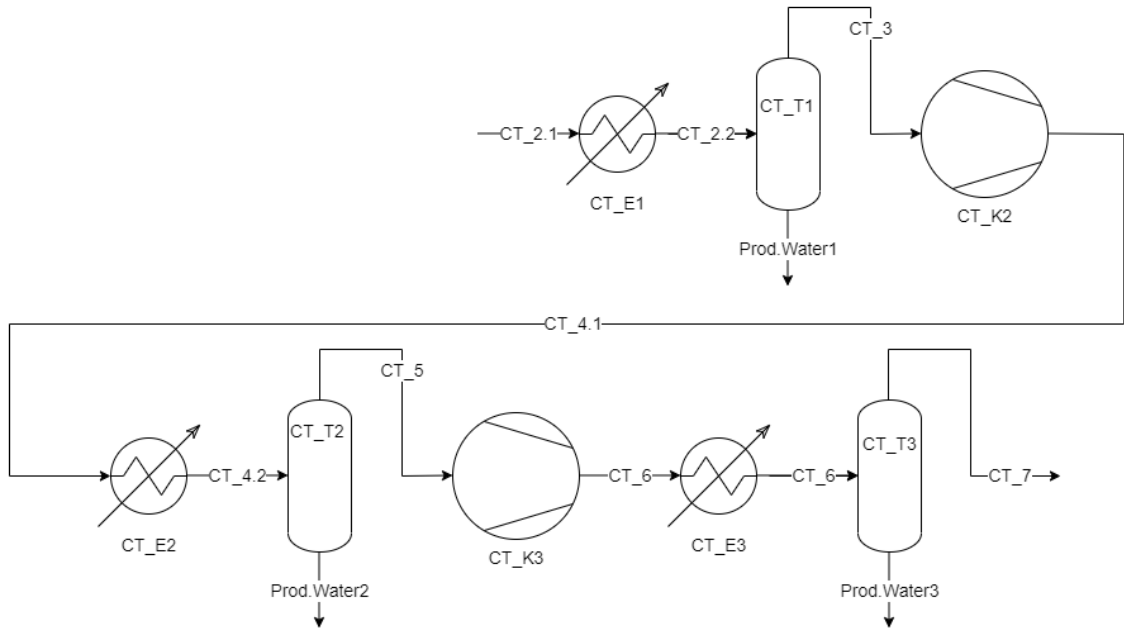


Figure 9: Cooling loop for ship transport of dehydrated CO_2 .

4.3 Post-treatment

Ship transport After the CO₂ has been dehydrated, cooling will be required, and the CO₂ stream will pass through a heat exchanger with the ammonia, to reach -30°C. The pressure is adjusted up to be 15bar.

Dense Phase transport For dense phase transport, it will be necessary to compress the CO₂ stream further as a gas, which is then cooled down into a liquid at 20°C. The stream is then pumped up meet the pressure requirement of 100bar after it is cooled down to 20°C.

Supercritical transport The compression process for transport in the supercritical state is similar to that of dense phase transport, but less cooling is required. After compression in a gaseous state, the fluid is cooled to 21°C and then pumped up to 150bar. As the compression is adiabatic, the temperature will then increase to the desired 40°C.

4.4 Cooling system

The cooling system will be identical for all the transport which is to be done by ship, apart from the volumes of ammonia required and duties.

In the cooling system, ammonia gas is compressed from 0.8 bar to 4 bar, before being cooled down to 20°C with cooling water. It is then re-compressed to 8.7 bar before again being cooled down to 20°C. During this cooling, the gas will enter a liquid phase. By then decompressing the ammonia to 0.8bar, the ammonia will cool down to -37.6°C, both through the Joule Thomson effect and by evaporation.

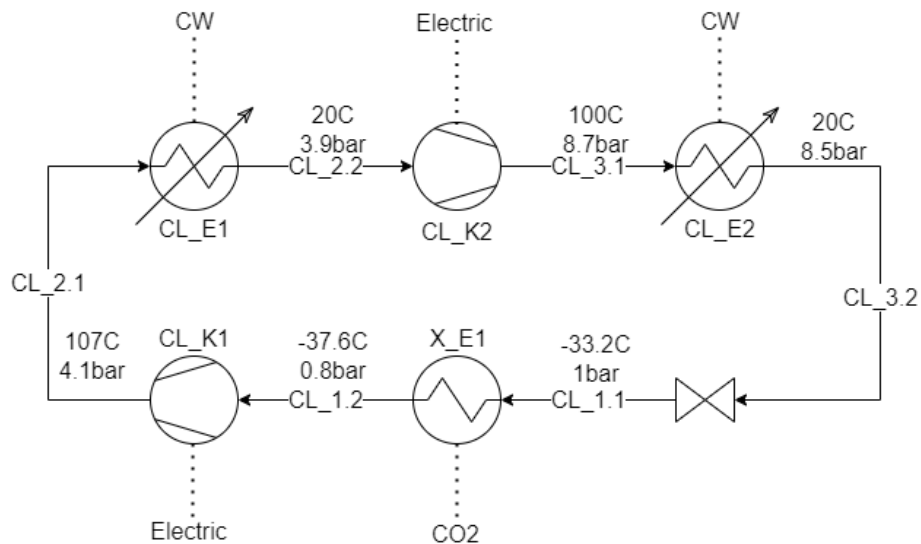


Figure 10: Cooling loop for ship transport of dehydrated CO₂.

4.5 Case A - Molecular sieve adsorption

After the compression train, Stream 7 enters the operating molecular sieve bed. There is a valve deciding how much produced, water-”free” CO₂ is used for regeneration. Depending on the amount of water coming into the molecular sieve, the need for regeneration gas will vary. From Andreassen 2022, 15% is sufficient and has been calculated for a very similar scenario. This regeneration stream is then heated to increase the temperature in the molecular sieve bed to 230°C, which evaporates the water. The stream used for regeneration is then returned to the cooling train. The water from the regenerating bed will then be knocked out into the produced water.

As *Aspen Hysys* does not have a model for molecular sieves, a component splitter that all the water, is used for simulations. This will provide sufficient results for this thesis, but should not be trusted blindly for the exact composition of the end product.

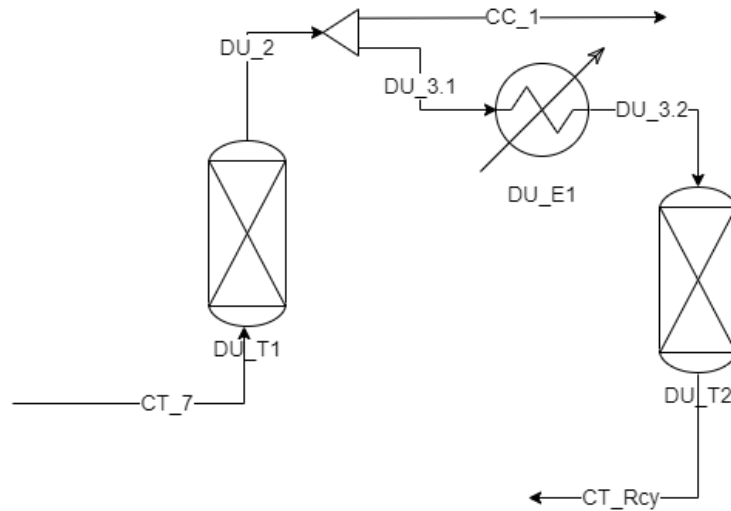


Figure 11: Dehydration after compressor train, with the use of molecular sieves, Case A

4.6 Case B1 - TEG absorption column

For case B1, the CO_2 stream enters an absorption column from the bottom, and lean TEG is injected at the top of the column. The water is absorbed into the TEG, and rich TEG is taken out at the bottom of the column. The rich TEG will then be regenerated by differences in boiling point, using 2 flash tanks and 2 distillation columns. This is done to separate out relatively pure TEG and water, as well as to recycle as little CO_2 as possible. This dehydration process will have minor losses of TEG into the CO_2 , and the produced water. The lost volumes are low but will need to be replaced in order to keep the process continuous. A makeup stream containing fresh TEG is therefore injected into the regenerated TEG prior before it enters the absorption column.

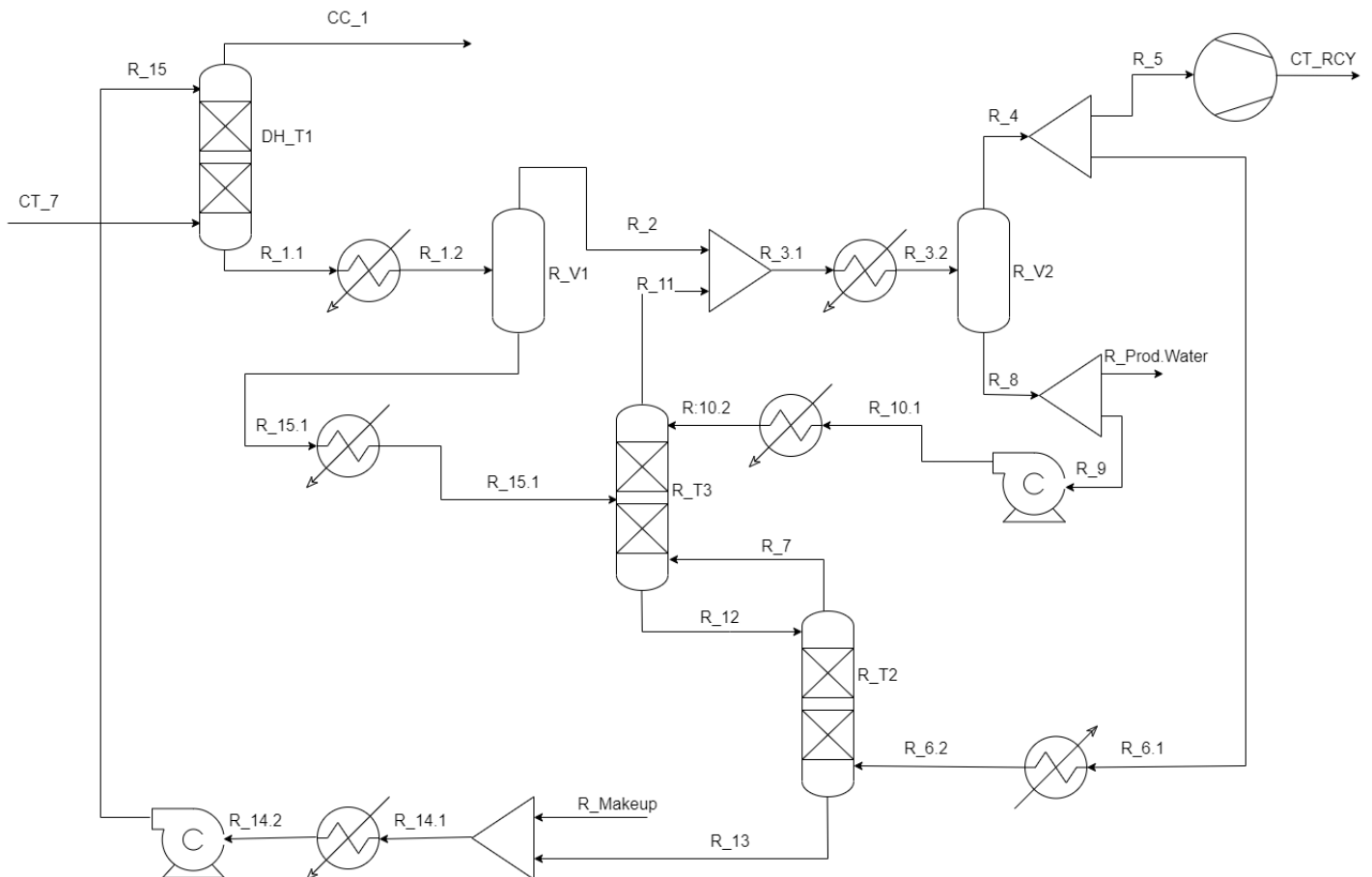


Figure 12: Dehydration and regeneration for Case B1, Dehydration by TEG absorption column.

4.8 Case C1 - Pressure temperature swing with Joule Thomson valve

For the temperature-pressure swing with a Joule Thomson valve, the compressor duties are increased. Lean MEG is injected into the main stream, preventing hydrate formation and freezing, before the pressure is decreased in a valve.

This valve decreases the temperature to knock out enough water alongside the MEG to meet the transport requirements in a knock-out drum. The rich MEG is then heated, and what is left in a vapor phase is recirculated back to the compressor train, while the liquid enters a distillation column, operating at 0.6bar. This pressure makes for a good separation of the water and MEG. The bottom temperature of the column is 139°C, which is slightly above the degeneration temperature of the MEG. The top stream will consist mostly of water and is discarded as produced water.

The now lean MEG is pumped up to the same pressure as the CO₂ stream before the valve, and a makeup flow of MEG is injected to compensate for lost MEG.

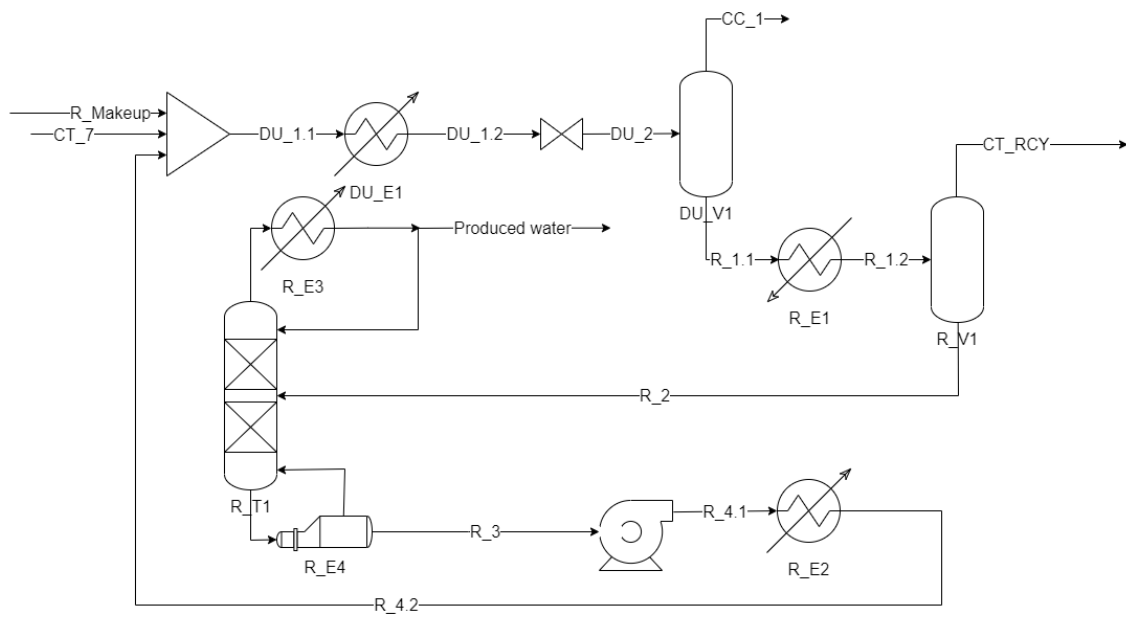


Figure 14: tekst her

4.9 Case C2 - Pressure temperature swing with turbo-expander

This method is similar to that of C1, but the CO_2 stream is decompressed through a turbo-expander rather than a valve. With adiabatic operation, this will take energy from the CO_2 stream while it is expanding, thus further cooling it. At the same time, mechanical energy is gained, which may be utilized for powering pumps or compressors with low energy losses.

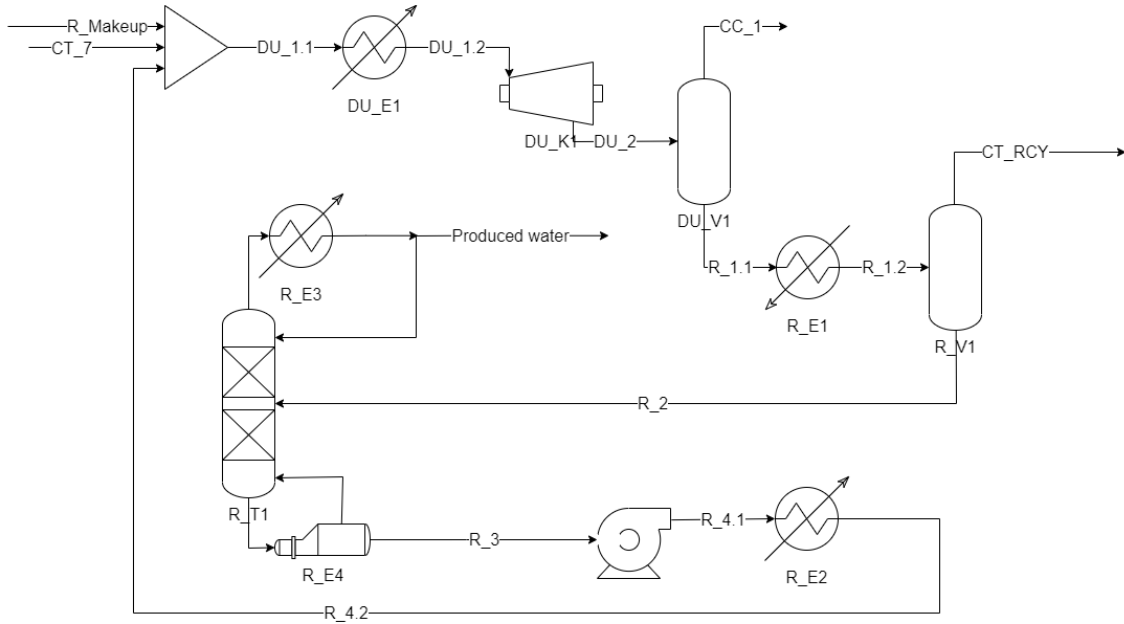


Figure 15: tekst her

5 Sizing and cost estimate of equipment

Equipment sizing is often important in preliminary studies, both because they give approximations for the spatial requirement of processes, and also to estimate the cost of equipment. For sizing, R. Sinnott 2020 is used as the main source when applicable. All equipment is scaled up 10% in order to make room for flow variations and to increase robustness. Cost estimates are made with cost factors from 2017, and adjusted by the CEPCI index at a later stage.

5.1 Heat exchangers

The heat transfer area of heat exchangers is calculated by the following equation:

$$A_{HEX} = \frac{Q}{U\Delta T_{lm}} \quad (8)$$

For all heat exchangers, the area is calculated for a counter-current configuration, apart from the heat exchanger that cools down the dehydrated CO₂ to -30°C. The equations used for calculating ΔT_{lm} for counter-current and co-current heat exchangers are shown in Equation 9 and 10, respectively.

$$\Delta T_{lm} = \frac{(T_H^{in} - T_C^{out}) - (T_H^{out} - T_C^{in})}{\ln\left(\frac{(T_H^{in} - T_C^{out})}{(T_H^{out} - T_C^{in})}\right)} \quad (9)$$

$$\Delta T_{lm} = \frac{(T_H^{in} - T_C^{in}) - (T_H^{out} - T_C^{out})}{\ln\left(\frac{(T_H^{in} - T_C^{in})}{(T_H^{out} - T_C^{out})}\right)} \quad (10)$$

The overall heat transfer coefficients used in calculating the heat exchanger area are shown in the table 2. All values selected within ranges presented by[R. Sinnott 2020].

Table 2: Table of the overall heat transfer coefficient used for sizing heat exchangers.

Type	Hot fluid	Cold Fluid	U(W/m ² C)
Cooler	Gas	CW	150
Heat exchanger	Gas	Gas	30
Heat exchanger	Gas	Gas	30
Cooler	Liquid CO2	CW	500
Cooler	Glycol	CW	500
Condenser	CO2	CW	1000
Condenser	Ammonia	CW	850
Condenser/evaporator	CO2	Ammonia	1250
Heater	Steam	gas	160
Reboiler	Steam	Glycol	1000

To calculate the cost of heat exchangers, "U-tube shell and tube" type heat exchangers are used for most instances. This type of heat exchanger has a lower limit of 10m², so when the heat transfer area is lower than this, "double pipe" heat exchangers are selected instead. These have a lower limit of 1m². [R. Sinnott 2020] 10% heat transfer area is added for cost estimates.

5.2 Molecular sieve packed beds

The molecular sieve beds are sized to have a loading capacity for the sieves to remove all water from the CO₂ stream for their operational time. As mentioned in Section 3.1, the molecular sieves in LPG treatment will typically be in operational state for 10 hours before regeneration. Under perfect conditions, this would suffice, but localized flow variations within the packed bed are expected, so some additional capacity is built in. 15% more molecular sieves are expected to handle the non-uniform flow and an additional 10% is added for the cost estimates.

The water mass entering the molecular sieves in this timespan is 1146.4kg, and by having a ratio of $\frac{m_{\text{water}}}{m_{\text{molecular sieve}}} = 19$, the required mass of molecular sieves is 6033 kg. The density of molecular sieves is 721 kg/m³, which gives a required molecular sieve volume of 8.4m³. [SPI-Chem Molecular Sieve Type 3A n.d.]

Kolmetz and Sari 2014 suggests a packing height which is a minimum of equal to the diameter, or at least 6ft(2m), whichever is highest, while Sanchez et al. 2016 had the best results in general packed beds when a ratio between packed height Z and diameter D is $\sim \frac{Z}{D} = 2.5$. As these results do not contradict each other, a height of 2.5 times the diameter is used. The molecular sieves do not require additional free space in the column.

The reactor is sized like a cylinder

$$h = 5 \cdot \sqrt[3]{\frac{V}{5\pi}} = 4.06m \quad (11)$$

The temperature of the materials will be up to 234°C, which makes the maximum stress 12.9ksi. The diameter will be 1.62m, and the minimum thickness will be 7mm. giving a steel weight of 1167kg. R. Sinnott 2020

The materials cost for the reactor shell will then be

$$C = 15000 + 68 * 1167(\text{kg})^{0.85} = 42512(\text{USD}) \quad (12)$$

The cost of molecular sieves must then be added:

One source of cost gives 4.74USD/kg for 3A molecular sieves, making the cost of the sieves 28596USD per reactor. BTS_Engineering n.d.

From the experience of Hammerfest LNG, the molecular sieves are expected to have a lifetime of 2 – 3 years before they need to be replaced. Secker and Bergene 2011

5.3 Membrane contactor

The area is directly calculated in Mahdi’s membrane contactor module, with fixed parameters that are viable with a Teflon AF2400 membrane. The chosen parameters are shown in Table 3.

Table 3: Input parameters for the membrane contactor model.

Parameter	Value	Unit
Permeance	1500	GPU
Dense layer thickness	1	μm
Inner diameter of porous support	0.5	mm
Outer diameter of porous support	0.55	mm
Porosity of porous support	0.75	phi
Inner diameter of shell	0.45	m
Length	0.8	m

From this, the membrane contactor model calculated the required number of tubes to be $4.767 \cdot 10^6$, and the required membrane area is 13180m^2 .

Due to a lack of commercial pricing, it is taken an estimated cost of 20\$ per m^3 , similarly to the estimates made for PTFE hollow fiber membranes in [Usman et al. 2018]. The cost of materials for the membrane contactor will then be:

$$C_{\text{membrane}} = 25 \frac{\text{USD}}{\text{m}^2} \cdot 13180\text{m}^2 \cdot 1.1 = 329500\text{USD}$$

5.4 Separator columns

The TEG absorption column is designed by first finding the diameter required to have a vapor velocity of $1\text{m}/\text{s}$. This is found from the volumetric flow:

$$D = 2 \sqrt{\frac{5809\text{m}^3/\text{hour}}{3600\text{s}/\text{hour} \cdot 1\text{m}/\text{s}}} = 1.61\text{m}$$

Since this is below 8ft(2.4m), a packed column will be more cost-effective than a trayed column. The choice of packing material size is also based on the diameter of the column; R. Sinnott 2020 suggests using packing with a size of 50 – 75mm. 50mm stainless pall rings are chosen, and these rings will give a HETP, height equivalent to a theoretical plate, value of 075 – 1m. The packing is then designed for a HETP value of 1m, which will give a packing volume of 19.32m^3 . With random packing such as pall rings, it will be necessary to have support for the packing, distributors, and some free volume for liquid and vapor holdup below and above the packing, respectively. To account for this, 30% height is added, making the real height of the column 4m .

The column shell is then calculated like the knockout drums, giving a wall thickness of 11mm, shell mass of 1781kg, and a cost of 40907USD. The cost of the packing must be added. The price of stainless pall rings is $7700\text{USD}/\text{m}^3$, making the cost of packing material 148764 USD, giving a total cost for the absorption column $C_{\text{absorber}} = 185100$ USD.

The same method is used for sizing and cost estimates of other columns, both stripping and distillation columns.

5.5 Pressure altering equipment

Compressor

The compressors are all set to be centrifugal when applicable, operating by increasing the kinetic energy in a gas by passing it through an impeller connected to an electric motor. Centrifugal compressors are rather uncomplicated and suited for all applications in this thesis. Centrifugal compressors typically have an efficiency in the range 70 – 85% [Simpson 2017], so 75% adiabatic efficiency is set for all compressors used in this thesis to give the best possible comparison. Compressors with a duty ≤ 75 kW are sized as blowers. The compressors are not sized in detail, as the cost may be estimated from only the duties. [R. Sinnott 2020].

Pumps

The pumps are all set to be explosion-proof motor pumps, when applicable. These pumps have a minimum duty of 75 kW, so pumps with a lower duty single-stage centrifugal pumps are selected. For smaller pumps, single stage centrifugal pumps are selected. Since these pumps can handle as low volume flows as 0.2 L/s, they are suitable for all applications of pumps in this report. The ability to cost estimate all pumps with the same equation is the reason for selecting single-stage centrifugal pumps. The technical details of the pumps selected are not necessary, as it is only used for cost estimates.

Turbo-expander

The turbo-expander is comparable to that of a pump, with the stream moving in the opposite direction, turning the impeller and generating shaft work. The turbo-expander will typically have an efficiency close to 90% [Bloch and Soares 2001], which is selected for the processes in this thesis. Because of this, the turbo-expander is cost-estimated like a compressor. The turbo-expander will have to be able to handle multiphase flows, and that aspect is not considered for the selected method for cost estimation.

5.6 CEPCI

Chemical Engineering Plant Cost Index, CEPCI, is a valuable tool for keeping track of costs associated with constructing chemical plants and the associated equipment. By tracking historical costs for specific parts of process equipment in addition to the change in prices over time, it is possible to use historical data to estimate the cost of the same equipment years later. The CEPCI index changes over years with increase or decrease caused by changes in the cost of services, materials, and currency changes. Table 4 shows the relevant table for this thesis.

The CEPCI index is used in the following way:

$$\text{Cost, year A} = \text{Cost, year B} \cdot \frac{\text{Cost index, year A}}{\text{Cost index, year B}} \quad (13)$$

Table 4: Table showing the CEPCI indexed from 2001 to 2022. Values from [2023]

Year	Cost Index
2022	816.0
2021	708.0
2020	596.2
2019	607.5
2018	603.1
2017	567.5
2016	541.7
2015	556.8
2014	576.1
2013	567.3
2012	584.6
2011	585.7
2010	550.8
2009	521.9
2008	575.4
2007	525.4
2006	499.6
2005	468.2
2004	444.2
2003	402.0
2002	395.6
2001	394.3

5.7 Overall Cost

For the overall cost, the following values have been used: The average electric cost for energy-intensive industries in Norway for 2022. [SSB n.d.] Cooling water prices from a report for the Norwegian Environmental Agency from 2019. [Kvinge et al. n.d.] Gas prices for an average of the European Union, averaged for 2017-2021, and an efficiency of 90% heating efficiency. [Aizarani 20223] Glycol prices are from market evaluations, averaged for 2022 Alerts 2023 [Mike 2023]

All values are first converted to USD and then adjusted to 2022 inflation levels using CEPCI indexes. The utility prices are shown in Table 5

Table 5: Cost of utilities used in this work, adjusted to 2022 value.

Adjusted utilities	Cost	Unit
Cooling water	0.0014	USD/ m^3
Power	52.41	USD/MWh
Gas	34.09	USD/MWh
Steam	37.88	USD/MWh
MEG	0.98	USD/kg
TEG	1.90	USD/kg

5.7.1 Parameters for cost estimation

The cost estimation for equipment is heavily based on R. Sinnott 2020, and follow the equation below:

$$C_e = a + bS^n \quad (14)$$

Here, C_e is the equipment cost. a, b and N are specific constants for the given type of equipment, and S is the size parameter.

Table 6: Cost parameters used for cost estimation, to be used with Equation 14

Equipment	Unit for S	a	b	n
Centrifugal compressor	Duty, kW	490 000	16 800	0.6
Blower	Flowrate, m^3/h	3 800	49	0.8
U-tube shell and tube heat exchanger	Area, m^2	24 000	46	1.2
Double pipe heat exchanger	Area, m^2	1 600	2 100	1
Raschig ring packing, 304ss	Volume, m^3	0	7 300	1
Vertical pressure vessels, 304ss	Mass, kg	15 000	68	0.85
Explosion proof motor pump	Duty, kW	-950	1 770	0.6
Single stage centrifugal pump	Duty, kW	6 900	206	0.9

5.7.2 Inside battery limits plant cost

For cost estimates on installed facilities, the equipment cost must be multiplied by the following factors to include related expenses that are not shown from the equipment cost alone. The factors here are what is included for "inside battery limit", the *ISBL*, cost. These costs account for other on-site expenses that are related to the construction of the process.

Equations used are shown below, and the symbols are shown in table 15 to include other expenses related to it:

$$C = \Sigma C_e[(1 + f_p)f_m + (f_{er} + f_{el} + f_i + f_c + f_s + f_l)] = 3.2C_e \quad (15)$$

Table 7: Cost factors used for including additional expenses related to the capital cost for the entire project. to be used in combination with Equation 15.

Explanation	Symbol	Value
Metal cost ratio	f_m	1
Equipment erection	f_{er}	0.3
Piping	f_p	0.8
Instrumental/control	f_i	0.3
Electrical	f_{el}	0.2
Civil	f_c	0.3
Structures, buildings	f_s	0.2
Lagging, paint	f_l	0.1

In addition to the ISBL costs, there will typically be off-site costs related to the construction of such facilities, but these are not considered in this thesis. They will typically be $\sim 40\%$ of the ISBL cost. [R. Sinnott 2020]

6 Results

In this section, the results are presented and discussed.

6.1 Summary of results

A summary of the main economical results is presented in Table 8. Here, the cost of major equipment, operational cost, and mass of dehydrated CO₂ for the various dehydration processes and transportation states are presented. For yearly utility cost and production of dehydrated CO₂, it is estimated 8000 operational hours per year.

Case	Equipment cost (MUSD)	ISBL Cost (MUSD)	Utility cost cost (MUSD/year)	Dehydrated CO2 (ton/year)	End product state
A	17.49	55.95	8.02	1484.34	Liquid
B1	15.25	48.80	8.62	1485.05	Liquid
B2	15.16	48.53	7.62	1486.29	Liquid
C1	21.00	67.20	9.74	1485.63	Liquid
C2	20.91	66.92	9.13	1485.80	Liquid
A	16.55	52.96	7.67	1485.06	Dense phase
B1	15.42	49.35	6.85	1485.05	Dense phase
B2	15.16	48.51	6.83	1486.29	Dense phase
C1	17.28	55.30	9.77	1485.03	Dense phase
C2	23.06	73.80	8.58	1483.46	Dense phase
A	16.52	52.87	7.43	1485.06	Supercritical fluid
B1	15.31	49.00	6.80	1485.05	Supercritical fluid
B2	15.03	48.11	6.84	1486.29	Supercritical fluid
C1	17.16	54.92	7.78	1485.03	Supercritical fluid
C2	22.47	71.91	8.51	1483.46	Supercritical fluid

Table 8: Overview of the costs of major equipment, capital cost, operational cost and amount of dehydrated CO₂ produced with the various methods for the three different states: Liquid, dense phase and supercritical fluid.

6.2 End Product

The quality of the end product, i.e. the dehydrated CO₂ is important for selecting the potential use cases for the dehydration methods. The stream compositions and operating conditions for the dehydrated CO₂ is presented in Table 9, Table 10, and Table 11 below. These values are calculated using *Aspen Hysys V.12.1*.

Table 9: Table showing the compositions of the dehydrated CO₂ after the different cases, for ship transport. Case A uses molecular sieves, Case B1 uses TEG absorption in an absorption column, Case B2 uses TEG absorption with membrane contactor, Case C1 uses pressure-temperature swing with a Joule Thomson valve and Case C2 uses pressure-temperature swing by turbo-expander.

Case	Case A	Case B1	Case B2	Case C1	Case C2
Temperature [C]	-30	-30	-30	-30	-30
Pressure [kPa]	1560	1517	1517	1520	1520
Vapor Fraction	0	0	0	0	0
Total mass flow [kg/h]	185542	185631	185786	185704	185725
Total molar flow [kmol/h]	4216.5	4218.6	4220.6	4220.2	4220.7
CO ₂ [kmol/h]	4214.9	4216.9	4218.9	4218.6	4219.1
H ₂ O [ppm molar]	0.0	29.6	29.0	30.7	30.7
N ₂ [ppm molar]	318	318	318	318	318
O ₂ [ppm molar]	41.1	41.1	41.1	41.1	41.1
MEA [ppm molar]	0	2.41	2.68	6.22E-04	6.22E-04
TEG [kmol/h]	0	0.49	0	0	0
MEG [ppm molar]	0	0	0	0.13	0.13

Table 10: Table showing the compositions of the dehydrated CO₂ after the different cases, for dense phase pipeline transport. Case A uses molecular sieves, Case B1 uses TEG absorption in an absorption column, Case B2 uses TEG absorption with membrane contactor, Case C1 uses pressure-temperature swing with a Joule Thomson valve and Case C2 uses pressure-temperature swing by turbo-expander.

Case	Case A	Case B1	Case B2	Case C1	Case C2
Temperature [C]	20	20	20	20	20
Pressure [kPa]	15000	15000	15000	15000	15000
Vapor Fraction	0	0	0	0	0
Total mass flow [kg/h]	185633	185631	185786	185629	185432
Total molar flow [kmol/h]	4218.5	4218.6	4220.6	4218.7	4214.0
CO ₂ [kmol/h]	4217.0	4216.9	4218.9	4216.8	4212.4
H ₂ O [ppm molar]	0	29.6	29.0	98.3	97.1
N ₂ [ppm molar]	318	318	318	318	318
O ₂ [ppm molar]	41.1	41.1	41.1	41.1	41.1
MEA [ppm molar]	0	2.41	2.68	2.68E-02	2.68E-02
TEG [kmol/h]	0	0.486	0	0	0
MEG [ppm molar]	0	0	0	0.321	0.318

Table 11: Table showing the compositions of the dehydrated CO₂ after the different cases, for supercritical fluid pipeline transport. Case B1 uses TEG absorption in an absorption column, Case B2 uses TEG absorption with membrane contactor, Case C1 uses pressure-temperature swing with a Joule Thomson valve and Case C2 uses pressure-temperature swing by turbo-expander.

Case	Case A	Case B1	Case B2	Case C1	Case C2
Temperature [C]	39.7	40	20	20	20
Pressure [kPa]	15000	15000	15000	15000	15000
Vapor Fraction	0	0	0	0	0
Total mass flow [kg/h]	185633	185631	185786	185629	185432
Total molar flow [kmol/h]	4218.5	4218.6	4220.6	4218.7	4214.0
CO ₂ [kmol/h]	4217.0	4216.9	4218.9	4216.8	4212.4
H ₂ O [kmol/h]	0.0	29.6	29.0	98.3	97.1
N ₂ [kmol/h]	318	318	318	318	318
O ₂ [kmol/h]	41.1	41.1	41.1	41.1	41.1
MEA [kmol/h]	0	2.41	2.67	2.68E-02	2.68E-02
TEG [kmol/h]	0	0.49	0	0	0
MEG [kmol/h]	0	0.00	0	0.32	0.32

6.2.1 Purity of end product

As seen in Table 9, the end composition in the dehydrated streams is quite similar for all dehydration methods, and there is no issue with achieving the right operating conditions of $\leq -30^{\circ}\text{C}$ and $\geq 15\text{bar}$.

However, using pressure-temperature swing does not reach sufficiently low water content, rendering it an infeasible process to dehydrate the CO_2 for ship transport in a liquid state, following the requirements set in the *Northern lights* project.

From the table, some losses of CO_2 are observed. These calculations indicate that molecular sieves will have the highest loss of CO_2 . The losses are minor in comparison to how much CO_2 is treated, but should ideally be reduced. All CO_2 losses are expected to be through produced water, and treatment of this may help recapture the CO_2 . This CO_2 would most likely require additional dehydration, so all CO_2 losses cause inefficiency.

The end products will also have more oxygen than the desired concentration of ≤ 10 ppm molar, implying that the specification may not be met with only these dehydration processes for the given feed stream. Other methods for oxygen removal will be necessary to further reduce the oxygen and prevent the outlined issues related to increased O_2 concentrations. However, de-oxygenation methods are beyond the scope of this thesis.

For the pressure-temperature swing methods, there is some loss of MEG into the product stream. This is not an issue for CO_2 that will be stored, but may be a consideration if the CO_2 is intended for other uses.

In case B1, dehydration with TEG in an absorption column will give some loss of TEG into the product stream. This TEG may freeze at lower temperatures and increased pressure if it accumulates, which would be problematic in the transportation stage. This will not be an issue if it occurs when the CO_2 is in storage.

It should be noted that the membrane contactor is set up to work in an ideal scenario, and minor TEG leakage into the product stream might be more realistic. The TEG losses would still be expected to be significantly lower than with conventional absorption columns.

For pipeline transport, all methods produce CO_2 with sufficiently low water concentration. The same trends for glycol loss into the dehydrated CO_2 and a higher oxygen content than desired are still present. As the CO_2 transported by pipeline will not reach as low temperatures as the liquid CO_2 , it is expected that TEG freezing is less of an issue.

6.3 Produced water

The combined composition and mass of produced water for the different cases are shown below:

Table 12: Composition produced water from the various processes, for liquid state transport.

Case	Case A	Case B1	Case B2	Case C1	Case C2
Mass [kg/hour]	1872	1867	1863	1882	1880
CO ₂ [kg/hour]	9.9	13.8	13.4	23.7	23.6
H ₂ O [kg/hour]	1580	1854	1834	1853	1851
N ₂ [kg/hour]	5.3E-05	7.3E-05	7.1E-05	8.5E-05	8.5E-05
O ₂ [kg/hour]	1.8E-06	2.1E-06	2.1E-06	2.7E-06	2.7E-06
MEA [kg/hour]	0.685	0.015	0.002	0.892	0.914
TEG [kg/hour]	0	0.047	0.004	0	0
MEG[kg/hour]	0	0	0	4.07	4.13

For these processes, the waste product is captured as one stream of "produced water". The produced water is removed at several stages in the processes and most of it comes from the knock-out drums. The reason for handling it like one big stream is that most facilities would have a combined collection of all the produced water, either for further treatment or for direct emissions. All the processes have some losses of CO₂ dissolved into the produced water, and molecular sieve adsorption has the lowest losses here, with only ~ 10 kg lost. Absorption with TEG has higher losses of 13.6kg/hour, and pressure-swing dehydration has the highest losses of 23.6 kg/hour. This will affect the efficiency of the dehydration processes, but these fractions are small when considering the larger scale.

N₂ and O₂ in the produced water are considered an environmental non-issue, as they are already the main components in the air.

The MEA emissions are significantly lower in the TEG absorption cases. This does not imply that the MEA is suddenly removed within the process, but rather implies that there is some accumulation of MEA in the regeneration loop, at this MEA is not found in the dehydrated CO₂.

Some method to remove this accumulated MEA should be implemented but is not present in the models used for simulations in this thesis. One source of error is losses through the membrane contactor, as the stream compositions were copied and pasted between different files, which might have caused some unintended losses.

TEG will only be present in the dehydration with TEG absorption, and the losses through produced water are highest for the conventional absorption column. This is likely caused by the higher CO₂ concentration in the regeneration system, which necessitates a more complicated system than the membrane contactor. However, the amount of TEG lost through the produced water is low, and is expected to not cause issues for emitting the produced water. This will also be low enough to not be considered a significant waste of resources.

Like for TEG, MEG will only be present in the produced water for processes requiring this chemical. About kg of MEG is lost through the pressure-temperature swing processes. Since MEG lost through produced water is a loss of a resource, this amount should be reduced if possible. However, the economic loss from this is marginal.

6.4 Heat exchangers

A general overview of the most important information about the heat exchangers for the various processes is shown in Table 13. The most important factors from this table are the hot and cold utility, in addition to the equipment cost.

Table 13: Overview of key information about the heat exchangers for the various processes, for transportation of liquid CO₂. *Case C1 and Case C2 have a pinch region instead of a pinch point.

Case	Case A	Case B1	Case B2	Case C1	Case C2
T _{pinch} Shift	135.9	120	120	134.9-144.3	134.9-144.3
Number of exchangers	8	14	15	11	11
Cold utility [MW]	41.22	38.55	39.02	39.99	42.51
Mass CW [ton/h]	3438	3223	3255	3336	3553
Hot utility	1010	942	892	113	114
Mass Steam [ton/h]	2.08	1.94	1.84	0.23	0.23
Energy saving potential [kW]	0	57	0	20	64
Cost [MUSD]	1.859	1.539	1.571	2.077	2.221

From the results, the heat exchanger networks are well integrated, as there is not much more energy that can be reused by further heat integration. Minor improvements in energy efficiency are possible, but the cost will likely not be worth it.

6.5 Compressors, pumps, turbo-expanders

Table 14 shows a summary of the combined cost and duties for pressure-altering equipment.

Table 14: Summary of compressors, pumps, and turbo-expanders showing the duties and equipment cost.

Case & Transport state	Duty [MW]	Equipment cost [MUSD]
Case A Liquid	18.32	3.57
Case B1 Liquid	19.77	3.60
Case B2 Liquid	17.31	3.76
Case C1 Liquid	23.06	4.53
Case C2 Liquid	21.51	5.49
Case A Dense Phase	17.44	2.98
Case B1 Dense Phase	15.43	4.93
Case B2 Dense Phase	15.45	3.87
Case C1 Dense Phase	18.32	3.89
Case C2 Dense Phase	20.22	5.23
Case A Supercritical State	16.89	3.00
Case B1 Supercritical State	15.45	3.89
Case B2 Supercritical State	15.48	3.87
Case C1 Supercritical State	18.32	3.89
Case C2 Supercritical State	20.05	5.23

From Table 14, it is observed a trend that the equipment cost related to compression and decompression is lowest for the molecular sieve adsorption in Case A. This makes sense as this process has the fewest compression operations, and compressors have a high fixed cost. Since Case A has a high recycling rate due to the regeneration of molecular sieves, this raises the compressor's duty. TEG absorption has a lower combined compression duty, which also makes sense as there is not as much recycling of CO₂. The pressure-temperature swing methods in Case C1 and Case C2 have

compression of CO₂ that is subsequently depressurized. Due to the efficiencies of compressors and pumps, it makes sense that this will cause some energy losses.

6.6 Separators

Below, it will be presented the cost of the different separation columns, and it is differentiated between packed columns and the knock-out drums.

Table 15: Table showing sizing and cost estimates for all packed columns. The packing material is stainless raschig rings, and the sizing and cost estimation is done in the same way as Section 5.4.

Case	Volume packing [m ³]	Packing size [mm]	Height [m]	Diameter [m]	Cost [kUSD]	Phase
Case B1	19.32	50	4	1.61	189.67	Liquid
Case B1	1.33	38	3	0.87	13.05	Liquid
Case B1	0.33	38	6	30.46	5.29	Liquid
Case B1	19.32	50	4	1.61	189.67	Dense Phase
Case B1	1.33	38	3	0.87	13.05	Dense Phase
Case B1	0.33	38	6	30.46	5.29	Dense Phase
Case B1	19.32	50	4	1.61	189.67	Critical State
Case B1	1.33	38	3	0.87	13.05	Critical State
Case B1	0.33	38	6	30.46	5.29	Critical State
Case B2	1.28	38	3	0.85	13.21	Liquid
Case B2	0.15	25	4	0.25	3.66	Liquid
Case B2	1.28	38	3	0.85	13.21	Dense Phase
Case B2	0.15	25	4	0.25	3.66	Dense Phase
Case B2	1.28	38	3	0.85	13.21	Critical State
Case B2	0.15	25	4	0.25	3.66	Critical State
Case C1	0.31	25	6.5	0.28	5.53	Liquid
Case C1	0.31	25	6.5	0.28	5.53	Dense Phase
Case C1	0.31	25	6.5	0.28	5.53	Critical State
Case C2	0.31	25	6.5	0.28	5.51	Liquid
Case C2	0.31	25	6.5	0.28	5.51	Dense Phase
Case C2	0.31	25	6.5	0.28	5.51	Critical State

Table 16: Overview of cost of knock-out drums for all cases. Note that the height and diameter are made with *Aspen Hysys* 'Quick-size' function.

Case	Cost [MUSD]	Phase
Case A	8.260	Liquid
Case A	8.260	Dense Phase
Case A	8.260	Critical State
Case B1	6.822	Liquid
Case B1	6.822	Dense Phase
Case B1	6.822	Critical State
Case B2	6.817	Liquid
Case B2	6.817	Dense Phase
Case B2	6.817	Critical State
Case C1	10.004	Liquid
Case C1	8.423	Dense Phase
Case C1	8.423	Critical State
Case C2	9.179	Liquid
Case C2	11.302	Dense Phase
Case C2	10.959	Critical State

Upon comparison of the costs in the different types of separator columns, it is observed that the knock-out drums are a significantly larger expense than the packed columns, despite the use of expensive stainless steel packing. The "Quick-size" function used for this sizing does not give any insight on calculation detail. Since this makes for a relatively large cost in this thesis it must be considered an error source that reduces the accuracy of the total equipment cost.

6.7 Energy integration

6.8 Heat exchanger networks

Heat integration was also done for all cases, and the heat exchanger networks for all methods are shown below. These values represent the heat exchanger networks for ship transport. Corresponding figures for dense phase and supercritical state transport can be seen in Appendix C.

The heat exchanger networks show the stream temperatures and which streams they interchange energy with. Heat exchangers are represented with squares, and dashed lines show which streams they exchange heat. Heat exchangers without dashed lines are either coolers or heaters, using cooling water or steam, respectively. The color of the heat exchangers indicates whether the stream is a hot or cold stream. Blue heat exchangers have cold streams entering and the stream is heated up, while red exchangers represent hot streams being cooled down.

The names of heat exchangers only represent where in the process the streams are located, and exchangers with a name starting with X exchange energy internally within the process. It should be noted that heat exchangers that only exchange heat with steam or cooling water is not included here.

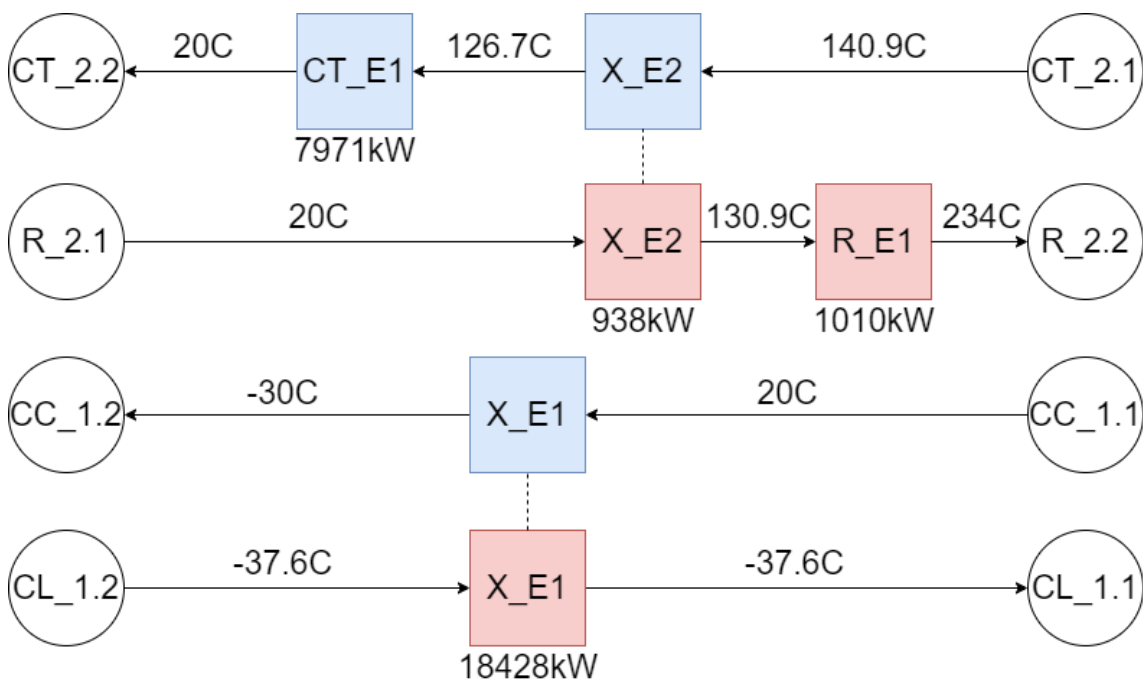


Figure 16: Heat exchanger network for case A, molecular sieve adsorption, for liquid phase transport. Note that streams that are cooled with only cooling water or heated by only steam is not included.

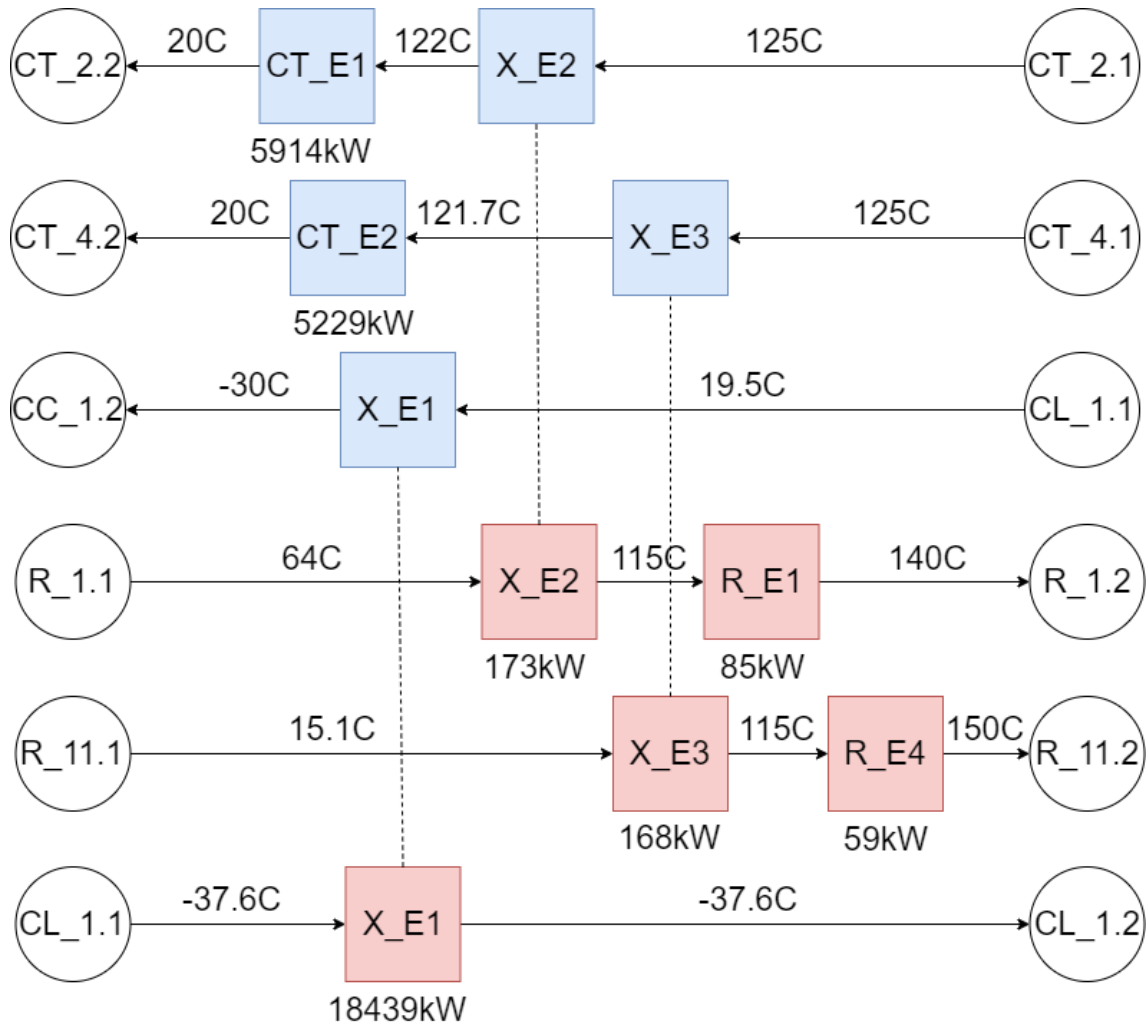


Figure 17: Heat exchanger network for case B1, TEG absorption with packed column, for liquid phase transport. Note that streams that are cooled with only cooling water or heated by only steam is not included.

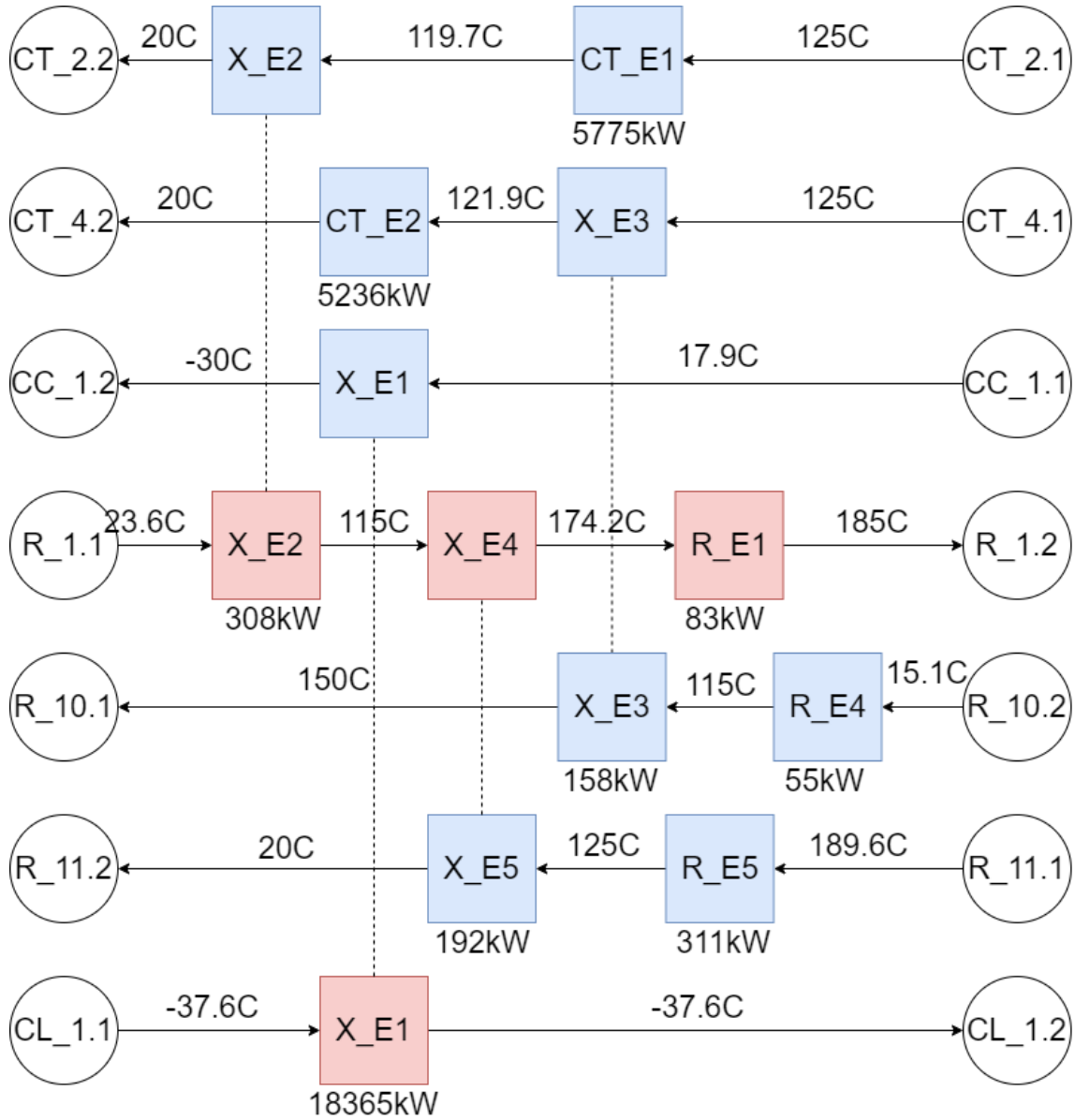


Figure 18: Heat exchanger network for case B2 TEG absorption with membrane contactor, for liquid phase transport. Note that streams that are cooled with only cooling water or heated by only steam is not included.

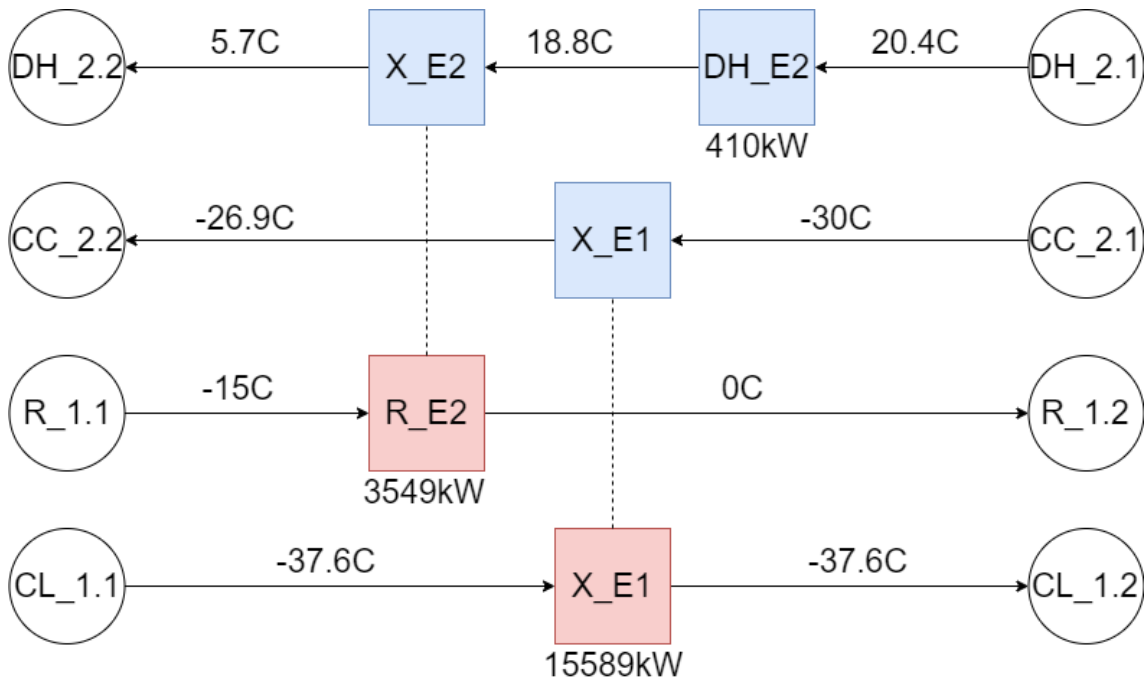


Figure 19: Heat exchanger network for case C1, pressure -temperature swing by Joule Thomson valve, for liquid phase transport. Note that streams that are cooled with only cooling water or heated by only steam is not included.

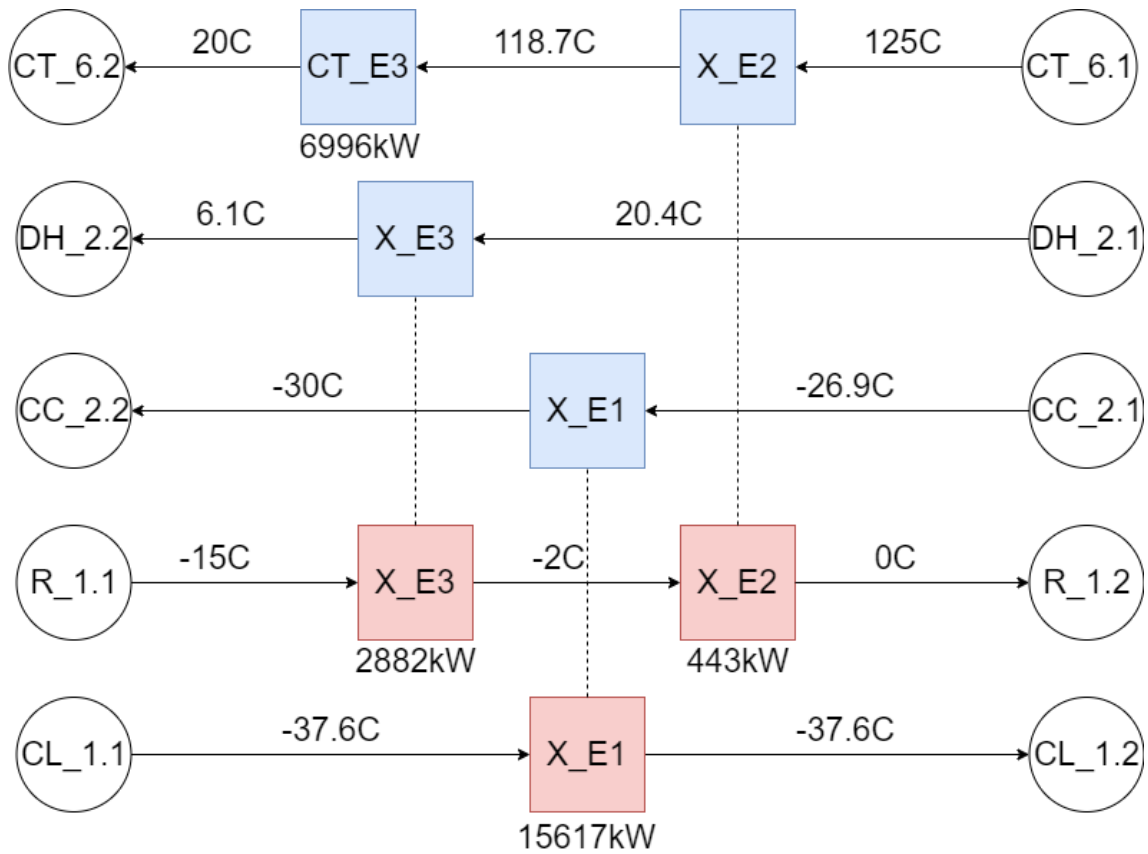


Figure 20: Heat exchanger network for case C2, pressure-temperature swing with turbo-expander, for liquid phase transport. Note that streams that are cooled with only cooling water or heated by only steam is not included

6.9 The membrane contactor model

The membrane contactor model used for the simulations is a known source of error. It is based on work done in Ahmadi et al. 2021, and the model was unable to function in its current configuration with more components than water, CO₂, CH₄ and TEG. The membrane contactor was made for subsea dehydration where these components were in focus. The membrane contactor therefore had to run on its own *Aspen Hysys* file, and for iterations, the stream composition was copied and pasted between the main file and the membrane contactor file. It is therefore expected that there has been some minor changes to the stream composition, which may affect the outcome.

The membrane contactor was only used with one set of parameters for the membrane, which are not certain to be optimal. This was done as a time saving measure as there were significant issues with both getting the membrane contactor to run and to achieving a steady state where both files converged, and the mass balances were acceptable.

Despite these issues with the membrane contactor, the results are still valuable, as they show that the desired separation is achievable with a membrane contactor. If there is a better setup for a membrane contactor, these will only affect the results shown in this thesis in a positive manner.

6.10 Makeup glycol

The makeup glycol will be an additional expense when considering the most suitable dehydration method, as both TEG absorption and pressure-temperature swing will require a continuous refill of glycol. In addition to being an expense, it will cause an additional logistical consideration. The required glycol to be refilled into the processes are shown below.

Case	Transport Phase	Glycol	Mass [kg/hour]
B1	All	TEG	0.358
B2	All	TEG	3.4
C1	Liquid	MEG	4.7
C1	Dense phase	MEG	3.4
	Supercritical state	MEG	
C2	All	MEG	4.4

Table 17: Table showing the required makeup of glycol for the various cases. Note that no makeup glycol is required for Case A

Despite the amounts of glycol needed to be refilled into the processes being low, there is expected some degradation of the MEG due to the regeneration boiler operating at a temperature where thermal degradation may occur. The losses from MEG degradation is not studied in this thesis, but should be further investigated before implementing a regeneration loop for MEG.

6.11 Energy sources

Electricity

For all processes in this thesis, the intended energy supply for all compressors and pumps is electricity. This is as simple energy source to convert into shaft work for such applications. Another alternative energy source for this is using turbines and combustion of fuels such as natural gas. A common shaft between the turbine and a compressor or a pump will have low associated energy loss. However, incineration of more fossil fuels is expected to be counter-productive to the main goal of CCS, unless the CO₂ is captured. As most electricity produced in Norway is produced from low-carbon sources, electric energy is chosen for all compression.

The cost of electricity is found from the average cost of electricity for energy-intensive industries in Norway in 2022, and is 52.41 USD/MW. Due to large fluctuations in the Norwegian energy market, it is possible that this cost would be larger for newly established facilities.

Cooling water

Due to the abundance of freshwater in Norway, the cost of cooling water is low, and most of the cost is related to pumping it to the desired location. The cooling water is supplied at 10°C which is heated up to 20°C, giving a cooling efficiency of 11.99kW per ton/h.

From an analysis of the costs of CCS projects, the cost of cooling water is estimated to be 0.0014 USD/m³. It should be noted that this would not be applicable for offshore operation, as seawater would require some treatment prior to use.

Steam

All applications of steam are based on the use of high-pressure steam at 250°C and 39.13bar, condensing to a liquid at the same temperature. Condensation of water at this fixed temperature, will supply 485.5kW of heat per kg/h of steam.

For the cost analysis, the steam is heated by natural gas at 90% efficiency in a closed steam loop. The cost is based on the average cost of natural gas for households in the European Union, averaged over the years 2017-2021, and inflation adjusted with the CEPCI index. Heating with natural gas is not optimal, and the heating should rather be performed with "waste heat" from other processes, if possible. High pressure steam at 250°C and 39.13bar has been used for all applications, but may not be the best option. If lower grade energy - such as medium pressure steam at 200°C is sufficient, this will usually be a better use of resources.

6.12 Pipeline transport

Pipeline transport can be used for CO₂ in both dense phase and supercritical state. However, if the transport is intended to be in *Norway*, there will be challenges related to transporting the CO₂ in supercritical state for longer distances, as the temperature must be above 31°C. This will either require significant effort in insulating the pipeline and or heating the fluid during transportation to combat heat loss to surroundings. This might not be an issue for short-distance transport, and an example of areas where the supercritical state may be utilized is offshore applications. For long-distance transport of the CO₂ in pipeline, transporting dense phase CO₂ will be a more appropriate alternative.

6.13 Economy

In the table below, the most important numbers for an economical analysis are presented.

Table 18: Summary of costs and tax savings related to each process. The capital cost is the "inside battery limit" plant cost from Table 8, plus additional 40% to include expenses outside the battery limit. Tax savings is the reduction CO₂ taxes based on the amount of dehydrated CO₂.

Case	Capital cost [MUSD]	Utility cost [MUSD/year]	Dehydrated CO ₂ [kton/y]	Tax savings [MUSD/y]	End product state
A	78.33	8.02	1484.34	117.77	Liquid
B1	68.32	8.62	1485.05	117.83	Liquid
B2	67.94	7.62	1486.29	117.93	Liquid
C1	94.08	9.74	1485.63	117.88	Liquid
C2	93.69	9.13	1485.80	117.89	Liquid
A	74.14	7.67	1485.06	117.83	Dense phase
B1	69.09	6.85	1485.05	117.83	Dense phase
B2	67.91	6.83	1486.29	117.93	Dense phase
C1	77.42	9.77	1485.03	117.83	Dense phase
C2	103.32	8.58	1483.46	117.70	Dense phase
A	74.02	7.43	1485.06	117.83	Supercritical fluid
B1	68.60	6.80	1485.05	117.83	Supercritical fluid
B2	67.35	6.84	1486.29	117.93	Supercritical fluid
C1	76.89	7.78	1485.03	117.83	Supercritical fluid
C2	100.68	8.51	1483.46	117.70	Supercritical fluid

Table 18 shows that if the savings on CO₂ tax is considered as revenue, the revenue would be higher than the capital cost and utility cost combined. But, since the dehydration process does not include all the costs related to carbon capture and storage, it is important to not interpret this as if all the processes have a break-even within the first year. What the table does show is that dehydration of CO₂ has a low cost as compared to the overall savings that can be made through CCS. The CO₂ tax is expected to increase in the future as countries strive to meet their environmental goals, thus further motivating emission reduction. It is also important to keep in mind that all costs presented in this thesis are rough estimates. From R. Sinnott 2020, which has been used as the main source for cost estimation, the accuracy of these estimates is expected to be $\pm 30 - 50\%$. The more work is put into the design details, the better estimates can be achieved.

6.13.1 Cost trends

The major trends for equipment cost are that the pressure-temperature swing methods are the most expensive. This is explained by the high cost of having large high-duty compressors, in addition to knock-out drums thick enough to operate at elevated pressures. Using a turbo-expander is significantly more expensive than a Joule-Thomson valve for both dense phase and supercritical state, but the equipment cost is similar between those two methods for liquid CO₂ transport. Due to the large and expensive knock-out drums, this may be an issue from using *Aspen Hysys* "quick sizing" function for estimating the column size. The cheapest equipment is that used for TEG absorption, and for all cases, using a membrane contactor is slightly less expensive than a conventional absorption column. The cost of these two processes are within the margin of error. Molecular sieves have an equipment cost between the cheaper TEG absorption, and the more expensive pressure-temperature swing for all cases.

The lowest operational cost for liquid transport is with case B2, the membrane contactor. Case B1, the absorption column has a higher cost than B2 and A. For dense phase and supercritical state CO₂, the operational cost difference between B1 and B2 is low. The difference in compression work required for case B1 between pipeline and shipping transport is significantly more than the corresponding difference for Case B2. This might indicate that there is some inefficiency error in Case B1 for ship transport.

For both liquid and dense phase transport, C2 has a lower operational cost than C1, which intuitively makes sense. However, for supercritical fluid, the operational cost for C1 is significantly higher than for C2. In order to explain this, it is necessary to look at the stream sizes, as the recycle stream is significantly larger for C2.

6.14 Absorption column vs. membrane contactor

The membrane contactor has advantages when compared to the conventional TEG absorption column in that the membrane contactors have a much smaller configuration, and have a more linear economy of scale.

The absorption columns will need a minimum size regardless of the operating volumes, while the membrane contactor can be built to exactly the required size, giving an advantage in economy of scale. The membrane contactors are typically made in modular configurations, enabling swapping out the membrane contactor for maintenance or replacement with a brief downtime. For maintenance of absorption columns, the downtime will be longer, and swapping them out will usually be a much more complicated process. The main advantage of the absorption column is that it is a mature technology, with a longer expected lifetime.

7 Conclusion & Further Work

7.1 Conclusion

For transportation of CO₂ in liquid state, molecular sieves, TEG absorption with a conventional absorption column, and TEG absorption with a membrane contactor are techniques that achieve the *Northern lights* project specification for gas composition of ≤ 30 ppm molar water, and are considered to be viable methods. The pressure-temperature swing processes are unable to achieve sufficiently low water composition and are not advisable for **Northern Lights**' use.

The lowest capital and operational cost are observed with the TEG absorption membrane contactor, making this the recommended method for producing dehydrated CO₂ ready to be transported by ship in a liquid state. The membrane contactor is a fairly untested method for such an application, but after large scaling testing, it is potentially a viable option for CO₂ dehydration. Both molecular sieves and TEG absorption columns are well-tested for the application, and are good options. The molecular sieves have a higher operational cost, while the TEG absorption column has a higher capital cost. As the two latter methods are more mature technologies, they might still be favored by industry at this point in time.

With pipeline transport in dense phase or as a supercritical fluid, slightly more water is allowed in the dehydrated CO₂. With a maximum concentration of 100ppm molar, all processes tested in this thesis are viable options.

For transport by pipeline, both in dense phase and as a supercritical fluid, the two methods with TEG absorption have the lowest operational and capital cost. The membrane contactor has a slightly lower capital cost, and the operational costs are so similar that no recommendation between these two should be made solely on the operational cost. Adsorption with molecular sieves is a better alternative than pressure-temperature swing, regardless if a turbo expander or a Joule Thomson valve is used.

All processes end up with a higher O₂ concentration in the final product, making it necessary to have a different feed stream or an added de-oxygenation process if specification from *Northern lights* of ≤ 10 ppm molar is to be achieved.

When comparing the costs of dehydration processes to the CO₂ tax, it is found that the cost of dehydration is small in comparison. In lack of knowledge on the total cost of capture, transport and storage of CO₂, it is difficult to make a good economical analysis.

7.2 Further work

In order to better determine the best method, more feed streams should be tested to ensure that the separation still satisfies the limitations on the water content in the end product. If one method is more robust, it will often be a better alternative despite being more expensive. If the O₂ concentrations remain at a level higher than the transport specification for other streams, it should be implemented a de-oxygenation process in combination with the dehydration.

For all the processes it has been made an attempt to find the most effective solution for dehydration, but no systematic optimization was done. By optimizing the process for a range of feed stream compositions, it will be clear which method is best suited. Especially the membrane contactor has potential for optimization, at the complications with implementing this model made it necessary to use the first membrane contactor configuration that converged.

A detailed study on the expected wear on equipment would also be valuable, especially for the membrane contactor and molecular sieves as these are considered to be the weak points and are expected to need replacement before more rigid equipment such as tanks. Due to the complications *Equinor* has experienced with the use of molecular sieves, alternative adsorption agents and methods to expand the lifetime of 3A molecular sieves should be explored.

The actual TEG losses through membrane contactors should also be explored. The model used in this thesis works with an ideal scenario and steady state. However, for real application, it is expected some pressure swings during operation that might cause bubbling or wetting. Some work on this subject has been done with natural gas instead of CO₂ on lab scale [Ahmadi et al. 2021], but large-scale testing will be required before practical implementation.

A detailed economical analysis would be highly relevant for the implementation of any of these processes. The results presented here show that the dehydration cost will be lower than the reduced cost of CO₂ taxes, but the economical aspect must also include the other costs related to CCS, such as the amine scrubbing, transport and the storage process. Comparing the cost of transportation by ship and by pipeline would also affect the actual need for a dehydration process.

Bibliography

- (2023). URL: https://personalpages.manchester.ac.uk/staff/tom.rodgers/Interactive_graphs/CEPCI.html?reactors%5C%2FCEPCI%5C%2Findex.html.
- Ahmadi, Mahdi et al. (2021). ‘Subsea natural gas dehydration in a membrane contactor with turbulence promoter: An experimental and modeling study’. In: *Chemical Engineering Journal* 404, p. 126535. ISSN: 1385-8947. DOI: 10.1016/j.cej.2020.126535. URL: <https://www.sciencedirect.com/science/article/pii/S1385894720326632>.
- Aizarani, Jessica (20223). *EU: Industrial Natural Gas Prices 2021*. URL: <https://www.statista.com/statistics/1047070/natural-gas-price-european-union/#:~:text=In%5C%202021%5C%2C%5C%20the%5C%20natural%5C%20gas,euro%5C%20cents%5C%20per%5C%20kilowatt%5C%20hour..>
- Alerts, Intratec (2023). *Triethylene glycol price*. URL: <https://www.intratec.us/chemical-markets/triethylene-glycol-price>.
- Andreassen, A. (2022). ‘Prosjektoppgave: Process concepts for dehydration of captured CO₂’. In: Ashour, Ibrahim et al. (2011). ‘Applications of equations of state in the oil and gas industry’. In: *Thermodynamics-Kinetics of Dynamic Systems* 1, pp. 165–178.
- Basile, Angelo and Kamran Ghasemzadeh (2019). *Current Trends and Future Developments on (bio-) Membranes: Microporous Membranes and Membrane Reactors*. Elsevier.
- Bloch, Heinz P and Claire Soares (2001). *Turboexpanders and process applications*. Gulf professional publishing.
- BTS.Engineering (n.d.). *Molecular Sieve 3A, 2,0-3,5mm BTS Engineering*. URL: https://bts.net.ua/eng/molekularnoe_sito_3a_4a_5a_13x1/molekularnoe_sito_3a1/molekulyarne_sito_3a-2-0-3-5mm-molecular-sieve-upakovka-15kg/.
- Cordray, Dennis R. et al. (1996). ‘Solid - liquid phase diagram for ethylene glycol + water’. In: *Fluid Phase Equilibria* 117.1. Proceedings of the Seventh International Conference on Fluid Properties and Phase Equilibria for Chemical Process Design, pp. 146–152. ISSN: 0378-3812. DOI: [https://doi.org/10.1016/0378-3812\(95\)02947-8](https://doi.org/10.1016/0378-3812(95)02947-8). URL: <https://www.sciencedirect.com/science/article/pii/0378381295029478>.
- Dabrowski, A (2001). ‘Adsorption—from theory to practice’. In: *Advances in colloid and interface science* 93.1-3, pp. 135–224.
- Equinor (May 2019). ‘Northern Lights Project Concept report’. In: RE-PM673-00001.
- Farag, Hassan A.A. et al. (2011). ‘Natural gas dehydration by desiccant materials’. In: *Alexandria Engineering Journal* 50.4, pp. 431–439. ISSN: 1110-0168. DOI: <https://doi.org/10.1016/j.aej.2011.01.020>. URL: <https://www.sciencedirect.com/science/article/pii/S1110016811000457>.
- Forse, Alexander C and Phillip J Milner (2021). ‘New chemistry for enhanced carbon capture: beyond ammonium carbamates’. In: *Chemical Science* 12.2, pp. 508–516.
- François, Maxime (2020). ‘Stability of dehydration glycols MEG and TEG’. MA thesis. NTNU.
- Fytianos, Georgios et al. (2016). ‘Corrosion Evaluation of MEA Solutions by SEM-EDS, ICP-MS and XRD’. In: *Energy Procedia* 86, pp. 197–204.
- Giakoumis, Zoitis et al. (2020). ‘Computational Investigation of a Multiphase Turbo Expander for Heat Pumps and Refrigeration Cycles’. In: *Turbo Expo: Power for Land, Sea, and Air*. Vol. 84140. American Society of Mechanical Engineers, V005T06A030.
- Ikhtlaq, M (1992). ‘Glycol dehydration of natural gas’. In: *Chemical Engineer (London);(United Kingdom)* 521.
- Jones, Matthew W et al. (2023). ‘National contributions to climate change due to historical emissions of carbon dioxide, methane, and nitrous oxide since 1850’. In: *Scientific Data* 10.1, p. 155.

-
- Kolmetz, K and RM Sari (2014). 'Kolmetz Handbook of Process Equipment Design'. In: *Malaysia: KLM Technology Group. Crude unit desalter system. Section Three–Refinery systems*, pp. 1–34.
- Kvinge, Bjørnar Andreas et al. (n.d.). 'Kostnader ved karbonfangst og-lagring i Norge'. In: ().
- Li, Wenyao et al. (2021). 'The role of hydrogen in the corrosion and cracking of steels-a review'. In: *Corrosion Communications* 4, pp. 23–32.
- Lin, Ronghong et al. (2014). 'Kinetics of water vapor adsorption on single-layer molecular sieve 3A: experiments and modeling'. In: *Industrial & Engineering Chemistry Research* 53.41, pp. 16015–16024.
- Makwashi, Nura et al. (2018). 'Pipeline gas hydrate formation and treatment: a review'. In: *3rd national engineering conference on building the gap between academia and industry, Faculty of Engineering, Bayero University, Kano*, pp. 2450–2454.
- Mike (June 2023). *Ethylene glycol price index*. URL: <https://businessanalytiq.com/procurementanalytics/index/ethylene-glycol-price-index/>.
- Mokhatab, Saeid, William A Poe and John Y Mak (2018). *Handbook of natural gas transmission and processing: principles and practices*. Gulf professional publishing.
- Munkejord, Svend Tollak, Morten Hammer and Sigurd W Løvseth (2016). 'CO2 transport: Data and models–A review'. In: *Applied Energy* 169, pp. 499–523.
- Nivargi, JP et al. (2005). 'TEG contactor for gas dehydration'. In: *Chemical engineering world* 40.9, p. 77.
- Okoli, Kenneth Ikechukwu (2017). 'Comparison of CO2 dehydration processes after CO2 capture'. MA thesis. Hogskolen i Sorost-Norge.
- Olivier, J, G Janssens-Maenhout and J Peters (2013). *Trends in global CO2 emissions : 2012 report*. Publications Office. DOI: doi/10.2788/33777.
- Patchigolla, Kumar and John E Oakey (2013). 'Design overview of high pressure dense phase CO2 pipeline transport in flow mode'. In: *Energy Procedia* 37, pp. 3123–3130.
- Pearson, Andy (2008). 'Refrigeration with ammonia'. In: *International journal of refrigeration* 31.4, pp. 545–551.
- Protocol, Montreal et al. (1987). 'Montreal protocol on substances that deplete the ozone layer'. In: *Washington, DC: US Government Printing Office* 26, pp. 128–136.
- R. Sinnott, G.Towler (2020). *Chemical Engineering Design*. 6th. Elsevier. ISBN: 978-0-08-102599-4. DOI: <https://doi.org/10.1016/B978-0-08-102599-4.00009-6>.
- Rathish, R Joseph et al. (2013). 'Corrosion resistance of nanoparticle-incorporated nano coatings'. In: *European Chemical Bulletin* 2.12, pp. 965–970.
- Roberts, Thomas and Sarah Mander (2011). 'Assessing public perceptions of CCS: Benefits, challenges and methods'. In: *Energy Procedia* 4. 10th International Conference on Greenhouse Gas Control Technologies, pp. 6307–6314. ISSN: 1876-6102. DOI: 10.1016/j.egypro.2011.02.646. URL: <https://www.sciencedirect.com/science/article/pii/S1876610211009258>.
- Sanchez, A Perez, EJ Perez Sanchez and R Segura Silva (2016). 'Design of a packed-bed absorption column considering four packing types and applying matlab'. In: *Nexo Revista Cientifica* 29.2, pp. 83–104.
- Secker, H. and E. Bergene (2011). 'Drying of CO2 in Process Applications using Molecular Sieves'. In: *Gas Processors Association - Europe*.
- Simpson, David A. (2017). 'Chapter Eight - Gas Compression'. In: *Practical Onshore Gas Field Engineering*. Ed. by David A. Simpson. Gulf Professional Publishing, pp. 513–571. ISBN: 978-0-12-813022-3. DOI: <https://doi.org/10.1016/B978-0-12-813022-3.00008-0>. URL: <https://www.sciencedirect.com/science/article/pii/B9780128130223000080>.
-

-
- SPI-Chem Molecular Sieve Type 3A* (n.d.). URL: <https://www.2spi.com/item/z02018/>.
- SSB (n.d.). URL: <https://www.ssb.no/energi-og-industri/energi/statistikk/elektrisitetspriser/artikler/rekordhoy-strompris-i-2022--dempet-av-stromstotte>.
- Swain, RL BIBB (2003). ‘Development and operation of the molecular sieve: an industry standard’. In: *The alcohol textbook*, pp. 337–341.
- Usman, Muhammad, Magne Hillestad and Liyuan Deng (2018). ‘Assessment of a membrane contactor process for pre-combustion CO₂ capture by modelling and integrated process simulation’. In: *International Journal of Greenhouse Gas Control* 71, pp. 95–103.
- Utslipp til luft* (Dec. 2022). URL: <https://www.norskpetroleum.no/miljo-og-teknologi/utslipp-til-luft/>.
- Witkowski, Andrzej, Mirosław Majkut and Sebastian Rulik (Mar. 2014). ‘Analysis of pipeline transportation systems for carbon dioxide sequestration’. In: *Archives of Thermodynamics* 35, s. 117–140. DOI: 10.2478/aoter-2014-0008.
- Zhang, Heng et al. (2021). ‘Study on the performance of CO₂ capture from flue gas with ceramic membrane contactor’. In: *Separation and Purification Technology* 265, p. 118521.
- Zhang, Xiaoxue, Saara Heinonen and Erkki Levänen (2014). ‘Applications of supercritical carbon dioxide in materials processing and synthesis’. In: *Rsc Advances* 4.105, pp. 61137–61152.
- Zhu, Xiang Y, John Lubeck and John J Kilbane (2003). ‘Characterization of microbial communities in gas industry pipelines’. In: *Applied and Environmental Microbiology* 69.9, pp. 5354–5363.

Appendix

A Cost and utilities

In this appendix, equipment and utility costs are sorted by categories and presented for each process.

Equipment	Cost [USD]	
Flash tanks	11876966	
Heat Exchangers	1859283	
Molecular sieve	179444	
Compressors/Pumps	3569361	
Total	17485055	

Utilities	Cost [USD/year]	
Electricity [kW]	18316kW	7679357
Hot Utility [kW]	1010kW	306065
Cooling Water [m^3/h]	3467m ³ /h	38865
Total	8024287	

Table 19: Equipment and utility cost for case A, molecular sieve dehydration for liquid transport.

Equipment	Cost [USD]	
Flash tanks	11876966	
Heat Exchangers	1509139	
Molecular sieve	179444	
Compressors/Pumps	2984270	
Total	16549820	

Utilities	Cost [USD/year]	
Electricity [kW]	17443	7313334
Hot utility [kW]	1068	323641
Cooling Water [m^3/h]	2921.9	32754
Total	7669729	

Table 20: Equipment and utility cost for case A, molecular sieve dehydration for dense phase transport.

Equipment	Cost [USD]	
Flash tanks	11876966	
Heat Exchangers	1462653	
Molecular sieve	179444	
Compressors/Pumps	3002414	
Total	16521478	
Utilities	Cost [USD/year]	
Electricity [kW]	16889	7081058
Hot utility [kW]	1068	323641
Cooling Water [m^3/h]	2639.1	29584
Total		7434283

Table 21: Equipment and utility cost for case A, molecular sieve dehydration for supercritical state transport.

Equipment	Cost [USD]	
Flash tanks	9808909	
Heat Exchangers	1540464	
Abs./Dist. Columns	299086	
Compressors/Pumps	3601798	
Total	15250258	
Utilities	Cost [USD/year]	
Electricity [kW]	19769kW	8288557
Hot utility [kW]	941.9kW	285429
Cooling Water [m^3/h]	3334.7m ³ /h	37382
TEG [kg/h]	0.358kg/h	5436
Total		8616803

Table 22: Equipment and utility cost for case B1, TEG absorbtion with column, for liquid transport.

Equipment	Cost [USD]	
Flash tanks	9808909	
Heat Exchangers	1428168	
Abs./Dist. Columns	299086	
Compressors/Pumps	3886621	
Total	15422784	
Utilities	Cost [USD/year]	
Electricity [kW]	15426kW	6467665
Hot utility [kW]	1133.9kW	343611
Cooling Water [m^3/h]	2664.1m ³ /h	29864
TEG [kg/h]	0.358kg/h	5436
Total		6846577

Table 23: Equipment and utility cost for case B1, TEG absorbtion with column, for dense phase transport.

Equipment	Cost [USD]	
Flash tanks	9808909	
Heat Exchangers	1313893	
Abs./Dist. Columns	299086	
Compressors/Pumps	3889587	
Total	15311475	
Utilities	Cost [USD/year]	
Electricity [kW]	15454kW	6479405
Hot utility [kW]	941.9kW	285429
Cooling Water [m^3/h]	2521.7m ³ /h	28268
TEG [kg/h]	0.358kg/h	5436
Total		6798537

Table 24: Equipment and utility cost for case B1, TEG absorbtion with column, for supercritical state transport.

Equipment	Cost [USD]	
Flash tanks	9801727	
Heat Exchangers	1579240	
Abs./Dist. Columns	24251	
Compressors/Pumps	3759471	
Membrane Contactor	473774	
Total	15164689	
Utilities	Cost [USD/year]	
Electricity [kW]	17307kW	7256313
Hot utility [kW]	892kW	270307
Cooling Water [m^3/h]	3453m ³ /h	38708
TEG [kg/h]	3.36kg/h	51017
Total		7616345

Table 25: Equipment and utility cost for case B2, TEG absorbtion with membrane contactor, for liquid transport.

Equipment	Cost [USD]	
Flash tanks	9801727	
Heat Exchangers	1466776	
Abs./Dist. Columns	24251	
Compressors/Pumps	3865380	
Membrane Contactor	473774	
Total	15158134	
Utilities	Cost [USD/year]	
Electricity [kW]	15451kW	6478147
Hot utility [kW]	892kW	270307
Cooling Water [m^3/h]	2830m ³ /h	31724
TEG [kg/h]	3.36kg/h	51017
Total		6831196

Table 26: Equipment and utility cost for case B2, TEG absorbtion with membrane contactor, for dense phase transport.

Equipment	Cost [USD]	
Flash tanks	9801727	
Heat Exchangers	1338528	
Abs./Dist. Columns	24251	
Compressors/Pumps	3868687	
Membrane Contactor	473774	
Total	15033192	
Utilities	Cost [USD/year]	
Electricity [kW]	15482kW	6491144
Hot utility [kW]	892kW	270307
Cooling Water [m^3/h]	2595m ³ /h	29090
TEG [kg/h]	3.36kg/h	51017
Total		6841559

Table 27: Equipment and utility cost for case B2, TEG absorption with membrane contactor, for supercritical state transport.

Equipment	Cost [USD]	
Flash tanks	14384128	
Heat Exchangers	2076786	
Abs./Dist. Columns	7949	
Compressors/Pumps	4531127	
Total	20999991	
Utilities	Cost [USD/year]	
Electricity [kW]	23057	9667117.6
Hot utility [kW]	113	34243.0
Cooling Water [m^3/h]	604	6770.8
MEG [kg/h]	4.7	36834.5
Total		9744966

Table 28: Equipment and utility cost for case C1, pressure-temperature swing for liquid transport.

Equipment	Cost [USD]	
Flash tanks	12110955	
Heat Exchangers	1275984	
Abs./Dist. Columns	7949	
Compressors/Pumps	3886338	
Total	17281227	
Utilities	Cost [USD/year]	
Electricity [kW]	23057kW	9667118
Hot utility	123kW	37273
Cooling Water [m^3/h]	3098.3m ³ /h	34732
MEG [kg/h]	3.4kg/h	26646
Total		9765769

Table 29: Equipment and utility cost for case C1, pressure-temperature swing for dense phase transport.

Equipment	Cost [USD]	
Flash tanks	12110955	
Heat Exchangers	1158233	
Abs./Dist. Columns	7949	
Compressors/Pumps	3886338	
Total	17163477	
Utilities	Cost [USD/year]	
Electricity [kW]	18323kW	7682292
Hot utility	123kW	37273
Cooling Water [m^3/h]	2863.3m ³ /h	32097
MEG [kg/h]	3.4kg/h	26646
Total		7778308

Table 30: Equipment and utility cost for case C1, pressure-temperature swing with joule thomson valve, for supercritical state transport.

Equipment	Cost [USD]	
Flash tanks	13197395	
Heat Exchangers	2220501	
Abs./Dist. Columns	7922	
Compressors/Pumps	5486214	
Total	20912033	
Utilities	Cost [USD/year]	
Electricity [kW]	21508kW	9017668
Hot utility [kW]	114kW	34546
Cooling Water [m^3/h]	3658m ³ /h	41006
MEG [kg/h]	4.4kg/h	34483
Total		9127703

Table 31: Equipment and utility cost for case C2, pressure-temperature swing with turbo-expander, for liquid transport.

Equipment	Cost [USD]	
Flash tanks	16250839	
Heat Exchangers	1574215	
Abs./Dist. Columns	7922	
Compressors/Pumps	5228709	
Total	23061686	
Utilities	Cost [USD/year]	
Electricity [kW]	20217kW	8476390
Hot utility [kW]	114kW	34546
Cooling Water [m^3/h]	3282.1m ³ /h	36792
MEG [kg/h]	4.4kg/h	34483
Total		8582211

Table 32: Equipment and utility cost for case C2, pressure-temperature swing with turbo-expander, for dense phase transport.

Equipment	Cost [USD]	
Flash tanks	15757150	
Heat Exchangers	1481231	
Abs./Dist. Columns	7922	
Compressors/Pumps	5226934	
Total	22473237	

Utilities		Cost [USD/year]
Electricity [kW]	20048kW	8405533
Hot utility [kW]	114kW	34546
Cooling Water [m^3/h]	3044.1m ³ /h	34124
MEG [kg/h]	4.4kg/h	34483
Total		8508686

Table 33: Equipment and utility cost for case C2, pressure-temperature swing with turbo-expander, for supercritical state transport.

Table 34: Parameters used for cost estimates for knock-out drums for Case A, molecular sieve adsorption.

Case A	Name	Stream in	D[m]	h[m]	P[bar]	S	t_w[mm]	Shell mass [kg]	Cost [USD]
Liquid	CT-V1	CT_2.2	8.8392	30.9372	4.6	20	17	116837	1381733
Liquid	CT-V2	CT_4.2	11.43	40	13.7	20	63	723927	6506533
Liquid	CT-V3	CT_6.2	3.505	12.27	15.9	20	23	24861	371925
Dense phase	CT-V1	CT_2.2	8.8392	30.9372		4.6	20	116837	1381733
Dense phase	CT-V2	CT_4.2	11.43	40		13.7	20	723927	6506533
Dense phase	CT-V3	CT_6.2	3.505	12.27		15.9	20	24861	371925
Supercritical	CT-V1	CT_2.2	8.8392	30.9372	4.6	20	17	116837	1381733
Supercritical	CT-V2	CT_4.2	11.43	40	13.7	20	63	723927	6506533
Supercritical	CT-V3	CT_6.2	3.505	12.27	15.9	20	23	24861	371925

Table 35: Parameters used for cost estimates for knock-out drums for Case B1, TEG absorption with absorption column.

B1	Name	Stream in	D[m]	h[m]	P[bar]	S	t_w[mm]	shell mass[kg]	Cost[uscd]
Liquid	CT_V1	CT_2.2	7.62	26.67	4.65	20	15	76616	965730
Liquid	CT_V2	CT_4.2	10.67	37.34	13.9	20	60	600811	5553330
Liquid	CT_V3	CT_6.2	3.2	11.2	16.1	20	21	18917	295153
Liquid	R_V1	R_1.2	0.6096	3.353	5.3	20	2	103	4995
Liquid	R_V2	R_3.2	0.4572	2.515	130	20	1	29	2691
Dense Phase	CT_V1	CT_2.2	7.62	26.67	4.65	20	15	76616	965730
Dense Phase	CT_V2	CT_4.2	10.67	37.34	13.9	20	60	600811	5553330
Dense Phase	CT_V3	CT_6.2	3.2	11.2	16.1	20	21	18917	295153
Dense Phase	R_V1	R_1.2	0.6096	3.353	5.3	20	2	103	4995
Dense Phase	R_V2	R_3.2	0.4572	2.515	130	20	1	29	2691
Supercritical	CT_V1	CT_2.2	7.62	26.67	4.65	20	15	76616	965730
Supercritical	CT_V2	CT_4.2	10.67	37.34	13.9	20	60	600811	5553330
Supercritical	CT_V3	CT_6.2	3.2	11.2	16.1	20	21	18917	295153
Supercritical	R_V1	R_1.2	0.6096	3.353	5.3	20	2	103	4995
Supercritical	R_V2	R_3.2	0.4572	2.515	1.3	20	1	29	2691

Table 36: Parameters used for cost estimates for knock-out drums for Case B2, TEG absorption with membrane contactor.

B1	Name	Stream in	D[m]	h[m]	P[bar]	S	t_w[mm]	shell mass[kg]	Cost[uscd]
B1	Name	Stream in	D[m]	h[m]	P[bar]	S	t_w[mm]	shell mass[kg]	Cost[uscd]
Liquid	CT_V1	CT_2.2	7.62	26.67	4.65	20	15	76616	965730
Liquid	CT_V2	CT_4.2	10.67	37.34	13.9	20	60	600811	5553330
Liquid	CT_V3	CT_6.2	3.2	11.2	16.1	20	21	18917	295153
Liquid	R_V1	R_2.2	0.4572	2.515	1.3	20	1	29	2691
Dense Phase	CT_V1	CT_2.2	7.62	26.67	4.65	20	15	76616	965730
Dense Phase	CT_V2	CT_4.2	10.67	37.34	13.9	20	60	600811	5553330
Dense Phase	CT_V3	CT_6.2	3.2	11.2	16.1	20	21	18917	295153
Dense Phase	R_V1	R_2.2	0.4572	2.515	1.3	20	1	29	2691
Supercritical	CT_V1	CT_2.2	7.62	26.67	4.65	20	15	76616	965730
Supercritical	CT_V2	CT_4.2	10.67	37.34	13.9	20	60	600811	5553330
Supercritical	CT_V3	CT_6.2	3.2	11.2	16.1	20	21	18917	295153
Supercritical	R_V1	R_2.2	0.4572	2.515	1.3	20	1	29	2691

Table 37: Parameters used for cost estimates for knock-out drums for Case C1, pressure-temperature swing with Joule-Thomson valve.

C1	Name	Stream in	D[m]	h[m]	P[bar]	S	t_w[mm]	shell mass[kg]	Cost[usd]
Liquid	CT_V1	CT_2.2	9.906	34.67	4.5	20	18	155372	1760136
Liquid	CT_V2	CT_4.2	12.04	42.14	13.3	20	65	828862	7299752
Liquid	CT_V3	CT_6.2	4.724	16.54	39.6	20	26	51059	684421
Liquid	DH_V1	DH_3	2.134	7.468	22	20	19	7611	136937
Liquid	R_V1	R_1.2	5.029	17.6	1.1	20	3	6674	122626
Dense Phase	CT_V1	CT_2.2	7.772	27.2	4.6	20	15	79697	998591
Dense Phase	CT_V2	CT_4.2	10.67	37.34	13.6	20	59	590798	5474584
Dense Phase	CT_V3	CT_6.2	4.267	14.94	40.6	20	71	113758	1350754
Dense Phase	DH_V1	DH_3	3.81	13.33	22	20	34	43400	596306
Dense Phase	R_V1	R_1.2	0.4572	2.515	1.1	20	1	29	2691
Supercritical	CT_V1	CT_2.2	7.772	27.2	4.6	20	15	79697	998591
Supercritical	CT_V2	CT_4.2	10.67	37.34	13.6	20	59	590798	5474584
Supercritical	CT_V3	CT_6.2	4.267	14.94	40.6	20	71	113758	1350754
Supercritical	DH_V1	DH_3	3.81	13.33	22	20	34	43400	596306
Supercritical	R_V1	R_1.2	0.4572	2.515	1.1	20	1	29	2691

Table 38: Parameters used for cost estimates for knock-out drums for Case C2, pressure-temperature swing with turbo-expander.

C2	Name	Stream in	D[m]	h[m]	P [bar]	S	t_w [mm]	shell mass [kg]	Cost [usd]
Liquid	CT_V1	CT_2.2	9.7536	34.1376	4.5	20	18	150633	1714436
Liquid	CT_V2	CT_4.2	11.89	41.61	13.3	20	64	795806	7051597
Liquid	CT_V3	CT_6.2	4.724	16.54	39.6	20	76	149248	171040
Liquid	DH_V1	DH_3	2.134	7.468	22	20	19	7611	136937
Dense phase	R_V1	R_1.2	4.572	16	1.1	20	3	5516	104513
Dense phase	CT_V1	CT_2.2	9.601	33.6	4.5	20	18	145941	1668977
Dense phase	CT_V2	CT_4.2	12.19	42.67	13.8	20	68	888962	7747182
Dense phase	CT_V3	CT_6.2	4.572	16	41.4	20	77	141568	1626410
Dense phase	DH_V1	DH_3	2.134	7.468	22	20	19	7611	136937
Dense phase	R_V1	R_1.2	5.029	17.6	1.1	20	3	6674	122626
Supercritical	CT_V1	CT_2.2	9.449	33.07	4.6	20	18	141365	1624430
Supercritical	CT_V2	CT_4.2	12.04	42.14	13.94	20	68	867117	7585092
Supercritical	CT_V3	CT_6.2	4.42	15.47	41.49	20	75	128891	1501870
Supercritical	DH_V1	DH_3	2.134	7.468	22	20	19	7611	136937
Supercritical	R_V1	R_1.2	4.724	16.54	1.1	20	3	5892	110452

B Composite curves and heat exchangers

This appendix will show the shifted composite curves related to the different processes in addition to the corresponding heat exchanger networks.

Case A Liquid

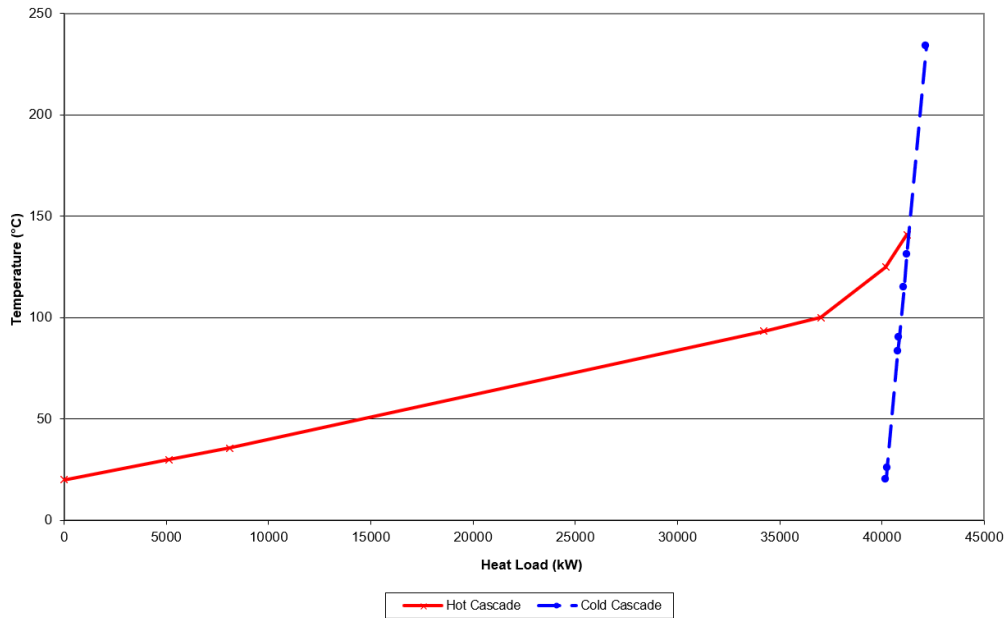


Figure 21: Shifted composite curve for Case Case A liquid phase transport, with $\Delta T = 10^\circ\text{C}$.

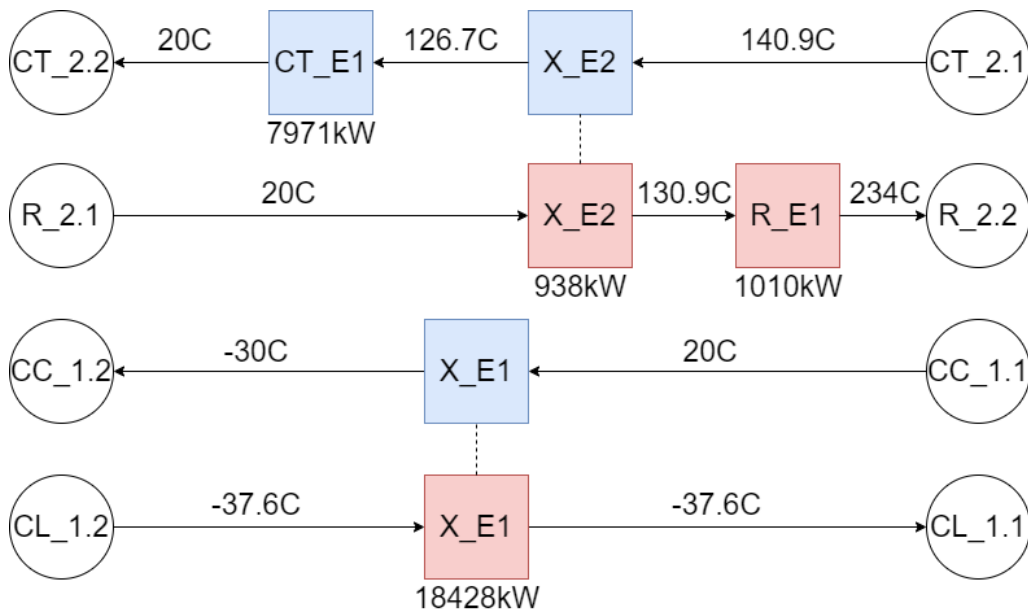


Figure 22: Heat integration network for case A, liquid phase transport.

Case A Dense phase

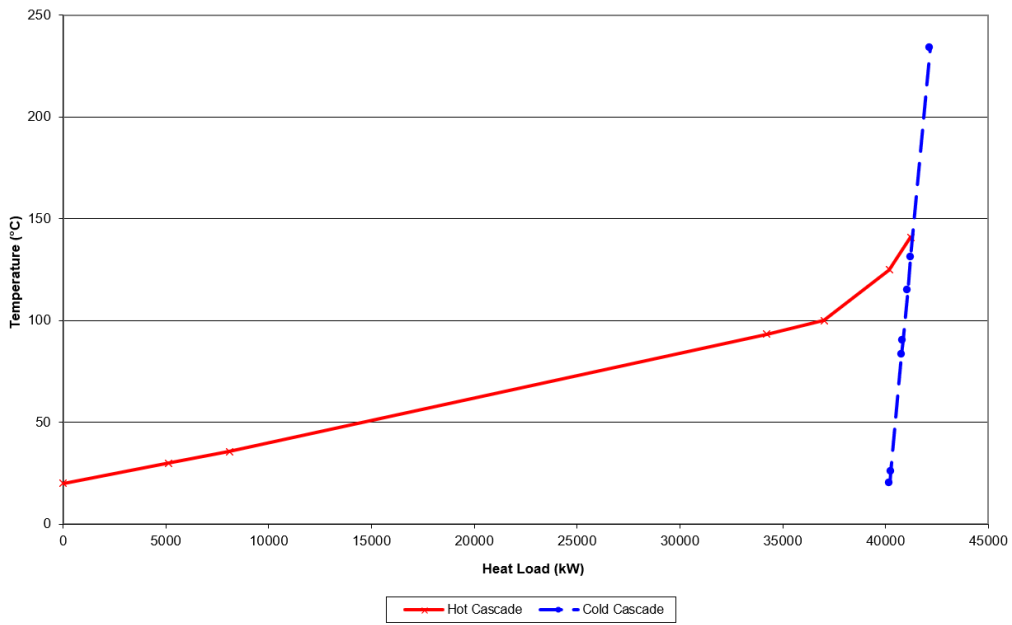


Figure 23: Shifted composite curve for Case A dense phase transport with $\Delta T = 10^\circ\text{C}$.

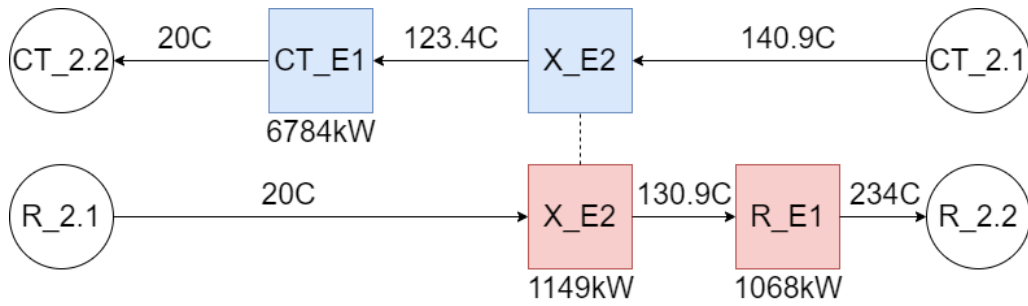


Figure 24: Heat integration network for case A, dense phase transport.

Case A supercritical

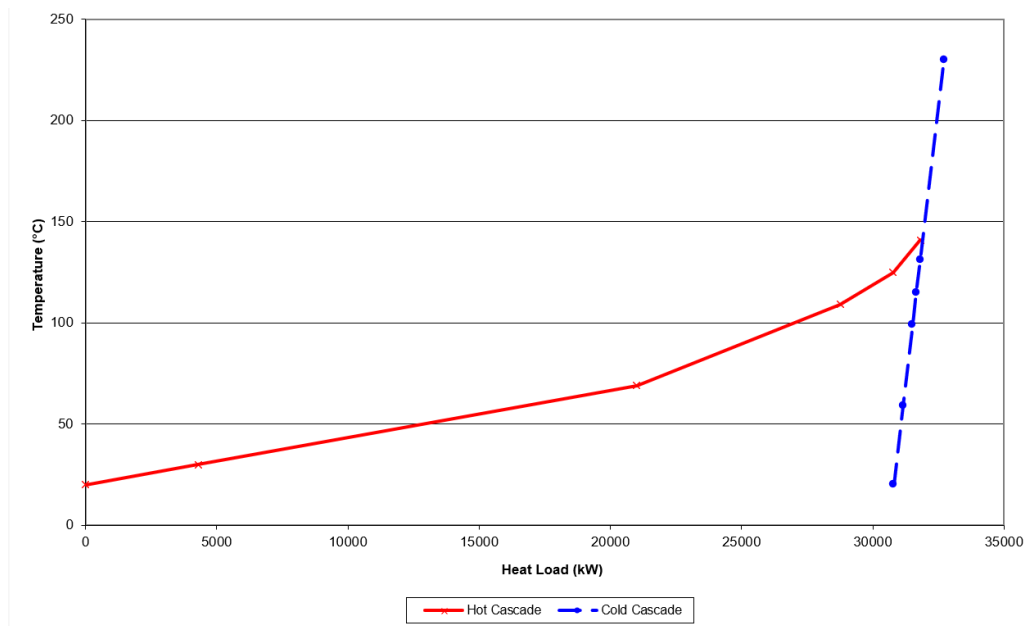


Figure 25: Shifted composite curve for Case A supercritical state transport with $\Delta T = 10^\circ\text{C}$.

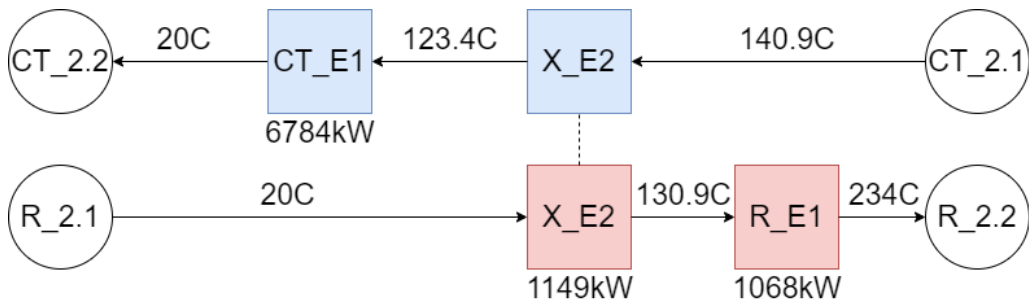


Figure 26: Heat integration network for case A, supercritical state transport.

Case B1 Liquid

Composite curves are:

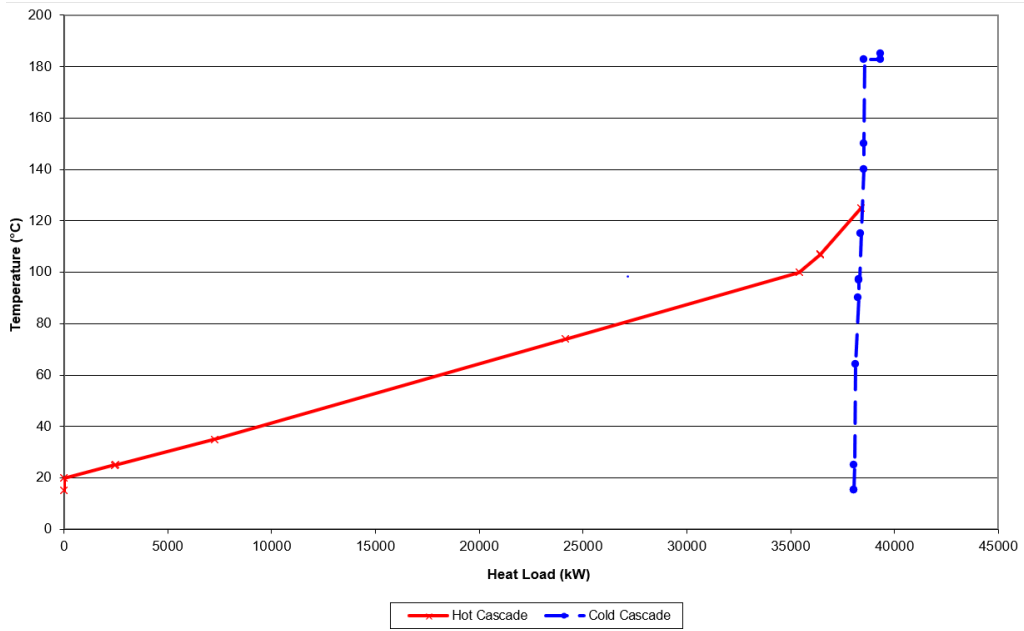


Figure 27: Shifted composite curve for Case B1 liquid phase transport, with $\Delta T = 10^\circ\text{C}$.

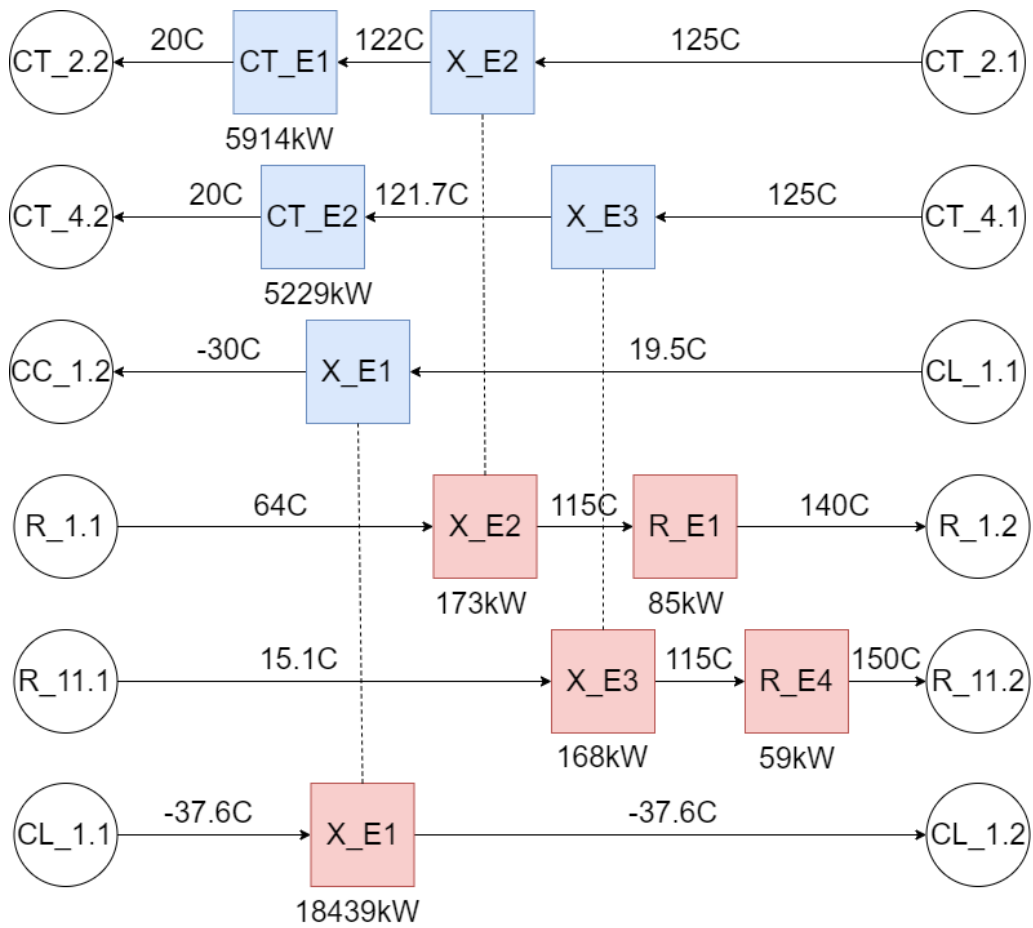


Figure 28: Heat integration network for case B1, liquid phase transport.

Case B1 Dense Phase

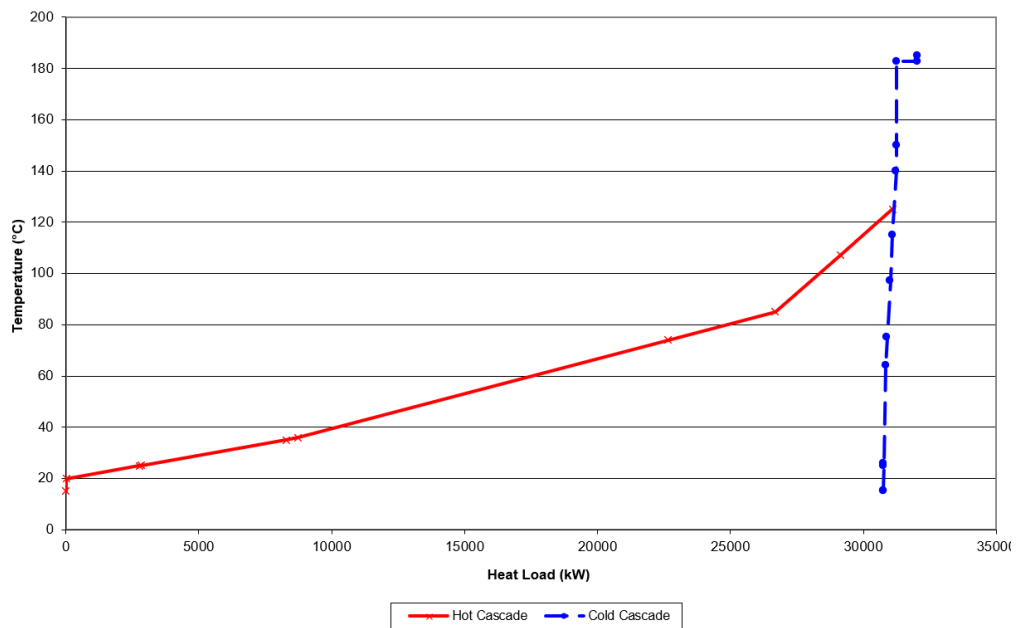


Figure 29: Shifted composite curve for Case B1 dense phase transport, with $\Delta T = 10^\circ\text{C}$.

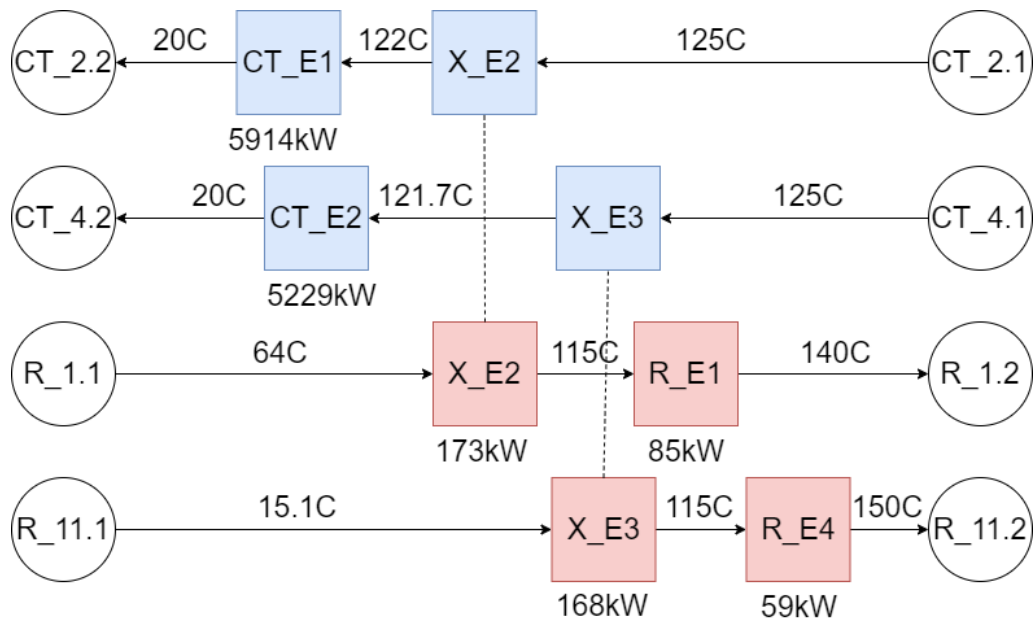


Figure 30: Heat integration network for case B1, dense phase transport.

Case B1 Critical

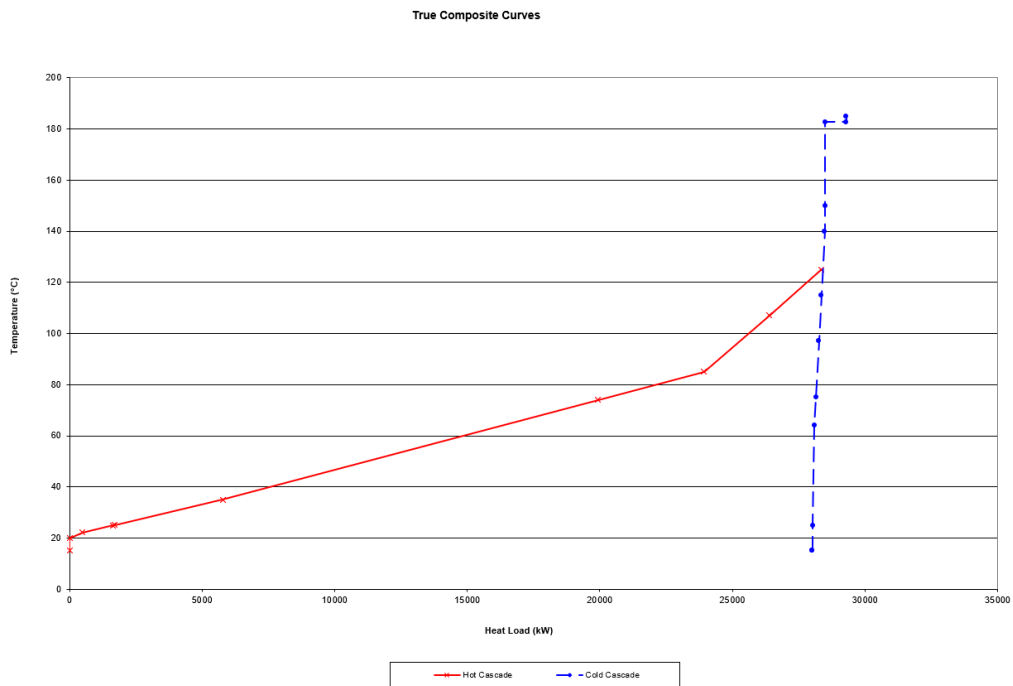


Figure 31: Shifted composite curve for Case B1 supercritical state transport with $\Delta T = 10^\circ\text{C}$.

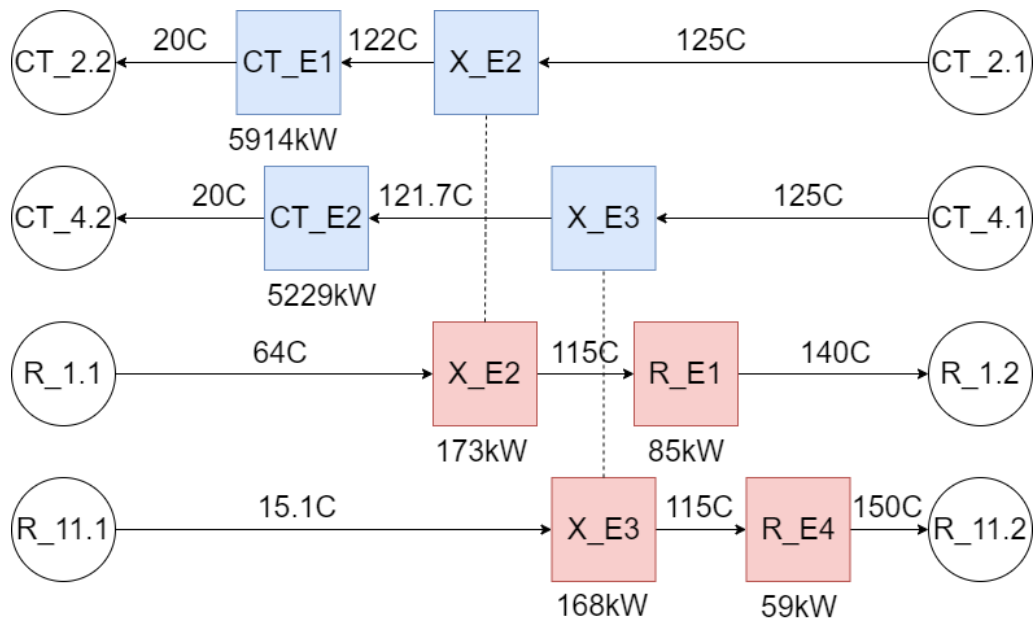


Figure 32: Heat integration network for case B2, supercritical state transport.

Case B2 Liquid

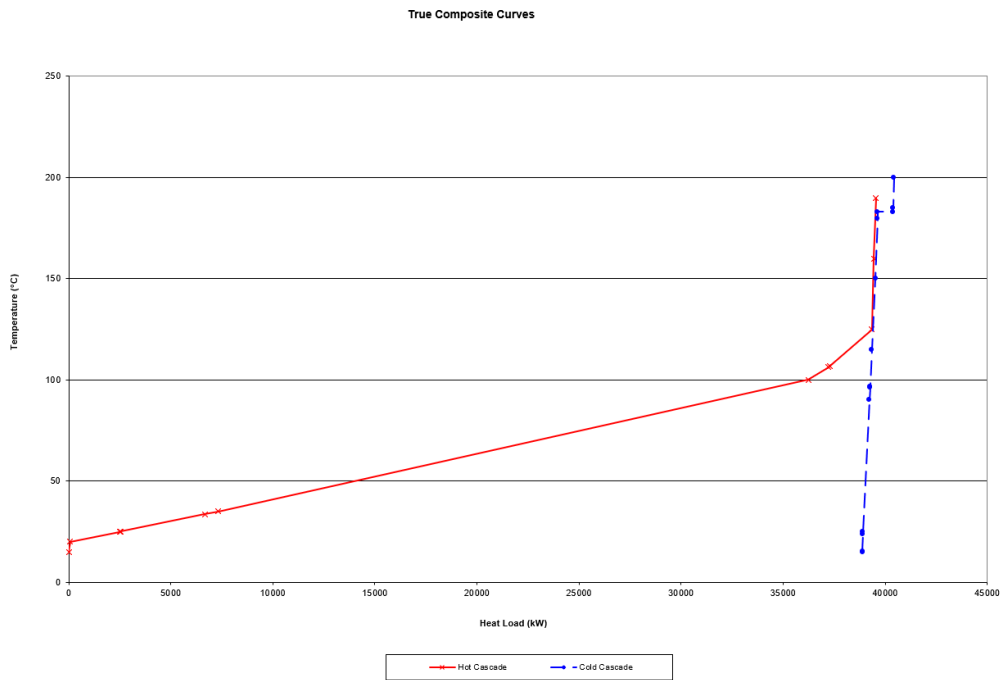


Figure 33: Shifted composite curve for Case B2 liquid phase transport, with $\Delta T = 10^\circ\text{C}$.

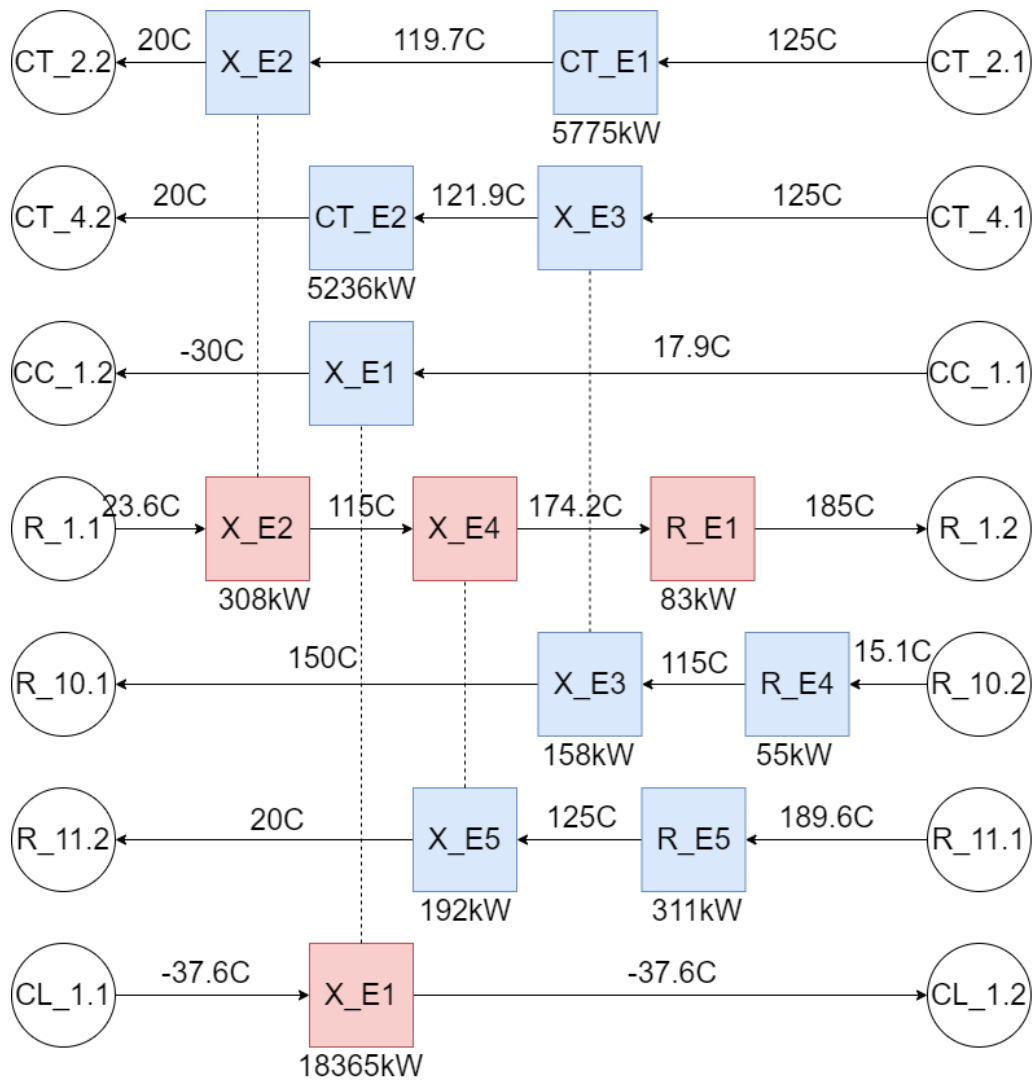


Figure 34: Heat integration network for case B2, liquid phase transport.

Case B2 Dense

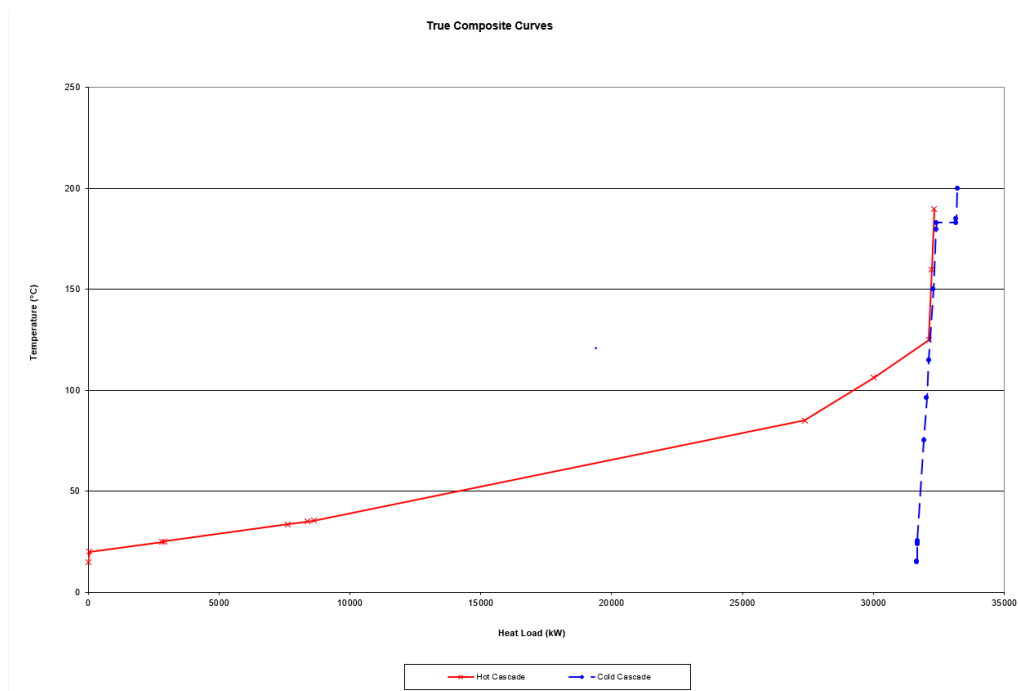


Figure 35: Shifted composite curve for Case B2 dense phase transport with $\Delta T = 10^\circ\text{C}$.

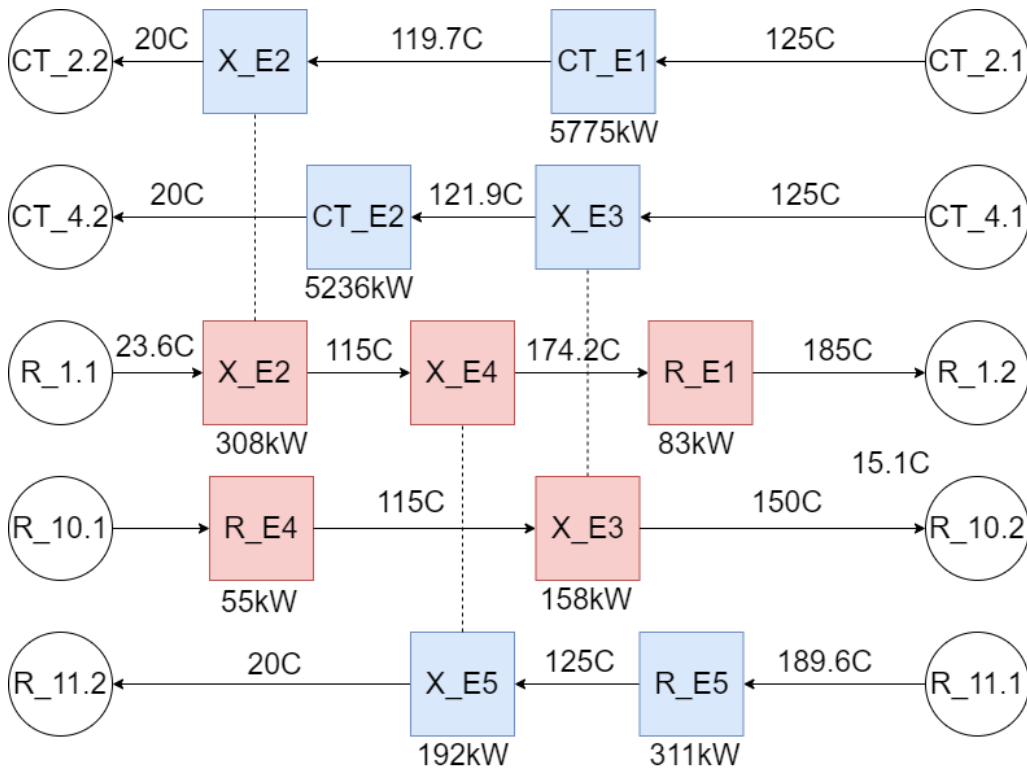


Figure 36: Heat integration network for case B2, dense phase transport.

Case B2 supercritical

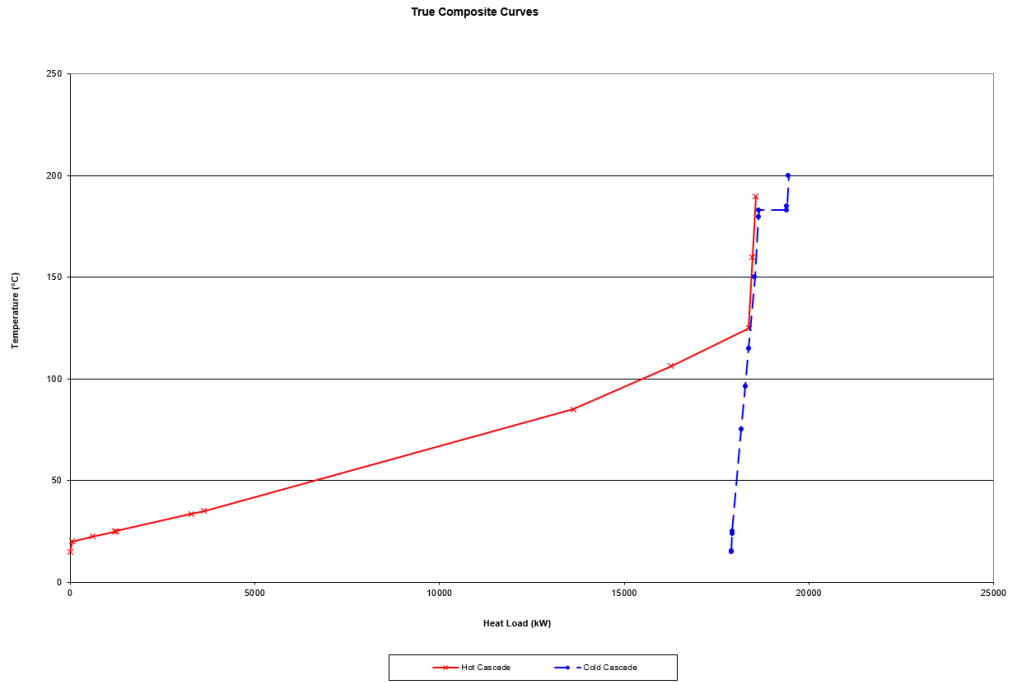


Figure 37: Shifted composite curve for Case B2 supercritical state transport with $\Delta T = 10^{\circ}\text{C}$.

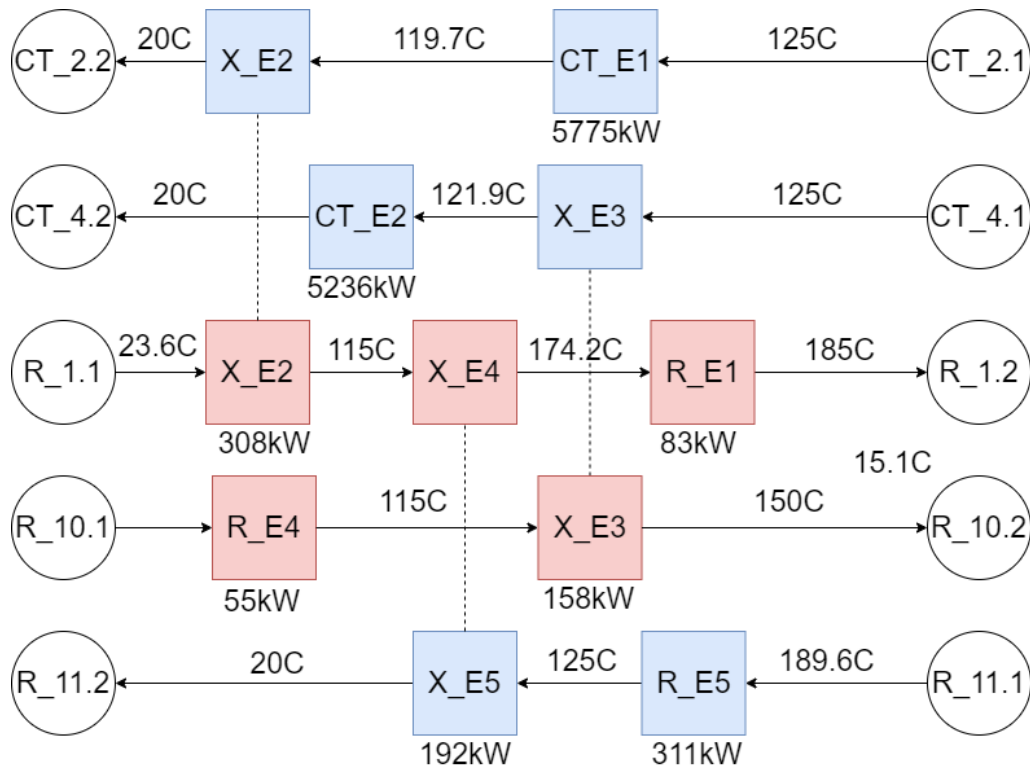


Figure 38: Heat integration network for case B2, supercritical state transport.

Case C1 ship

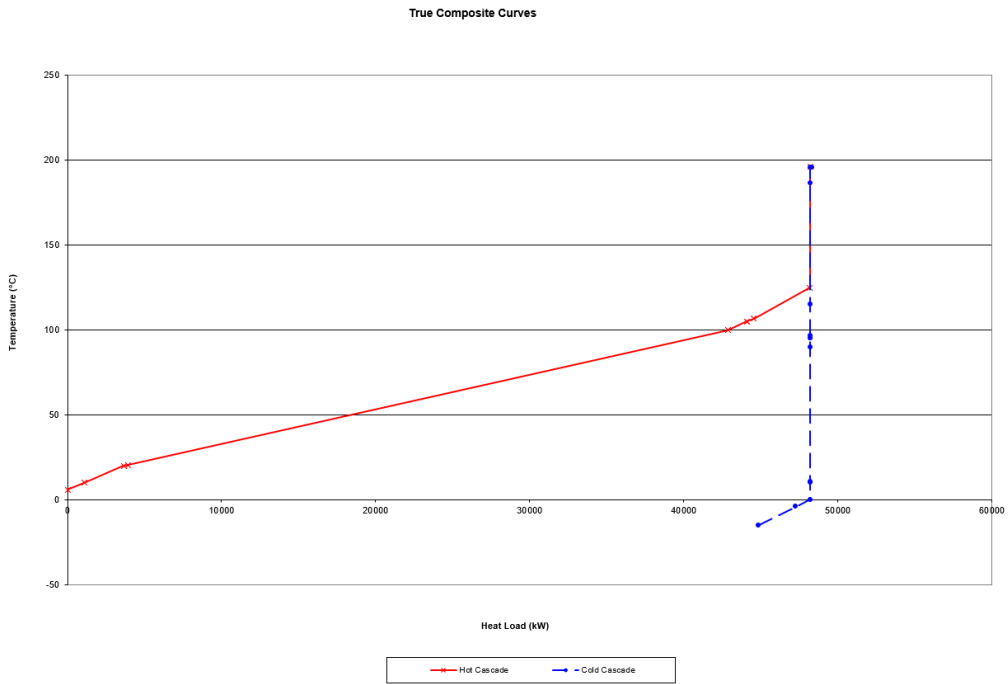


Figure 39: Shifted composite curve for Case C1 liquid phase transport, with $\Delta T = 10^\circ\text{C}$.

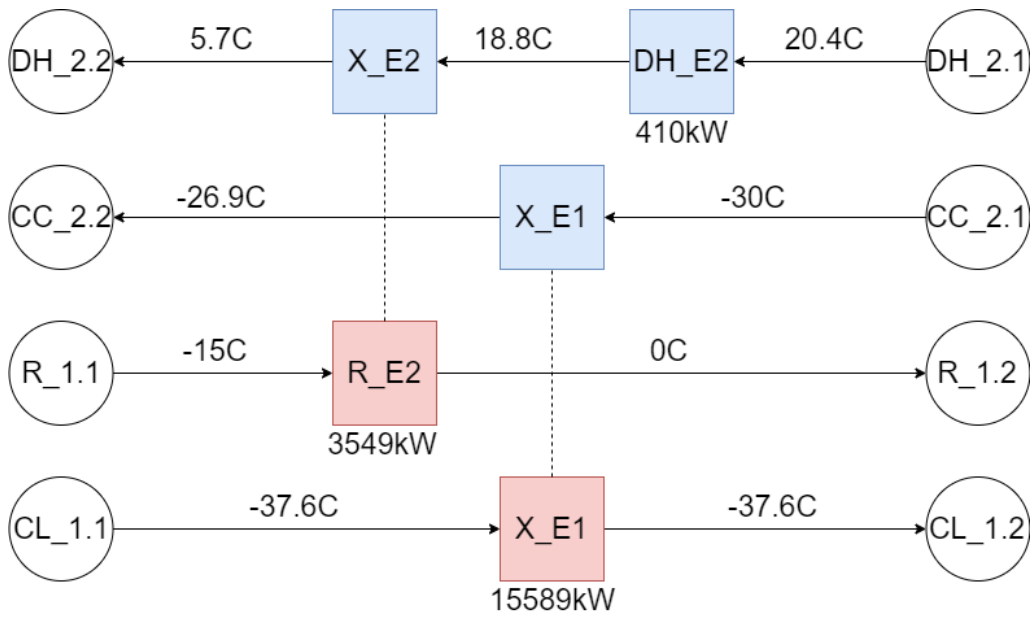


Figure 40: Heat integration network for case C1, liquid phase transport.

Case C1 Dense phase

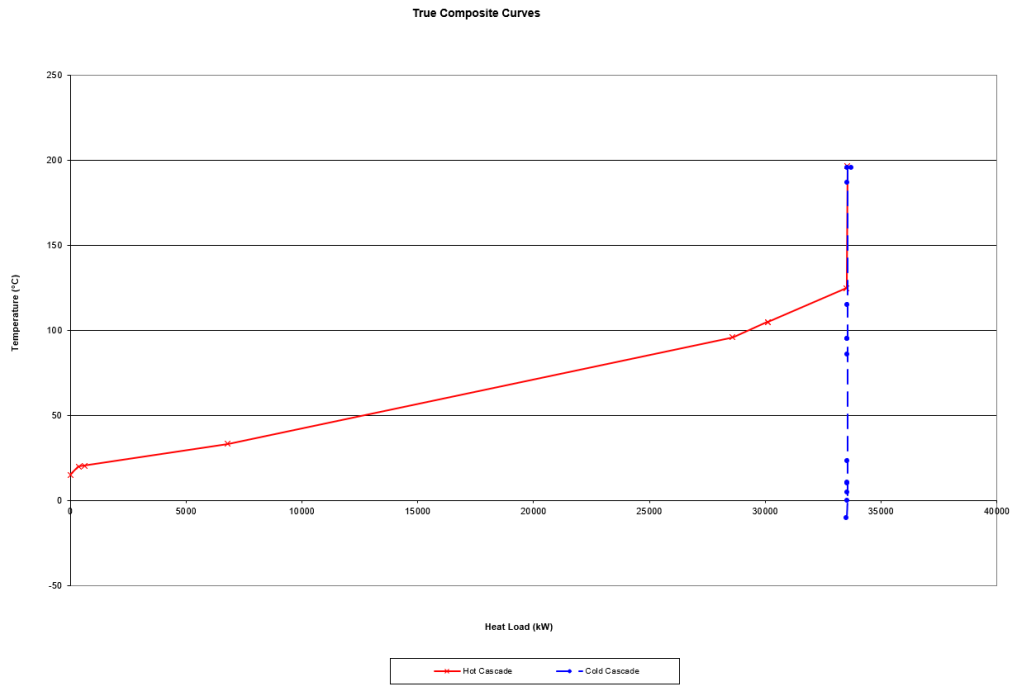


Figure 41: Heat integration network for case C1, dense phase transport.

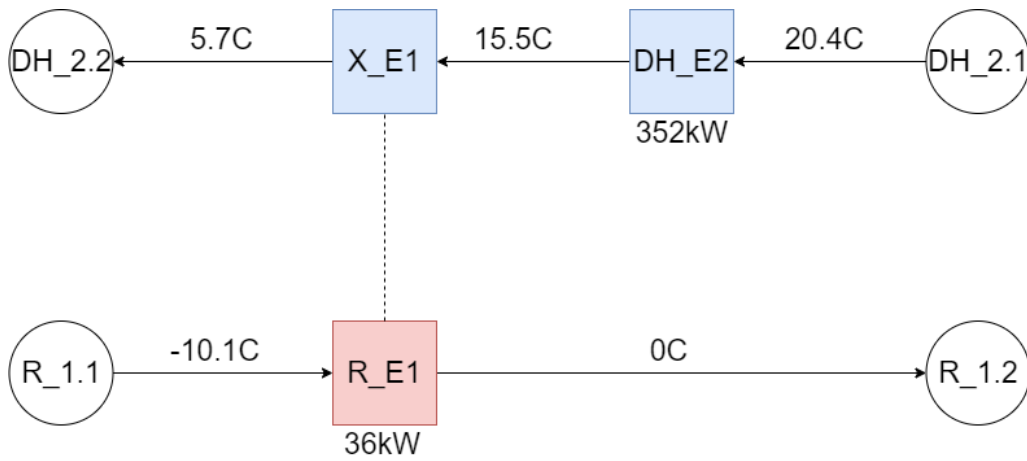


Figure 42: Heat integration network for case C1, dense phase transport.

Case C1 Critical

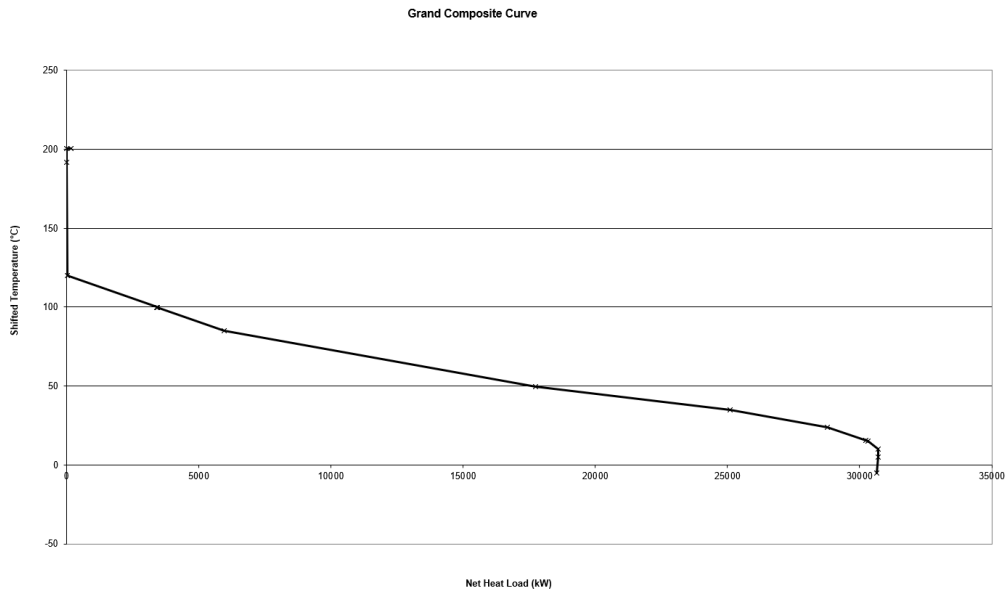


Figure 43: Shifted composite curve for Case B2 supercritical state transport with $\Delta T = 10^\circ\text{C}$.

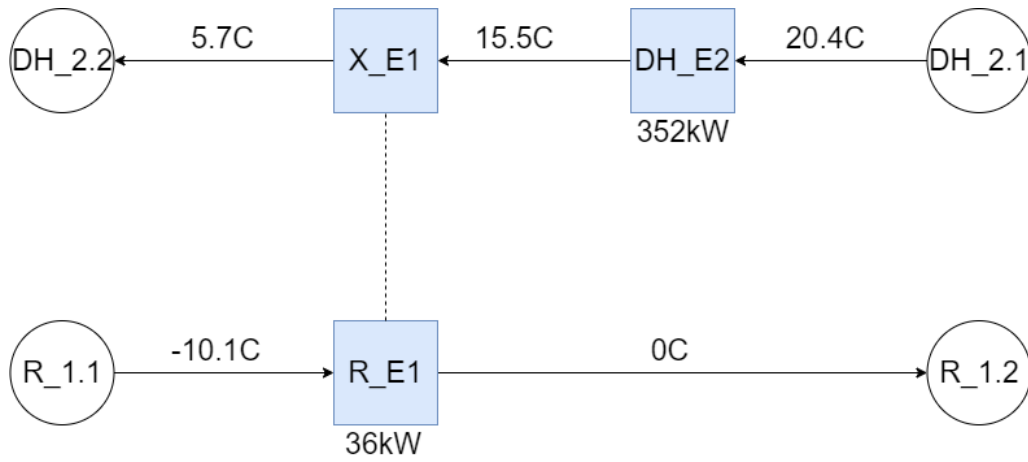


Figure 44: Heat integration network for case C1, supercritical state transport.

Case C2 Liquid

,

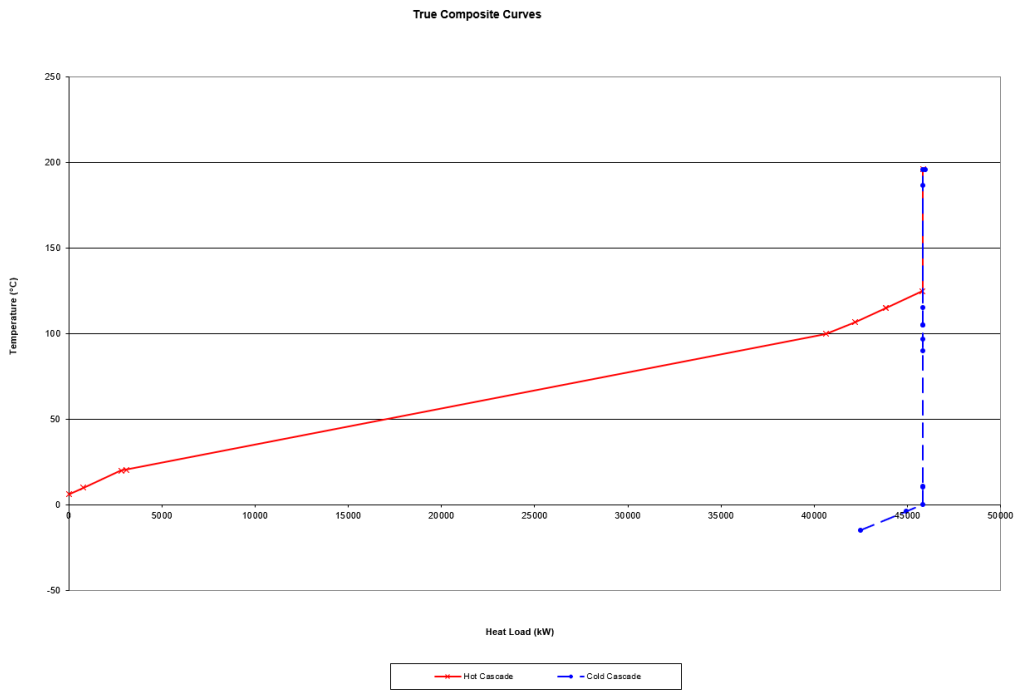


Figure 45: Shifted composite curve for Case C2 liquid phase transport, with $\Delta T = 10^\circ\text{C}$.

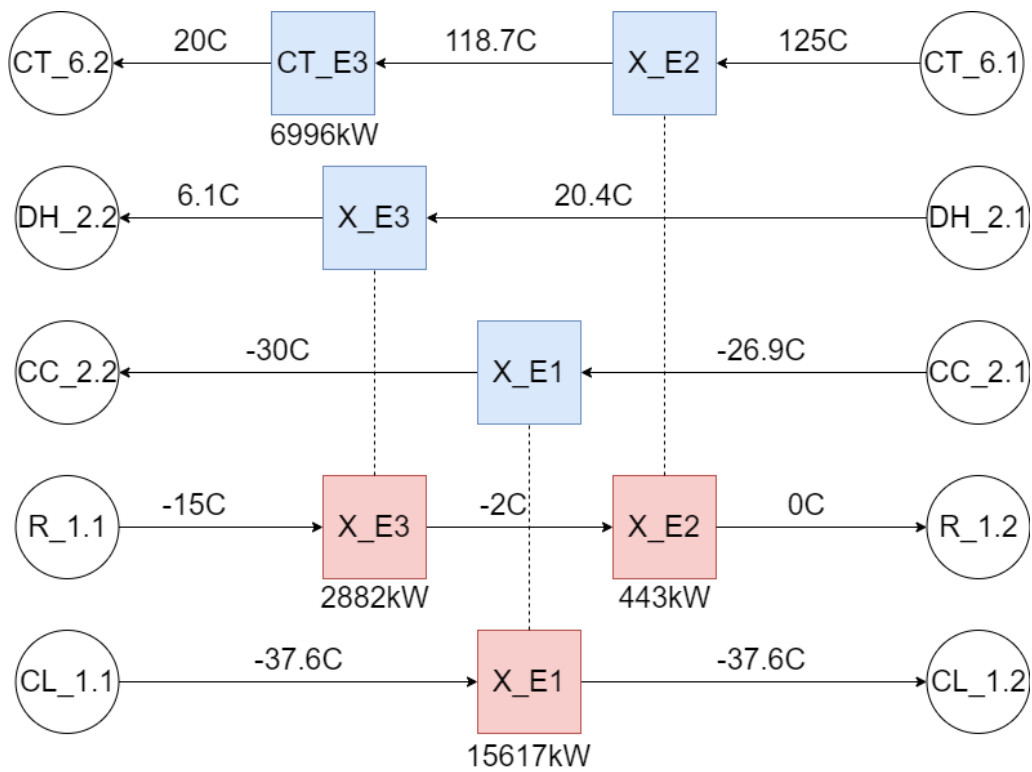


Figure 46: Heat integration network for case C2, liquid phase transport.

Case C2 Dense phase

Duties required:

,

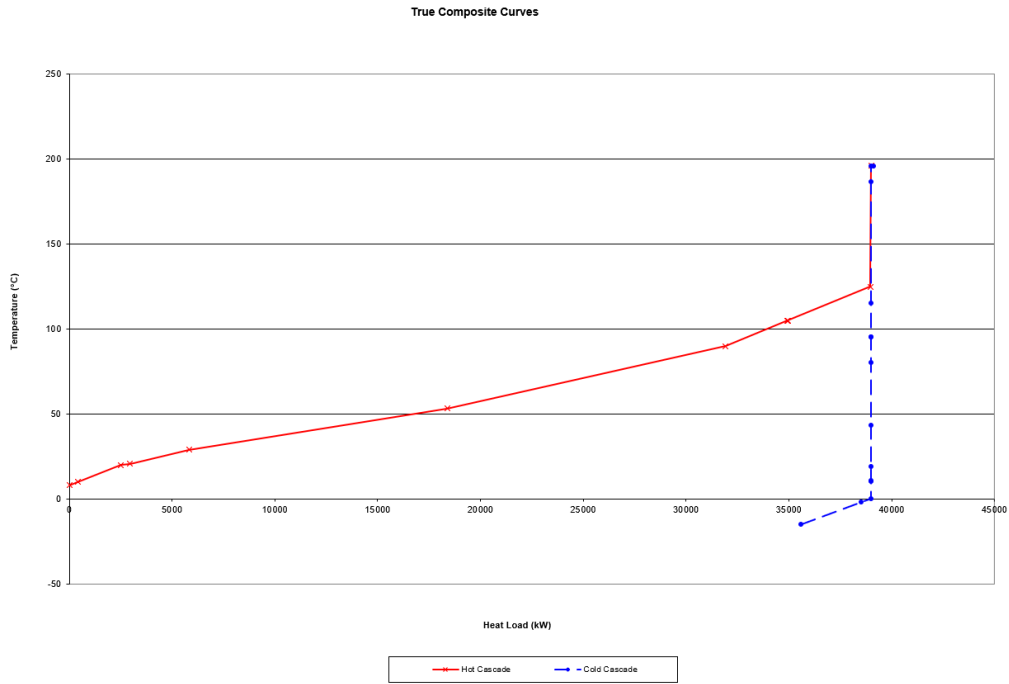


Figure 47: Shifted composite curve for Case C2 dense phase transport, with $\Delta T = 10^\circ\text{C}$.

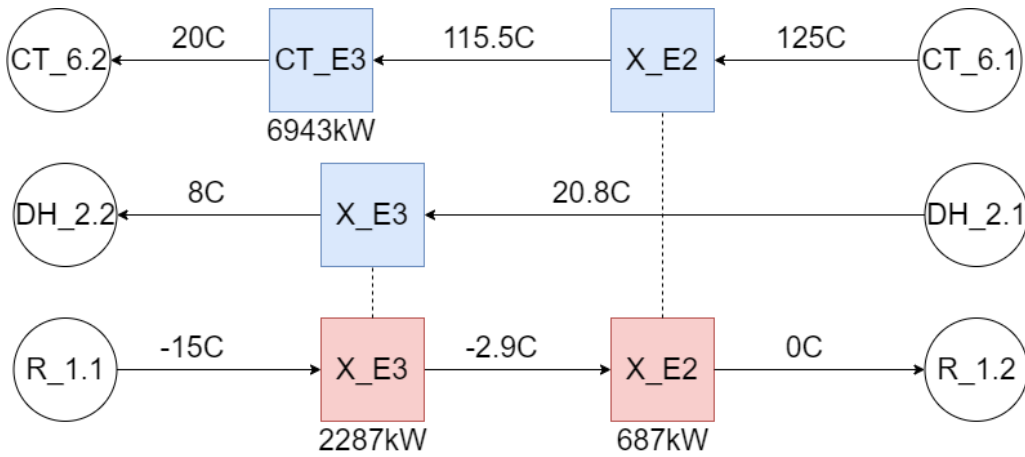


Figure 48: Heat integration network for case C2, dense phase transport.

Case C2 Supercritical

C Stream compositions

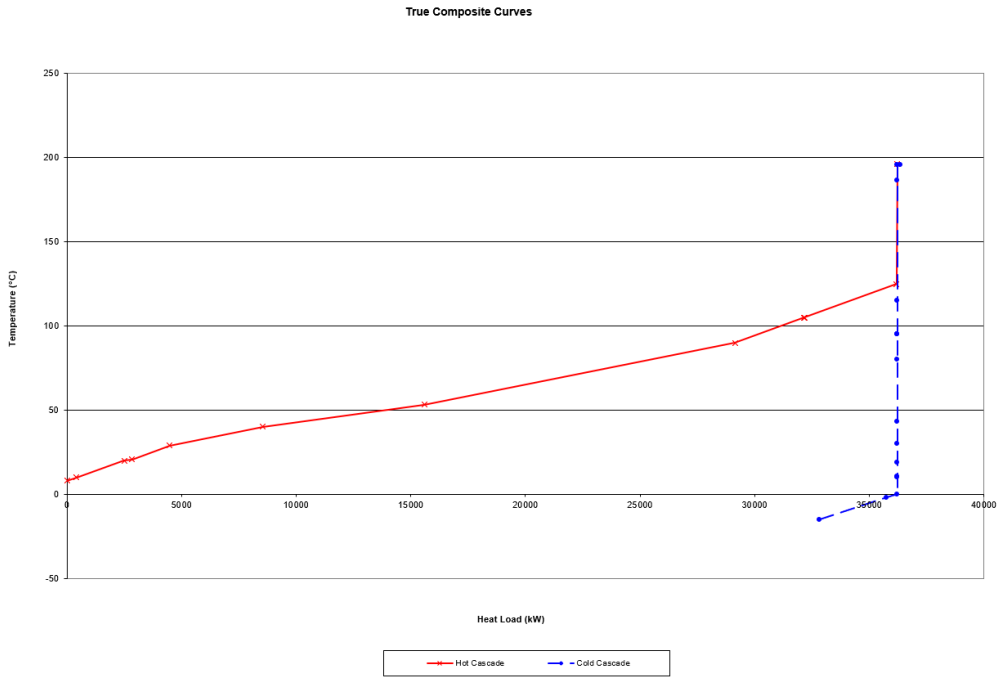


Figure 49: Shifted composite curve for Case supercritical state transport, with $\Delta T = 10^\circ\text{C}$.

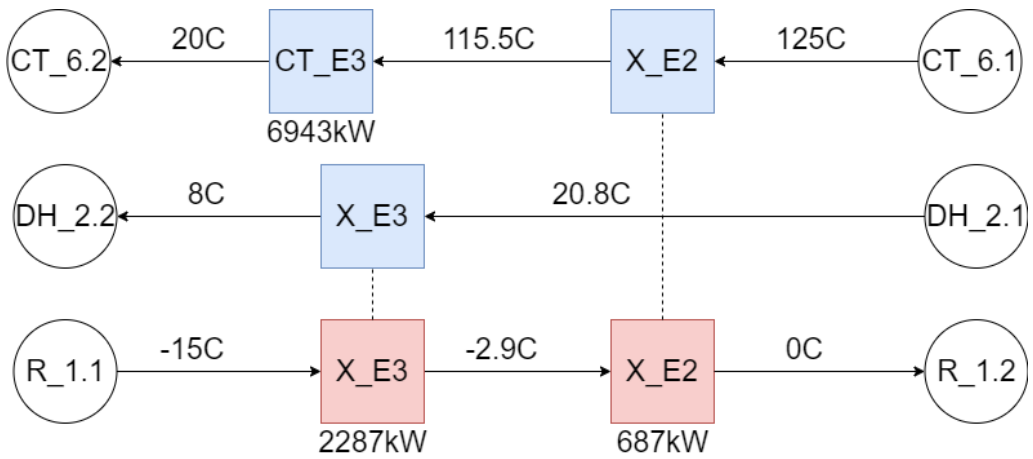


Figure 50: Heat integration network for case C2, supercritical state transport.

Table 39: Stream data for Case A, molecular sieve adsorption, for liquid transport.

Stream	Temperature [C]	Pressure [kPa]	Vapor Fraction	Total mass flow [kg/h]	Total molar flow [kmol/h]	CO2 [kmol/h]	H2O [kmol/h]	N2 [kmol/h]	O2 [kmol/h]	MEA [kmol/h]
CT_Feed	30.0	180	1	1.88E+05	4.32E+03	4.22E+03	1.03E+02	1.34E+00	1.73E-01	1.13E-02
CT_1	125.0	491	1	1.88E+05	4.32E+03	4.22E+03	1.03E+02	1.34E+00	1.73E-01	1.13E-02
CT_RCY	230.0	700	1	3.28E+04	7.51E+02	7.42E+02	9.37E+00	2.36E-01	3.05E-02	1.38E-01
CT_2.1	140.9	491	1	2.20E+05	5.07E+03	4.96E+03	1.12E+02	1.58E+00	2.04E-01	1.49E-01
CT_2.2	20.0	471	0.9830	2.20E+05	5.07E+03	4.96E+03	1.12E+02	1.58E+00	2.04E-01	1.49E-01
CT_3	19.7	451	1	2.19E+05	4.99E+03	4.96E+03	2.67E+01	1.58E+00	2.04E-01	1.49E-01
CT_4.1	125.0	1392	1	2.19E+05	4.99E+03	4.96E+03	2.67E+01	1.58E+00	2.04E-01	1.49E-01
CT_4.2	20.0	1372	0.9967	2.19E+05	4.99E+03	4.96E+03	2.67E+01	1.58E+00	2.04E-01	1.49E-01
CT_5	19.8	1351	1	2.18E+05	4.97E+03	4.96E+03	1.05E+01	1.58E+00	2.04E-01	1.48E-01
CT_6.1	35.7	1620	1	2.18E+05	4.97E+03	4.96E+03	1.05E+01	1.58E+00	2.04E-01	1.48E-01
CT_6.2	20.0	1600	0.9998	2.18E+05	4.97E+03	4.96E+03	1.05E+01	1.58E+00	2.04E-01	1.48E-01
CT_7	19.8	1580	1	2.18E+05	4.97E+03	4.96E+03	9.37E+00	1.58E+00	2.04E-01	1.38E-01
CT_Prod.Water1	19.7	451	0	1.55E+03	8.59E+01	2.09E-01	8.57E+01	1.72E-06	4.32E-08	3.12E-04
CT_Prod.Water2	19.8	1352	0	2.97E+02	1.63E+01	5.15E+00	1.62E+01	1.04E-06	2.64E-08	1.36E-04
CT_Prod.Water3	19.8	1580	0	2.16E+01	1.15E+00	1.37E-02	1.13E+00	1.20E-07	1.27E-08	1.09E-02
DH.2	20.0	1580	1	2.18E+05	4.96E+03	4.96E+03	0.00E+00	1.58E+00	2.04E-01	0.00E+00
CC.1.1	20.0	1580	1	1.86E+05	4.22E+03	4.21E+03	0.00E+00	1.34E+00	1.73E-01	0.00E+00
CC.1.2	-30.0	1560	0	1.86E+05	4.22E+03	4.21E+03	0.00E+00	1.34E+00	1.73E-01	0.00E+00
R.1.1	20.0	1580	1	3.27E+04	7.44E+02	7.44E+02	0.00E+00	2.36E-01	3.06E-02	0.00E+00
R.1.2	234.0	700	1	3.27E+04	7.44E+02	7.44E+02	0.00E+00	2.36E-01	3.06E-02	0.00E+00

Table 40: Stream data for Case A, molecular sieve adsorption, for dense phase transport.

Stream	Temperature [C]	Pressure [kPa]	Vapor Fraction	Total mass flow [kg/h]	Total molar flow [kmol/h]	CO2 [kmol/h]	H2O [kmol/h]	N2 [kmol/h]	O2 [kmol/h]	MEA [kmol/h]
CT_Feed	30.0	180	1	1.88E+05	4.32E+03	4.22E+03	1.03E+02	1.34E+00	1.73E-01	1.13E-02
CT_1	125.0	491	1	1.88E+05	4.32E+03	4.22E+03	1.03E+02	1.34E+00	1.73E-01	1.13E-02
CT_RCY	230.0	700	1	3.29E+04	7.51E+02	7.44E+02	6.36E+00	2.37E-01	3.06E-02	1.12E-01
CT_2.1	140.9	491	1	2.20E+05	5.07E+03	4.96E+03	1.09E+02	1.58E+00	2.04E-01	1.23E-01
CT_2.2	20.0	471	0.9836	2.20E+05	5.07E+03	4.96E+03	1.09E+02	1.58E+00	2.04E-01	1.23E-01
CT_3	19.7	451	1	2.19E+05	4.99E+03	4.96E+03	2.67E+01	1.58E+00	2.04E-01	1.23E-01
CT_4.1	125.0	1392	1	2.19E+05	4.99E+03	4.96E+03	2.67E+01	1.58E+00	2.04E-01	1.23E-01
CT_4.2	20.0	1372	0.9967	2.19E+05	4.99E+03	4.96E+03	2.67E+01	1.58E+00	2.04E-01	1.23E-01
CT_5	19.8	1352	1	2.19E+05	4.97E+03	4.96E+03	1.05E+01	1.58E+00	2.04E-01	1.23E-01
CT_6.1	109.1	3500	1	2.19E+05	4.97E+03	4.96E+03	1.05E+01	1.58E+00	2.04E-01	1.23E-01
CT_6.2	20.0	3480	0.9992	2.19E+05	4.97E+03	4.96E+03	1.05E+01	1.58E+00	2.04E-01	1.23E-01
CT_7	19.8	3460	1	2.19E+05	4.97E+03	4.96E+03	6.36E+00	1.58E+00	2.04E-01	1.23E-01
CT_Prod.Water1	19.7	451	0	1.50E+03	8.29E+01	2.02E-01	8.27E+01	1.66E-06	4.17E-08	2.49E-04
CT_Prod.Water2	19.8	1352	0	2.98E+02	1.64E+01	1.17E-01	1.62E+01	1.04E-06	2.64E-08	1.12E-04
CT_Prod.Water3	19.8	3460	0	7.91E+01	4.24E+00	8.86E-02	4.14E+00	9.83E-07	6.91E-08	1.10E-02
DH.2	20.0	3460	1	2.18E+05	4.96E+03	4.96E+03	0.00E+00	1.58E+00	2.04E-01	0.00E+00
CC.1	20.0	3460	1	1.86E+05	4.22E+03	4.22E+03	0.00E+00	1.34E+00	1.73E-01	0.00E+00
CC.2.1	90.0	7315	1	1.86E+05	4.22E+03	4.22E+03	0.00E+00	1.34E+00	1.73E-01	0.00E+00
CC.2.2	20.0	7295	0	1.86E+05	4.22E+03	4.22E+03	0.00E+00	1.34E+00	1.73E-01	0.00E+00
CC.3.1	32.8	15020	0	1.86E+05	4.22E+03	4.22E+03	0.00E+00	1.34E+00	1.73E-01	0.00E+00
CC.3.2	20.0	15000	0	1.86E+05	4.22E+03	4.22E+03	0.00E+00	1.34E+00	1.73E-01	0.00E+00
R.1.1	20.0	3460	1	3.28E+04	7.44E+02	7.44E+02	0.00E+00	2.37E-01	3.06E-02	0.00E+00
R.1.2	234.4	700	1	3.28E+04	7.44E+02	7.44E+02	0.00E+00	2.37E-01	3.06E-02	0.00E+00

Table 41: Stream data for Case A, molecular sieve adsorption, for supercritical state transport.

Stream name	Temperature [C]	Pressure [kPa]	Vapor Fraction	Total mass flow [kg/h]	Total molar flow [kmol/h]	CO2 [kmol/h]	H2O [kmol/h]	N2 [kmol/h]	O2 [kmol/h]	MEA [kmol/h]
CT_Feed	30.0	180	1	1.88E+05	4.32E+03	4.22E+03	1.03E+02	1.34E+00	1.73E-01	1.13E-02
CT_1	125.0	491	1	1.88E+05	4.32E+03	4.22E+03	1.03E+02	1.34E+00	1.73E-01	1.13E-02
CT_RCY	230.0	700	1	3.29E+04	7.51E+02	7.44E+02	6.36E+00	2.37E-01	3.06E-02	1.12E-01
CT_2.1	140.9	491	1	2.20E+05	5.07E+03	4.96E+03	1.09E+02	1.58E+00	2.04E-01	1.23E-01
CT_2.2	20.0	471	0.9836	2.20E+05	5.07E+03	4.96E+03	1.09E+02	1.58E+00	2.04E-01	1.23E-01
CT_3	19.7	451	1	2.19E+05	4.99E+03	4.96E+03	2.67E+01	1.58E+00	2.04E-01	1.23E-01
CT_4.1	125.0	1392	1	2.19E+05	4.99E+03	4.96E+03	2.67E+01	1.58E+00	2.04E-01	1.23E-01
CT_4.2	20.0	1372	0.9967	2.19E+05	4.99E+03	4.96E+03	2.67E+01	1.58E+00	2.04E-01	1.23E-01
CT_5	19.8	1352	1	2.19E+05	4.97E+03	4.96E+03	1.05E+01	1.58E+00	2.04E-01	1.23E-01
CT_6.1	109.1	3500	1	2.19E+05	4.97E+03	4.96E+03	1.05E+01	1.58E+00	2.04E-01	1.23E-01
CT_6.2	20.0	3480	0.9992	2.19E+05	4.97E+03	4.96E+03	1.05E+01	1.58E+00	2.04E-01	1.23E-01
CT_7	19.8	3460	1	2.19E+05	4.97E+03	4.96E+03	6.36E+00	1.58E+00	2.04E-01	1.12E-01
CT_Prod.Water1	19.7	451	0	1.50E+03	8.29E+01	2.02E-01	8.27E+01	1.66E-06	4.17E-08	2.49E-04
CT_Prod.Water2	19.8	1352	0	2.98E+02	1.64E+01	1.17E-01	1.62E+01	1.04E-06	2.64E-08	1.12E-04
CT_Prod.Water3	19.8	3460	0	7.91E+01	4.24E+00	8.86E-02	4.14E+00	9.83E-07	6.91E-08	1.10E-02
DH.2	20.0	3460	1	2.18E+05	4.96E+03	4.96E+03	0.00E+00	1.58E+00	2.04E-01	0.00E+00
CC.1	20.0	3460	1	1.86E+05	4.22E+03	4.22E+03	0.00E+00	1.34E+00	1.73E-01	0.00E+00
CC.2.1	69.0	5896	1	1.86E+05	4.22E+03	4.22E+03	0.00E+00	1.34E+00	1.73E-01	0.00E+00
CC.2.2	21.0	5876	0	1.86E+05	4.22E+03	4.22E+03	0.00E+00	1.34E+00	1.73E-01	0.00E+00
CC.3	39.7	1500	0	1.86E+05	4.22E+03	4.22E+03	0.00E+00	1.34E+00	1.73E-01	0.00E+00
R.1.1	20.0	3460	1	3.28E+04	7.44E+02	7.44E+02	0.00E+00	2.37E-01	3.06E-02	0.00E+00
R.1.2	234.4	700	1	3.28E+04	7.44E+02	7.44E+02	0.00E+00	2.37E-01	3.06E-02	0.00E+00

Table 42: A Critical state

Table 43: Stream data for Case B1, TEG absorption with absorption column, for liquid transport.

Stream	Temp. [C]	Pressure [kPa]	Vapor Fraction	Tot. mass flow [kg/h]	Tot. molar flow [kmol/h]	CO2 [kmol/h]	H2O [kmol/h]	N2 [kmol/h]	O2 [kmol/h]	MEA [kmol/h]	TEG [kmol/h]
CT_Feed	30.0	180	1	1.88E+05	4.32E+03	4.22E+03	1.03E+02	1.34E+00	1.73E-01	1.13E-02	0.00E+00
CT_RCY	42.9	180	1	1.55E+02	3.54E+00	3.50E+00	4.71E-02	3.59E-04	6.93E-05	4.98E-09	3.55E-11
CT_1	30.0	180	1	1.88E+05	4.33E+03	4.22E+03	1.03E+02	1.34E+00	1.73E-01	1.13E-02	3.55E-11
CT_2.1	125.0	496	1	1.88E+05	4.33E+03	4.22E+03	1.03E+02	1.34E+00	1.73E-01	1.13E-02	3.55E-11
CT_2.2	20.0	476	0.9812	1.88E+05	4.33E+03	4.22E+03	1.03E+02	1.34E+00	1.73E-01	1.13E-02	3.55E-11
CT_3	19.7	456	1	1.86E+05	4.24E+03	4.22E+03	2.25E+01	1.34E+00	1.73E-01	1.13E-02	2.12E-11
CT_4.1	125.0	1420	1	1.86E+05	4.24E+03	4.22E+03	2.25E+01	1.34E+00	1.73E-01	1.13E-02	2.12E-11
CT_4.2	20.0	1400	0.9967	1.86E+05	4.24E+03	4.22E+03	2.25E+01	1.34E+00	1.73E-01	1.13E-02	2.12E-11
CT_5	19.8	1380	1	1.86E+05	4.23E+03	4.22E+03	8.80E+00	1.34E+00	1.73E-01	1.13E-02	1.75E-11
CT_6.1	35.0	1640	1	1.86E+05	4.23E+03	4.22E+03	8.80E+00	1.34E+00	1.73E-01	1.13E-02	1.75E-11
CT_6.2	20.0	1620	0.9998	1.86E+05	4.23E+03	4.22E+03	8.80E+00	1.34E+00	1.73E-01	1.13E-02	1.75E-11
CT_7	19.8	1600	1	1.86E+05	4.23E+03	4.22E+03	7.90E+00	1.34E+00	1.73E-01	1.13E-02	1.72E-11
CT_Prod.Water1	19.7	456	0	1.46E+03	8.08E+01	1.98E-01	8.06E+01	1.63E-06	4.10E-08	2.65E-05	1.43E-11
CT_Prod.Water2	19.8	1380	0	2.52E+02	1.38E+01	1.01E-01	1.37E+01	8.97E-07	2.29E-08	1.04E-05	3.74E-12
CT_Prod.Water3	19.8	1600	0	1.65E+01	9.02E-01	7.60E-03	8.95E-01	6.88E-08	1.76E-09	7.30E-07	2.47E-13
CC_1	21.8	1600	1	1.86E+05	4.22E+03	4.22E+03	1.25E-01	1.34E+00	1.73E-01	1.02E-02	2.05E-03
R_15	20.1	1600	0	3.52E+03	2.38E+01	1.14E-01	2.20E-01	6.44E-06	1.62E-06	1.59E-01	2.33E+01
R_1.1	64.0	1600	0.06	3.82E+03	3.51E+01	3.64E+00	8.00E+00	3.67E-04	7.13E-05	1.60E-01	2.33E+01
CC_2	19.5	1537	1	1.86E+05	4.22E+03	4.22E+03	1.25E-01	1.34E+00	1.73E-01	1.02E-02	2.05E-03
CC_3	-30.0	1517	0	1.86E+05	4.22E+03	4.22E+03	1.25E-01	1.34E+00	1.73E-01	1.02E-02	2.05E-03
R_1.2	140.0	550	0.1133	3.82E+03	3.51E+01	3.64E+00	8.00E+00	3.67E-04	7.13E-05	1.60E-01	2.33E+01
R_2	140.0	530	1	1.61E+02	3.98E+00	3.42E+00	5.53E-01	3.66E-04	6.95E-05	8.54E-04	3.18E-03
R_3.1	107.0	130	1	1.96E+03	9.64E+01	8.66E+00	8.77E+01	8.80E-04	1.70E-04	2.30E-03	3.59E-03
R_3.2	15.0	130	0.09	1.96E+03	9.64E+01	8.66E+00	8.77E+01	8.80E-04	1.70E-04	2.30E-03	3.59E-03
R_4	15.0	130	1	3.80E+02	8.71E+00	8.59E+00	1.16E-01	8.80E-04	1.70E-04	1.76E-08	8.78E-11
R_5	15.0	130	1	1.56E+02	3.57E+00	3.52E+00	4.74E-02	3.61E-04	6.96E-05	7.20E-09	3.60E-11
R_6.1	15.0	130	1	2.24E+02	5.14E+00	5.07E+00	6.82E-02	5.19E-04	1.00E-04	1.04E-08	5.18E-11
R_6.2	185.0	130	1	2.24E+02	5.14E+00	5.07E+00	6.82E-02	5.19E-04	1.00E-04	1.04E-08	5.18E-11
R_7	183.2	130	0.9938	3.39E+02	9.08E+00	4.95E+00	3.64E+00	5.13E-04	9.86E-05	2.03E-01	2.90E-01
R_8	15.0	130	0	1.58E+03	8.77E+01	6.73E-02	8.76E+01	1.51E-07	6.73E-09	2.30E-03	3.59E-03
R_9	15.0	130	0	1.44E+03	8.00E+01	6.14E-02	7.99E+01	1.37E-07	6.13E-09	2.10E-03	3.28E-03
R_10.1	15.1	1500	0	1.44E+03	8.00E+01	6.14E-02	7.99E+01	1.37E-07	6.13E-09	2.10E-03	3.28E-03
R_10.2	150.0	1000	0	1.44E+03	8.00E+01	6.14E-02	7.99E+01	1.37E-07	6.13E-09	2.10E-03	3.28E-03
R_11	105.4	130	1	1.80E+03	9.24E+01	5.23E+00	8.72E+01	5.14E-04	1.00E-04	1.45E-03	4.17E-04
R_12	182.6	130	0	3.64E+03	2.78E+01	9.96E-06	3.79E+00	7.67E-12	2.50E-11	3.85E-01	2.36E+01
R_13	187.5	130	0.0026	3.52E+03	2.38E+01	1.14E-01	2.20E-01	6.43E-06	1.62E-06	1.82E-01	2.33E+01
R_14.1	187.4	110	0.0032	3.52E+03	2.38E+01	1.14E-01	2.20E-01	6.43E-06	1.62E-06	1.82E-01	2.33E+01
R_14.2	20.0	90	0	3.52E+03	2.38E+01	1.14E-01	2.20E-01	6.43E-06	1.62E-06	1.82E-01	2.33E+01
R_Prod.Water	15.0	130	0	1.39E+02	7.71E+00	5.92E-03	7.70E+00	1.32E-08	5.91E-10	2.03E-04	3.17E-04
R_Makeup	20.0	110	0	3.58E-01	1.34E-03	0.00E+00	5.55E-06	0.00E+00	0.00E+00	0.00E+00	2.37E-03

Table 44: Stream data for Case B1, TEG absorption with absorption column, for dense phase transport.

Stream	Temp. [C]	Pressure [kPa]	Vapor Fraction	Total mass flow [kg/h]	Total molar flow [kmol/h]	CO2 [kmol/h]	H2O [kmol/h]	N2 [kmol/h]	O2 [kmol/h]	MEA [kmol/h]	TEG [kmol/h]
CT_Feed	30.0	180	1	1.88E+05	4.32E+03	4.22E+03	1.03E+02	1.34E+00	1.73E-01	1.13E-01	0.00E+00
CT_RCY	42.9	180	1	1.55E+02	3.54E+00	3.50E+00	4.71E-02	3.59E-04	6.93E-05	4.98E-09	3.55E-11
CT_1	30.0	180	1	1.88E+05	4.33E+03	4.22E+03	1.03E+02	1.34E+00	1.73E-01	1.13E-02	3.55E-11
CT_2.1	125.0	496	1	1.88E+05	4.33E+03	4.22E+03	1.03E+02	1.34E+00	1.73E-01	1.13E-02	3.55E-11
CT_2.2	20.0	476	0.9812	1.88E+05	4.33E+03	4.22E+03	1.03E+02	1.34E+00	1.73E-01	1.13E-02	3.55E-11
CT_3	19.7	456	1	1.86E+05	4.24E+03	4.22E+03	2.25E+01	1.34E+00	1.73E-01	1.13E-02	2.12E-11
CT_4.1	125.0	1420	1	1.86E+05	4.24E+03	4.22E+03	2.25E+01	1.34E+00	1.73E-01	1.13E-02	2.12E-11
CT_4.2	20.0	1400	0.9967	1.86E+05	4.24E+03	4.22E+03	2.25E+01	1.34E+00	1.73E-01	1.13E-02	2.12E-11
CT_5	19.8	1380	1	1.86E+05	4.23E+03	4.22E+03	8.80E+00	1.34E+00	1.73E-01	1.13E-02	1.75E-11
CT_6.1	35.0	1640	1	1.86E+05	4.23E+03	4.22E+03	8.80E+00	1.34E+00	1.73E-01	1.13E-02	1.75E-11
CT_6.2	20.0	1620	0.9998	1.86E+05	4.23E+03	4.22E+03	8.80E+00	1.34E+00	1.73E-01	1.13E-02	1.75E-11
CT_7	19.8	1600	1	1.86E+05	4.23E+03	4.22E+03	7.90E+00	1.34E+00	1.73E-01	1.13E-02	1.72E-11
CT_Prod.Water1	19.7	456	0	1.46E+03	8.08E+01	1.98E-01	8.06E+01	1.63E-06	4.10E-08	2.65E-05	1.43E-11
CT_Prod.Water2	19.8	1380	0	2.52E+02	1.38E+01	1.01E-01	1.37E+01	8.97E-07	2.29E-08	1.04E-05	3.74E-12
CT_Prod.Water3	19.8	1600	0	1.65E+01	9.02E-01	7.60E-03	8.95E-01	6.88E-08	1.76E-09	7.30E-07	2.47E-13
CC_1	21.8	1600	1	1.86E+05	4.22E+03	4.22E+03	1.25E-01	1.34E+00	1.73E-01	1.02E-02	2.05E-03
R_16	20.1	1600	0	3.52E+03	2.38E+01	1.14E-01	2.20E-01	6.44E-06	1.62E-06	1.59E-01	2.33E+01
R_1.1	64.0	1600	0.0558	3.82E+03	3.51E+01	3.64E+00	8.00E+00	3.67E-04	7.13E-05	1.60E-01	2.33E+01
CC_2.1	85.0	3167	1	1.86E+05	4.22E+03	4.22E+03	1.25E-01	1.34E+00	1.73E-01	1.02E-02	2.05E-03
CC_2.2	20.0	3147	1	1.86E+05	4.22E+03	4.22E+03	1.25E-01	1.34E+00	1.73E-01	1.02E-02	2.05E-03
CC_3.1	85.0	6319	1	1.86E+05	4.22E+03	4.22E+03	1.25E-01	1.34E+00	1.73E-01	1.02E-02	2.05E-03
CC_3.2	20.0	6299	0	1.86E+05	4.22E+03	4.22E+03	1.25E-01	1.34E+00	1.73E-01	1.02E-02	2.05E-03
CC_4.1	35.9	15020	0	1.86E+05	4.22E+03	4.22E+03	1.25E-01	1.34E+00	1.73E-01	1.02E-02	2.05E-03
CC_4.2	20.0	15000	0	1.86E+05	4.22E+03	4.22E+03	1.25E-01	1.34E+00	1.73E-01	1.02E-02	2.05E-03
R_1.2	140.0	550	0.1133	3.82E+03	3.51E+01	3.64E+00	8.00E+00	3.67E-04	7.13E-05	1.60E-01	2.33E+01
R_2	140.0	530	1	1.61E+02	3.98E+00	3.42E+00	5.53E-01	3.66E-04	6.95E-05	8.54E-04	3.18E-03
R_3.1	107.0	130	1	1.96E+03	9.64E+01	8.66E+00	8.77E+01	8.80E-04	1.70E-04	2.30E-03	3.59E-03
R_3.2	15.0	130	0.0903	1.96E+03	9.64E+01	8.66E+00	8.77E+01	8.80E-04	1.70E-04	2.30E-03	3.59E-03
R_4	15.0	130	1	3.80E+02	8.71E+00	8.59E+00	1.16E-01	8.80E-04	1.70E-04	1.76E-08	8.78E-11
R_5	15.0	130	1	1.56E+02	3.57E+00	3.52E+00	4.74E-02	3.61E-04	6.96E-05	7.20E-09	3.60E-11
R_6.1	15.0	130	1	2.24E+02	5.14E+00	5.07E+00	6.82E-02	5.19E-04	1.00E-04	1.04E-08	5.18E-11
R_6.2	185.0	130	1	2.24E+02	5.14E+00	5.07E+00	6.82E-02	5.19E-04	1.00E-04	1.04E-08	5.18E-11
R_7	183.2	130	0.9939	3.39E+02	9.08E+00	4.95E+00	3.64E+00	5.13E-04	9.86E-05	2.03E-01	2.90E-01
R_8	15.0	130	0	1.58E+03	8.77E+01	6.73E-02	8.76E+01	1.51E-07	6.73E-09	2.30E-03	3.59E-03
R_9	15.0	130	0	1.44E+03	8.00E+01	6.14E-02	7.99E+01	1.37E-07	6.13E-09	2.10E-03	3.28E-03
R_10.1	15.1	1500	0	1.44E+03	8.00E+01	6.14E-02	7.99E+01	1.37E-07	6.13E-09	2.10E-03	3.28E-03
R_10.2	150.0	1000	0	1.44E+03	8.00E+01	6.14E-02	7.99E+01	1.37E-07	6.13E-09	2.10E-03	3.28E-03
R_11	105.4	130	1	1.80E+03	9.24E+01	5.23E+01	8.72E+01	5.14E-04	1.00E-04	1.45E-03	4.17E-04
R_12	182.6	130	0	3.64E+03	2.78E+01	9.96E-06	3.79E+00	7.67E-12	2.50E-11	3.85E-01	2.36E+01
R_13	187.5	130	0.0027	3.52E+03	2.38E+01	1.14E-01	2.20E-01	6.43E-06	1.62E-06	1.82E-01	2.33E+01
R_14.1	187.4	110	0.0032	3.52E+03	2.38E+01	1.14E-01	2.20E-01	6.43E-06	1.62E-06	1.82E-01	2.33E+01
R_14.2	20.0	90	0	3.52E+03	2.38E+01	1.14E-01	2.20E-01	6.43E-06	1.62E-06	1.82E-01	2.33E+01
R_Prod.Water	15.0	130	0	1.39E+02	7.71E+00	5.92E-03	7.70E+00	1.32E-08	5.91E-10	2.03E-04	3.17E-04
R_Makeup	20.0	110	0	3.58E-01	1.34E-03	0.00E+00	5.55E-06	0.00E+00	0.00E+00	0.00E+00	1.33E-03

Table 45: Stream data for Case B1, TEG absorption with absorption column, for supercritical state transport.

Stream	Temp. [C]	Pressure [kPa]	Vapor Fraction	Total mass flow [kg/h]	Total molar flow [kmol/h]	CO2 [kmol/h]	H2O [kmol/h]	N2 [kmol/h]	O2 [kmol/h]	MEA [kmol/h]	TEG [kmol/h]
CT_Feed	30.0	180	1.00E+00	1.88E+05	4.32E+03	4.22E+03	1.03E+02	1.34E+00	1.73E-01	1.13E-02	0.00E+00
CT_RCY	42.9	180	1.00E+00	1.55E+02	3.54E+00	3.50E+00	4.71E+02	3.59E+04	6.93E-05	4.98E-09	3.55E-11
CT_1	30.0	180	1.00E+00	1.88E+05	4.33E+03	4.22E+03	1.03E+02	1.34E+00	1.73E-01	1.13E-02	3.55E-11
CT_2.1	125.0	496	1.00E+00	1.88E+05	4.33E+03	4.22E+03	1.03E+02	1.34E+00	1.73E-01	1.13E-02	3.55E-11
CT_2.2	20.0	476	9.81E-01	1.88E+05	4.33E+03	4.22E+03	1.03E+02	1.34E+00	1.73E-01	1.13E-02	3.55E-11
CT_3	19.7	456	1.00E+00	1.86E+05	4.24E+03	4.22E+03	2.25E+01	1.34E+00	1.73E-01	1.13E-02	2.12E-11
CT_4.1	125.0	1420	1.00E+00	1.86E+05	4.24E+03	4.22E+03	2.25E+01	1.34E+00	1.73E-01	1.13E-02	2.12E-11
CT_4.2	20.0	1400	9.97E-01	1.86E+05	4.24E+03	4.22E+03	2.25E+01	1.34E+00	1.73E-01	1.13E-02	2.12E-11
CT_5	19.8	1380	1.00E+00	1.86E+05	4.23E+03	4.22E+03	8.80E+00	1.34E+00	1.73E-01	1.13E-02	1.75E-11
CT_6.1	35.0	1640	1.00E+00	1.86E+05	4.23E+03	4.22E+03	8.80E+00	1.34E+00	1.73E-01	1.13E-02	1.75E-11
CT_6.2	20.0	1620	1.00E+00	1.86E+05	4.23E+03	4.22E+03	8.80E+00	1.34E+00	1.73E-01	1.13E-02	1.75E-11
CT_7	19.8	1600	1.00E+00	1.86E+05	4.23E+03	4.22E+03	7.90E+00	1.34E+00	1.73E-01	1.13E-02	1.72E-11
CT_Prod.Water1	19.7	456	0.00E+00	1.46E+03	8.08E+01	1.98E+01	8.06E+01	1.63E+00	4.10E-08	2.65E-05	1.43E-11
CT_Prod.Water2	19.8	1380	0.00E+00	2.52E+02	1.38E+01	1.01E-01	1.37E+01	8.97E-07	2.29E-08	1.04E-05	3.74E-12
CT_Prod.Water3	19.8	1600	0.00E+00	1.65E+01	9.02E-01	7.60E-03	8.95E-01	6.88E-08	1.76E-09	7.30E-07	2.47E-13
CC_1	21.8	1600	1.00E+00	1.86E+05	4.22E+03	4.22E+03	1.25E-01	1.34E+00	1.73E-01	1.02E-02	2.05E-03
R_15	20.1	1600	0.00E+00	3.52E+03	2.38E+01	1.14E-01	2.20E-01	6.44E-06	1.62E-06	1.59E-01	2.33E+01
R_1.1	64.0	1600	5.58E-02	3.82E+03	3.51E+01	3.64E+00	8.00E+00	3.67E-04	7.13E-05	1.60E-01	2.33E+01
CC_2	85.0	3147	1.00E+00	1.86E+05	4.22E+03	4.22E+03	1.25E-01	1.34E+00	1.73E-01	1.02E-02	2.05E-03
CC_3	20.0	3147	1.00E+00	1.86E+05	4.22E+03	4.22E+03	1.25E-01	1.34E+00	1.73E-01	1.02E-02	2.05E-03
CC_4	85.0	6319	1.00E+00	1.86E+05	4.22E+03	4.22E+03	1.25E-01	1.34E+00	1.73E-01	1.02E-02	2.05E-03
CC_5	22.2	6299	0.00E+00	1.86E+05	4.22E+03	4.22E+03	1.25E-01	1.34E+00	1.73E-01	1.02E-02	2.05E-03
CC_6	40.0	15000	0.00E+00	1.86E+05	4.22E+03	4.22E+03	1.25E-01	1.34E+00	1.73E-01	1.02E-02	2.05E-03
R_1.2	140.0	550	1.13E-01	3.82E+03	3.51E+01	3.64E+00	8.00E+00	3.67E-04	7.13E-05	1.60E-01	2.33E+01
R_2	140.0	530	1.00E+00	1.61E+02	3.98E+00	3.42E+00	5.53E-01	3.66E-04	6.95E-05	8.54E-04	3.18E-03
R_3.1	107.0	130	1.00E+00	1.96E+03	9.64E+01	8.66E+00	8.77E+01	8.80E-04	1.70E-04	2.30E-03	3.59E-03
R_3.2	15.0	130	9.03E-02	1.96E+03	9.64E+01	8.66E+00	8.77E+01	8.80E-04	1.70E-04	2.30E-03	3.59E-03
R_4	15.0	130	1.00E+00	3.80E+02	8.71E+00	8.59E+00	1.16E-01	8.80E-04	1.70E-04	1.76E-08	8.78E-11
R_5	15.0	130	1.00E+00	1.56E+02	3.57E+00	3.52E+00	4.74E-02	3.61E-04	6.96E-05	7.20E-09	3.60E-11
R_6.1	15.0	130	1.00E+00	2.24E+02	5.14E+00	5.07E+00	6.82E-02	5.19E-04	1.00E-04	1.04E-08	5.18E-11
R_6.2	185.0	130	1.00E+00	2.24E+02	5.14E+00	5.07E+00	6.82E-02	5.19E-04	1.00E-04	1.04E-08	5.18E-11
R_7	183.2	130	9.94E-01	3.39E+02	9.08E+00	4.95E+00	3.64E+00	5.13E-04	9.86E-05	2.03E-01	2.90E-01
R_8	15.0	130	0.00E+00	1.58E+03	8.77E+01	6.73E-02	8.76E+01	1.51E-07	6.73E-09	2.30E-03	3.59E-03
R_9	15.0	130	0.00E+00	1.44E+03	8.00E+01	6.14E-02	7.99E+01	1.37E-07	6.13E-09	2.10E-03	3.28E-03
R_10.1	15.1	1500	0.00E+00	1.44E+03	8.00E+01	6.14E-02	7.99E+01	1.37E-07	6.13E-09	2.10E-03	3.28E-03
R_10.2	150.0	1000	0.00E+00	1.44E+03	8.00E+01	6.14E-02	7.99E+01	1.37E-07	6.13E-09	2.10E-03	3.28E-03
R_11	105.4	130	1.00E+00	1.80E+03	9.24E+01	5.23E+00	8.72E+01	5.14E-04	1.00E-04	1.45E-03	4.17E-04
R_12	182.6	130	0.00E+00	3.64E+03	2.78E+01	9.96E-06	3.79E+00	7.67E-12	2.50E-11	3.85E-01	2.36E+01
R_13	187.5	130	2.69E-03	3.52E+03	2.38E+01	1.14E-01	2.20E-01	6.43E-06	1.62E-06	1.82E-01	2.33E+01
R_14.1	187.4	110	3.16E-03	3.52E+03	2.38E+01	1.14E-01	2.20E-01	6.43E-06	1.62E-06	1.82E-01	2.33E+01
R_14.2	20.0	90	0.00E+00	3.52E+03	2.38E+01	1.14E-01	2.20E-01	6.43E-06	1.62E-06	1.82E-01	2.33E+01
R_Prod.Water	15.0	130	0.00E+00	1.39E+02	7.71E+00	5.92E-03	7.70E+00	1.32E-08	5.91E-10	2.03E-04	3.17E-04
R_Makeup	20.0	110	0.00E+00	2.00E-01	1.34E-03	0.00E+00	5.55E-06	0.00E+00	0.00E+00	0.00E+00	1.33E-03

Table 46: Stream data for Case B2, TEG absorption with membrane contactor, for liquid transport.

Stream	Temp. [C]	Pressure [kPa]	Vapor Fraction	Total mass flow [kg/h]	Total molar flow [kmol/h]	CO2 [kmol/h]	H2O [kmol/h]	N2 [kmol/h]	O2 [kmol/h]	MEA [kmol/h]	TEG [kmol/h]
CT_Feed	30.0	180	1	1.88E+05	4.32E+03	4.22E+03	1.03E+02	1.34E+00	1.73E-01	1.13E-02	0.00E+00
CT_Split	180	180	1	5.12E+00	1.18E-01	1.15E-01	2.81E-03	3.66E-05	4.73E-06	3.10E-07	0.00E+00
CT_1	30.0	180	1	1.87E+05	4.32E+03	4.22E+03	1.03E+02	1.34E+00	1.73E-01	1.13E-02	0.00E+00
CT_2.1	125.0	496	1	1.87E+05	4.32E+03	4.22E+03	1.03E+02	1.34E+00	1.73E-01	1.13E-02	0.00E+00
CT_2.2	20.0	476	0.9812	1.87E+05	4.32E+03	4.22E+03	1.03E+02	1.34E+00	1.73E-01	1.13E-02	0.00E+00
CT_3	19.7	456	1	1.86E+05	4.24E+03	4.22E+03	2.25E+01	1.34E+00	1.73E-01	1.13E-02	0.00E+00
CT_4.1	125.0	1420	1	1.86E+05	4.24E+03	4.22E+03	2.25E+01	1.34E+00	1.73E-01	1.13E-02	0.00E+00
CT_4.2	20.0	1400	0.9967	1.86E+05	4.24E+03	4.22E+03	2.25E+01	1.34E+00	1.73E-01	1.13E-02	0.00E+00
CT_5	19.8	1380	1	1.86E+05	4.23E+03	4.22E+03	8.79E+00	1.34E+00	1.73E-01	1.13E-02	0.00E+00
CT_6.1	35.0	1640	1	1.86E+05	4.23E+03	4.22E+03	8.79E+00	1.34E+00	1.73E-01	1.13E-02	0.00E+00
CT_6.2	20.0	1620	0.9998	1.86E+05	4.23E+03	4.22E+03	8.79E+00	1.34E+00	1.73E-01	1.13E-02	0.00E+00
CT_7	19.8	1600	1	1.86E+05	4.23E+03	4.22E+03	7.90E+00	1.34E+00	1.73E-01	1.13E-02	0.00E+00
CT_Prod.Water1	19.7	456	0	1.46E+03	8.07E+01	1.98E-01	8.05E+01	1.63E-06	4.10E-08	2.65E-05	0.00E+00
CT_Prod.Water2	19.8	1380	0	2.52E+02	1.38E+01	1.01E-01	1.37E+01	8.97E-07	2.29E-08	1.04E-05	0.00E+00
CT_Prod.Water3	19.8	1600	0	1.64E+01	9.01E-01	7.58E-03	8.93E-01	6.87E-08	1.75E-09	7.29E-07	0.00E+00
CC_1	20.1	1600	1	1.86E+05	4.22E+03	4.22E+03	1.22E-01	1.34E+00	1.73E-01	1.13E-02	0.00E+00
R_12	20.1	1600	0	3.52E+03	2.40E+01	1.05E-01	5.81E-01	6.45E-06	1.60E-06	4.81E-05	2.33E+01
R_1.1	23.6	1597	0	3.65E+03	3.13E+01	0.00E+00	8.00E+00	0.00E+00	0.00E+00	0.00E+00	2.33E+01
CC_2	17.9	1537	1	1.86E+05	4.22E+03	4.22E+03	1.22E-01	1.34E+00	1.73E-01	1.13E-02	0.00E+00
CC_3	-30.0	1517	0	1.86E+05	4.22E+03	4.22E+03	1.22E-01	1.34E+00	1.73E-01	1.13E-02	0.00E+00
R_1.2	200.0	490	0	3.65E+03	3.13E+01	0.00E+00	8.00E+00	0.00E+00	0.00E+00	0.00E+00	2.33E+01
R_2.1	106.2	130	1	1.61E+03	8.53E+01	2.80E+00	8.25E+01	3.01E-04	5.74E-05	2.19E-06	3.02E-04
R_2.2	15.0	130	0.0325	1.61E+03	8.53E+01	2.80E+00	8.25E+01	3.01E-04	5.74E-05	2.19E-06	3.02E-04
R_3.1	15.0	130	1	1.21E+02	2.77E+00	2.74E+00	3.69E-02	3.01E-04	5.74E-05	5.65E-12	2.50E-12
R_3.2	185.0	130	1	1.21E+02	2.77E+00	2.74E+00	3.69E-02	3.01E-04	5.74E-05	5.65E-12	2.50E-12
R_4	185.6	130	0.9941	2.06E+02	6.08E+00	2.63E+00	3.24E+00	2.65E-04	5.12E-05	3.16E-05	2.11E-01
R_5	185.3	130	0.9932	2.14E+02	6.30E+00	2.74E+00	3.34E+00	3.01E-04	5.74E-05	3.28E-05	2.21E-01
R_6	130.0	183	0	3.61E+03	2.73E+01	6.11E-06	3.78E+00	4.84E-12	1.67E-11	7.96E-05	2.36E+01
R_7	15.0	130	0	1.49E+03	8.25E+01	6.33E-02	8.25E+01	1.52E-07	6.71E-09	2.19E-06	3.02E-04
R_8	15.0	130	0	1.35E+03	7.50E+01	5.75E-02	7.49E+01	1.38E-07	6.10E-09	1.99E-06	2.74E-04
R_9.1	15.1	1500	0	1.35E+03	7.50E+01	5.75E-02	7.49E+01	1.38E-07	6.10E-09	1.99E-06	2.74E-04
R_9.2	150.0	1000	0	1.35E+03	7.50E+01	5.75E-02	7.49E+01	1.38E-07	6.10E-09	1.99E-06	2.74E-04
R_10.1	189.6	130	0.0027	3.52E+03	2.40E+01	1.05E-01	5.81E-01	6.45E-06	1.60E-06	4.81E-05	2.33E+01
R_10.2	20.0	110	0	3.52E+03	2.40E+01	1.05E-01	5.81E-01	6.45E-06	1.60E-06	4.81E-05	2.33E+01
R_Prod.Water	15.0	130	0	1.36E+02	7.53E+00	5.77E-03	7.52E+00	1.39E-08	6.12E-10	2.00E-07	2.75E-05
R_Makeup	214.8	130	1	3.36E+00	1.10E-01	1.30E-05	9.93E-02	3.96E-07	1.69E-06	9.59E-07	1.05E-02

Table 47: Stream data for Case B2, TEG absorption with membrane contactor, for dense phase transport

Stream	Temp. [C]	Pressure [kPa]	Vapor Fraction	Total mass flow [kg/h]	Total molar flow [kmol/h]	CO2 [kmol/h]	H2O [kmol/h]	N2 [kmol/h]	O2 [kmol/h]	MEA [kmol/h]	TEG [kmol/h]
CT_Feed	30.0	180	1	1.88E+05	4.32E+03	4.22E+03	1.03E+02	1.34E+00	1.73E-01	1.13E-02	0.00E+00
CT_Split	30.0	180	1	5.12E+00	1.18E-01	1.15E-01	2.81E-01	3.66E-05	4.73E-06	3.10E-07	0.00E+00
CT_1	30.0	180	1	1.87E+05	4.32E+03	4.22E+03	1.03E+02	1.34E+00	1.73E-01	1.13E-02	0.00E+00
CT_2.1	125.0	496	1	1.87E+05	4.32E+03	4.22E+03	1.03E+02	1.34E+00	1.73E-01	1.13E-02	0.00E+00
CT_2.2	20.0	476	0.9812	1.87E+05	4.32E+03	4.22E+03	1.03E+02	1.34E+00	1.73E-01	1.13E-02	0.00E+00
CT_3	19.7	456	1	1.86E+05	4.24E+03	4.22E+03	2.25E+01	1.34E+00	1.73E-01	1.13E-02	0.00E+00
CT_4.1	125.0	1420	1	1.86E+05	4.24E+03	4.22E+03	2.25E+01	1.34E+00	1.73E-01	1.13E-02	0.00E+00
CT_4.2	20.0	1400	0.9967	1.86E+05	4.24E+03	4.22E+03	2.25E+01	1.34E+00	1.73E-01	1.13E-02	0.00E+00
CT_5	19.8	1380	1	1.86E+05	4.23E+03	4.22E+03	8.79E+00	1.34E+00	1.73E-01	1.13E-02	0.00E+00
CT_6.1	35.0	1640	1	1.86E+05	4.23E+03	4.22E+03	8.79E+00	1.34E+00	1.73E-01	1.13E-02	0.00E+00
CT_6.2	20.0	1620	0.9998	1.86E+05	4.23E+03	4.22E+03	8.79E+00	1.34E+00	1.73E-01	1.13E-02	0.00E+00
CT_7	19.8	1600	1	1.86E+05	4.23E+03	4.22E+03	7.90E+00	1.34E+00	1.73E-01	1.13E-02	0.00E+00
CT_Prod.Water1	19.7	456	0	1.46E+03	8.07E+01	1.98E-01	8.05E+01	1.63E-06	4.10E-08	2.65E-05	0.00E+00
CT_Prod.Water2	19.8	1380	0	2.52E+02	1.38E+01	1.01E-01	1.37E+01	8.97E-07	2.29E-08	1.04E-05	0.00E+00
CT_Prod.Water3	19.8	1600	0	1.64E+01	9.01E-01	7.58E-03	8.93E-01	6.87E-08	1.75E-09	7.29E-07	0.00E+00
CC_1	20.1	1600	1	1.86E+05	4.22E+03	4.22E+03	1.22E-01	1.34E+00	1.73E-01	1.13E-02	0.00E+00
R_12	20.1	1600	0	3.52E+03	2.40E+01	1.05E-01	5.81E-01	6.45E-06	1.60E-06	4.81E-05	2.33E+01
R_1.1	23.6	1597	0	3.65E+03	3.13E+01	0.00E+00	8.00E+00	0.00E+00	0.00E+00	0.00E+00	2.33E+01
CC_2.1	85.0	3230	1	1.86E+05	4.22E+03	4.22E+03	1.22E-01	1.34E+00	1.73E-01	1.13E-02	0.00E+00
CC_2.2	20.0	3210	1	1.86E+05	4.22E+03	4.22E+03	1.22E-01	1.34E+00	1.73E-01	1.13E-02	0.00E+00
CC_3.1	85.0	6445	1	1.86E+05	4.22E+03	4.22E+03	1.22E-01	1.34E+00	1.73E-01	1.13E-02	0.00E+00
CC_3.2	20.0	6425	0	1.86E+05	4.22E+03	4.22E+03	1.22E-01	1.34E+00	1.73E-01	1.13E-02	0.00E+00
CC_6.1	35.5	15020	0	1.86E+05	4.22E+03	4.22E+03	1.22E-01	1.34E+00	1.73E-01	1.13E-02	0.00E+00
CC_6.2	20.0	15000	0	1.86E+05	4.22E+03	4.22E+03	1.22E-01	1.34E+00	1.73E-01	1.13E-02	0.00E+00
R_1.2	200.0	490	0	3.65E+03	3.13E+01	0.00E+00	8.00E+00	0.00E+00	0.00E+00	0.00E+00	2.33E+01
R_2.1	106.2	130	1	1.61E+03	8.53E+01	2.80E+00	8.25E+01	3.01E-04	5.74E-05	2.19E-06	3.02E-04
R_2.2	15.0	130	0.0325	1.61E+03	8.53E+01	2.80E+00	8.25E+01	3.01E-04	5.74E-05	2.19E-06	3.02E-04
R_3.1	15.0	130	1	1.21E+02	2.77E+00	2.74E+00	3.69E-02	3.01E-04	5.74E-05	5.65E-12	2.50E-12
R_3.2	185.0	130	1	1.21E+02	2.77E+00	2.74E+00	3.69E-02	3.01E-04	5.74E-05	5.65E-12	2.50E-12
R_4	185.6	130	0.9941	2.06E+02	6.08E+00	2.63E+00	3.24E+00	2.65E-04	5.12E-05	3.16E-05	2.11E-01
R_5	185.3	130	0.9932	2.14E+02	6.30E+00	2.74E+00	3.34E+00	3.01E-04	5.74E-05	3.28E-05	2.21E-01
R_6	130.0	183	0	3.61E+03	2.73E+01	6.11E-06	3.78E+00	4.84E-12	1.67E-11	7.96E-05	2.36E+01
R_7	15.0	130	0	1.49E+03	8.25E+01	6.33E-02	8.25E+01	1.52E-07	6.71E-09	2.19E-06	3.02E-04
R_8	15.0	130	0	1.35E+03	7.50E+01	5.75E-02	7.49E+01	1.38E-07	6.10E-09	1.99E-06	2.74E-04
R_9.1	15.1	1500	0	1.35E+03	7.50E+01	5.75E-02	7.49E+01	1.38E-07	6.10E-09	1.99E-06	2.74E-04
R_9.2	150.0	1000	0	1.35E+03	7.50E+01	5.75E-02	7.49E+01	1.38E-07	6.10E-09	1.99E-06	2.74E-04
R_10.1	189.6	130	0.0027	3.52E+03	2.40E+01	1.05E-01	5.81E-01	6.45E-06	1.60E-06	4.81E-05	2.33E+01
R_10.2	20.0	110	0	3.52E+03	2.40E+01	1.05E-01	5.81E-01	6.45E-06	1.60E-06	4.81E-05	2.33E+01
R_Prod.Water	15.0	130	0	1.36E+02	7.53E+00	5.77E-03	7.52E+00	1.39E-08	6.12E-10	2.00E-07	2.75E-05
R_Makeup	214.8	130	1	3.36E+00	1.10E-01	1.30E-05	9.93E-02	3.96E-07	1.69E-06	9.59E-07	1.05E-02

Table 48: Stream data for Case B2, TEG absorption with membrane contactor, for supercritical state transport

Stream	Temp. [C]	Pressure [kPa]	Vapor Fraction	Total mass flow [kg/h]	Total molar flow [kmol/h]	CO2 [kmol/h]	H2O [kmol/h]	N2 [kmol/h]	O2 [kmol/h]	MEA [kmol/h]	TEG [kmol/h]
CT_Feed	30.0	180	1	1.88E+05	4.32E+03	4.22E+03	1.03E+02	1.34E+00	1.73E-01	1.13E-02	0.00E+00
CT_Split	30.0	180	1	5.12E+00	1.18E-01	1.15E-01	2.81E-03	3.66E-05	4.73E-06	3.10E-07	0.00E+00
CT_1	30.0	180	1	1.87E+05	4.32E+03	4.22E+03	1.03E+02	1.34E+00	1.73E-01	1.13E-02	0.00E+00
CT_2.1	125.0	496	1	1.87E+05	4.32E+03	4.22E+03	1.03E+02	1.34E+00	1.73E-01	1.13E-02	0.00E+00
CT_2.2	20.0	476	0.9812	1.87E+05	4.32E+03	4.22E+03	1.03E+02	1.34E+00	1.73E-01	1.13E-02	0.00E+00
CT_3	19.7	456	1	1.86E+05	4.24E+03	4.22E+03	2.25E+01	1.34E+00	1.73E-01	1.13E-02	0.00E+00
CT_4.1	125.0	1420	1	1.86E+05	4.24E+03	4.22E+03	2.25E+01	1.34E+00	1.73E-01	1.13E-02	0.00E+00
CT_4.2	20.0	1400	0.9967	1.86E+05	4.24E+03	4.22E+03	2.25E+01	1.34E+00	1.73E-01	1.13E-02	0.00E+00
CT_5	19.8	1380	1	1.86E+05	4.23E+03	4.22E+03	8.79E+00	1.34E+00	1.73E-01	1.13E-02	0.00E+00
CT_6.1	35.0	1640	1	1.86E+05	4.23E+03	4.22E+03	8.79E+00	1.34E+00	1.73E-01	1.13E-02	0.00E+00
CT_6.2	20.0	1620	0.9998	1.86E+05	4.23E+03	4.22E+03	8.79E+00	1.34E+00	1.73E-01	1.13E-02	0.00E+00
CT_7	19.8	1600	1	1.86E+05	4.23E+03	4.22E+03	7.90E+00	1.34E+00	1.73E-01	1.13E-02	0.00E+00
CT_Prod.Water1	19.7	456	0	1.46E+03	8.07E+01	1.98E-01	8.05E+01	1.63E-06	4.10E-08	2.65E-05	0.00E+00
CT_Prod.Water2	19.8	1380	0	2.52E+02	1.38E+01	1.01E-01	1.37E+01	8.97E-07	2.29E-08	1.04E-05	0.00E+00
CT_Prod.Water3	19.8	1600	0	1.64E+01	9.01E-01	7.58E-03	8.93E-01	6.87E-08	1.75E-09	7.29E-07	0.00E+00
CC_1	20.1	1600	1	1.86E+05	4.22E+03	4.22E+03	1.22E-01	1.34E+00	1.73E-01	1.13E-02	0.00E+00
R_11	20.1	1600	0	3.52E+03	2.40E+01	1.05E-01	5.81E-01	6.45E-06	1.60E-06	4.81E-05	2.33E+01
R_1.1	23.6	1597	0	3.65E+03	3.13E+01	0.00E+00	8.00E+00	0.00E+00	0.00E+00	0.00E+00	2.33E+01
CC_2	85.0	3230	1	1.86E+05	4.22E+03	4.22E+03	1.22E-01	1.34E+00	1.73E-01	1.13E-02	0.00E+00
CC_3	20.0	3210	1	1.86E+05	4.22E+03	4.22E+03	1.22E-01	1.34E+00	1.73E-01	1.13E-02	0.00E+00
CC_4	85.0	6445	1	1.86E+05	4.22E+03	4.22E+03	1.22E-01	1.34E+00	1.73E-01	1.13E-02	0.00E+00
CC_5	22.5	6425	0	1.86E+05	4.22E+03	4.22E+03	1.22E-01	1.34E+00	1.73E-01	1.13E-02	0.00E+00
CC_6	40.0	15000	0	1.86E+05	4.22E+03	4.22E+03	1.22E-01	1.34E+00	1.73E-01	1.13E-02	0.00E+00
R_1.2	200.0	490	0	3.65E+03	3.13E+01	0.00E+00	8.00E+00	0.00E+00	0.00E+00	0.00E+00	2.33E+01
R_2.1	106.2	130	1	1.61E+03	8.53E+01	2.80E+00	8.25E+01	3.01E-04	5.74E-05	2.19E-06	3.02E-04
R_2.2	15.0	130	0.0325	1.61E+03	8.53E+01	2.80E+00	8.25E+01	3.01E-04	5.74E-05	2.19E-06	3.02E-04
R_3.1	15.0	130	1	1.21E+02	2.77E+00	2.74E+00	3.69E-02	3.01E-04	5.74E-05	5.65E-12	2.50E-12
R_3.2	185.0	130	1	1.21E+02	2.77E+00	2.74E+00	3.69E-02	3.01E-04	5.74E-05	5.65E-12	2.50E-12
R_4	185.6	130	0.9941	2.06E+02	6.08E+00	2.63E+00	3.24E+00	2.65E-04	5.12E-05	3.16E-05	2.11E-01
R_5	185.3	130	0.9932	2.14E+02	6.30E+00	2.74E+00	3.34E+00	3.01E-04	5.74E-05	3.28E-05	2.21E-01
R_6	130.0	183	0	3.61E+03	2.73E+01	6.11E-06	3.78E+00	4.84E-12	1.67E-11	7.96E-05	2.36E+01
R_7	15.0	130	0	1.49E+03	8.25E+01	6.33E-02	8.25E+01	1.52E-07	6.71E-09	2.19E-06	3.02E-04
R_8	15.0	130	0	1.35E+03	7.50E+01	5.75E-02	7.49E+01	1.38E-07	6.10E-09	1.99E-06	2.74E-04
R_9.1	15.1	1500	0	1.35E+03	7.50E+01	5.75E-02	7.49E+01	1.38E-07	6.10E-09	1.99E-06	2.74E-04
R_9.2	150.0	1000	0	1.35E+03	7.50E+01	5.75E-02	7.49E+01	1.38E-07	6.10E-09	1.99E-06	2.74E-04
R_10.1	189.6	130	0.0027	3.52E+03	2.40E+01	1.05E-01	5.81E-01	6.45E-06	1.60E-06	4.81E-05	2.33E+01
R_10.2	20.0	110	0	3.52E+03	2.40E+01	1.05E-01	5.81E-01	6.45E-06	1.60E-06	4.81E-05	2.33E+01
R_Prod.Water	15.0	130	0	1.36E+02	7.53E+00	5.77E-03	7.52E+00	1.39E-08	6.12E-10	2.00E-07	2.75E-05
R_Makeup	214.8	130	1	3.36E+00	1.10E-01	1.30E-05	9.93E-02	3.96E-07	1.69E-06	9.59E-07	1.05E-02

Table 49: Stream data for Case C1, pressure-temperature swing with the use of Joule Thomson valve, for liquid transport

Stream	Temp. [C]	Pressure [kPa]	Vapor Fraction	Total mass flow [kg/h]	Total molar flow [kmol/h]	CO2 [kmol/h]	H2O [kmol/h]	N2 [kmol/h]	O2 [kmol/h]	MEA [kmol/h]	MEG [kmol/h]
CT_Feed	30.0	180	1	187500	4321.82147	4217.24659	103.049934	1.34031342	0.17329079	1.13E-02	0
CT_RCY	41.4	180	1	36602.9137	832.806216	830.913949	1.86877358	1.23E-02	2.12E-03	1.05E-03	7.99E-03
CT_1	31.8	180	1	224102.915	5154.62772	5048.16054	104.918707	1.35264446	0.17544303	1.24E-02	7.99E-03
CT_2.1	125.0	481	1	224102.915	5154.62772	5048.16054	104.918707	1.35264446	0.17544303	1.24E-02	7.99E-03
CT_2.2	20.0	461	0.9849	224102.915	5154.62772	5048.16054	104.918707	1.35264446	0.17544303	1.24E-02	7.99E-03
CT_3	19.7	441	1	222704.851	5077.30747	5047.97669	27.7902961	1.35264318	0.17544299	1.24E-02	2.52E-05
CT_4.1	125.0	1359	1	222704.851	5077.30747	5047.97669	27.7902961	1.35264318	0.17544299	1.24E-02	2.52E-05
CT_4.2	20.0	1339	0.9967	222704.851	5077.30747	5047.97669	27.7902961	1.35264318	0.17544299	1.24E-02	2.52E-05
CT_5	19.8	1319	1	222394.967	5060.27788	5047.85769	10.8797457	1.3526423	0.17544297	1.24E-02	1.68E-07
CT_6.1	125.0	3992	1	222394.967	5060.27788	5047.85769	10.8797457	1.3526423	0.17544297	1.24E-02	1.68E-07
CT_6.2	20.0	3972	0.9991	222394.967	5060.27788	5047.85769	10.8797457	1.3526423	0.17544297	1.24E-02	1.68E-07
CT_7	19.8	3952	1	222310.752	5055.72969	5047.77002	6.41922298	1.35264144	0.17544295	1.24E-02	4.75E-09
CT_Prod.Water1	19.7	441	0	1398.06317	77.3202526	0.18385384	77.1284106	1.28E-06	3.21E-08	2.26E-05	7.96E-03
CT_Prod.Water2	19.8	1319	0	309.884705	17.029588	0.11900023	16.9105504	8.87E-07	2.27E-08	1.14E-05	2.50E-05
CT_Prod.Water3	19.8	3952	0	84.2149955	4.54818954	8.77E-02	4.46052272	8.53E-07	2.24E-08	3.00E-06	1.63E-07
DH_1.1	20.4	3952	0.9966	222817.85	5064.29224	5047.77002	6.97161512	1.35264144	0.17544295	4.90E-02	7.97354206
DH_1.2	5.8	3932	0.8222	222817.85	5064.29224	5047.77002	6.97161512	1.35264144	0.17544295	4.90E-02	7.97354206
DH_2	-15.0	2200	0.8333	222817.85	5064.29224	5047.77002	6.97161512	1.35264144	0.17544295	4.90E-02	7.97354206
CC_1	-15.0	2200	1	185703.542	4220.21553	4218.57171	0.12942358	1.34051709	0.17335445	2.63E-06	5.32E-04
DH_4	20.0	3952	0	507.098184	8.56255596	0	0.55239215	0	0	3.66E-02	7.97354205
DH_5	-15.0	2200	0	37114.3075	844.076709	829.198319	6.84219154	1.21E-02	2.09E-03	4.90E-02	7.97301047
CC_2	-26.9	1540	0.9705	185703.542	4220.21553	4218.57171	0.12942358	1.34051709	0.17335445	2.63E-06	5.32E-04
CC_3	-30.0	1520	0	185703.542	4220.21553	4218.57171	0.12942358	1.34051709	0.17335445	2.63E-06	5.32E-04

Table 50: Stream data for Case C1, pressure-temperature swing with the use of Joule Thomson valve, for dense phase transport

Stream	Temp. [C]	Pressure [kPa]	Vapor Fraction	Total mass flow [kg/h]	Total molar flow [kmol/h]	CO2 [kmol/h]	H2O [kmol/h]	N2' [kmol/h]	O2 [kmol/h]	MEA [kmol/h]	MEG [kmol/h]
CT_Feed	30.0	180	1	1.88E+05	4.32E+03	4.22E+03	1.03E+02	1.34E+00	1.73E-01	1.13E-02	0.00E+00
CT_RCY	41.4	180	1	3.40E+02	7.74E+00	7.72E+00	1.84E-02	2.63E-05	6.86E-06	1.08E-05	7.13E-05
CT_1	30.0	180	1	1.88E+05	4.33E+03	4.22E+03	1.03E+02	1.34E+00	1.73E-01	1.14E-02	7.13E-05
CT_2.1	125.0	491	1	1.88E+05	4.33E+03	4.22E+03	1.03E+02	1.34E+00	1.73E-01	1.14E-02	7.13E-05
CT_2.2	20.0	471	0.9813	1.88E+05	4.33E+03	4.22E+03	1.03E+02	1.34E+00	1.73E-01	1.14E-02	7.13E-05
CT_3	19.7	451	1	1.86E+05	4.25E+03	4.22E+03	2.28E+01	1.34E+00	1.73E-01	1.13E-02	1.78E-07
CT_4.1	125.0	1391	1	1.86E+05	4.25E+03	4.22E+03	2.28E+01	1.34E+00	1.73E-01	1.13E-02	1.78E-07
CT_4.2	20.0	1371	0.9967	1.86E+05	4.25E+03	4.22E+03	2.28E+01	1.34E+00	1.73E-01	1.13E-02	1.78E-07
CT_5	19.8	1351	1	1.86E+05	4.24E+03	4.22E+03	8.94E+00	1.34E+00	1.73E-01	1.13E-02	1.20E-09
CT_6.1	125.0	4086	1	1.86E+05	4.24E+03	4.22E+03	8.94E+00	1.34E+00	1.73E-01	1.13E-02	1.20E-09
CT_6.2	20.0	4066	0.9992	1.86E+05	4.24E+03	4.22E+03	8.94E+00	1.34E+00	1.73E-01	1.13E-02	1.20E-09
CT_7	19.8	4046	1	1.86E+05	4.23E+03	4.22E+03	5.38E+00	1.34E+00	1.73E-01	1.13E-02	3.66E-11
CT_Prod.Water1	19.7	451	0	1.46E+03	8.05E+01	1.96E-01	8.03E+01	1.61E-06	4.04E-08	2.62E-05	7.12E-05
CT_Prod.Water2	19.8	1351	0	2.53E+02	1.39E+01	9.96E-02	1.38E+01	8.81E-07	2.25E-08	1.03E-05	1.77E-07
CT_Prod.Water3	19.8	4046	0	6.73E+01	3.63E+00	7.14E-02	3.56E+00	8.33E-07	2.18E-08	2.54E-06	1.16E-09
DH_1.1	20.7	4046	0.9960	1.87E+05	4.24E+03	4.22E+03	5.93E+00	1.34E+00	1.73E-01	4.79E-02	7.97E+00
DH_1.2	15.0	4026	0.9956	1.87E+05	4.24E+03	4.22E+03	5.93E+00	1.34E+00	1.73E-01	4.79E-02	7.97E+00
DH_2	-10.1	2200	0.9949	1.87E+05	4.24E+03	4.22E+03	5.93E+00	1.34E+00	1.73E-01	4.79E-02	7.97E+00
CC_1	-10.1	2200	1	1.86E+05	4.22E+03	4.22E+03	3.97E-01	1.34E+00	1.73E-01	9.86E-05	1.44E-03
R_6	20.0	4046	0	5.07E+02	8.56E+00	0.00E+00	5.52E-01	0.00E+00	0.00E+00	3.66E-02	7.97E+00
R_1.1	-10.1	2200	0	9.43E+02	2.14E+01	7.86E+00	5.54E+00	2.62E-05	6.85E-06	4.78E-02	7.97E+00
CC_2.1	96.0	7152	1	1.86E+05	4.22E+03	4.22E+03	3.97E-01	1.34E+00	1.73E-01	9.86E-05	1.44E-03
CC_2.2	20.0	7132	0	1.86E+05	4.22E+03	4.22E+03	3.97E-01	1.34E+00	1.73E-01	9.86E-05	1.44E-03
CC_3.1	33.2	15020	0	1.86E+05	4.22E+03	4.22E+03	3.97E-01	1.34E+00	1.73E-01	9.86E-05	1.44E-03
CC_3.2	20.0	15000	0	1.86E+05	4.22E+03	4.22E+03	3.97E-01	1.34E+00	1.73E-01	9.86E-05	1.44E-03
R_1.2	0.0	110	0.3613	9.44E+02	2.14E+01	7.87E+00	5.53E+00	2.63E-05	6.86E-06	4.78E-02	7.97E+00
R_2	0.0	110	1	3.40E+02	7.74E+00	7.72E+00	1.84E-02	2.63E-05	6.86E-06	1.08E-05	7.13E-05
R_3	0.0	110	0	6.04E+02	1.37E+01	1.45E-01	5.52E+00	3.85E-09	2.39E-09	4.78E-02	7.97E+00
R_4	196.0	110	0	4.97E+02	8.06E+00	8.22E-30	9.03E-02	8.04E-30	8.03E-30	2.14E-02	7.95E+00
R_5.1	196.8	4066	0	4.97E+02	8.06E+00	8.22E-30	9.03E-02	8.04E-30	8.03E-30	2.14E-02	7.95E+00
R_5.2	20.0	4046	0	4.97E+02	8.06E+00	8.22E-30	9.03E-02	8.04E-30	8.03E-30	2.14E-02	7.95E+00
R_Prod.Water	105.0	110	1	1.07E+02	5.62E+00	1.45E-01	5.43E+00	3.85E-09	2.39E-09	2.64E-02	2.01E-02
R_Makeup	29.5	4046	0	1.06E+01	4.99E-01	0.00E+00	8.32E+00	0.00E+00	0.00E+00	9.27E-01	1.34E+00

Table 51: Stream data for Case C1, pressure-temperature swing with the use of Joule Thomson valve, for supercritical state transport

Stream	Temp. [C]	Pressure [kPa]	Vapor Fraction	Total mass flow [kg/h]	Total molar flow [kmol/h]	CO2 [kmol/h]	H2O [kmol/h]	N2 [kmol/h]	O2 [kmol/h]	MEA [kmol/h]	MEG [kmol/h]
CT_Feed	30.0	180	1	1.88E+05	4.32E+03	4.22E+03	1.03E+02	1.34E+00	1.73E-01	1.13E-02	0.00E+00
CT_RCY	41.4	180	1	3.40E+02	7.74E+00	7.72E+00	1.84E-02	2.63E-05	6.86E-06	1.08E-05	7.13E-05
CT_1	30.0	180	1	1.88E+05	4.33E+03	4.22E+03	1.03E+02	1.34E+00	1.73E-01	1.14E-02	7.13E-05
CT_2.1	125.0	491	1	1.88E+05	4.33E+03	4.22E+03	1.03E+02	1.34E+00	1.73E-01	1.14E-02	7.13E-05
CT_2.2	20.0	471	0.9813	1.88E+05	4.33E+03	4.22E+03	1.03E+02	1.34E+00	1.73E-01	1.14E-02	7.13E-05
CT_3	19.7	451	1	1.86E+05	4.25E+03	4.22E+03	2.28E+01	1.34E+00	1.73E-01	1.13E-02	1.78E-07
CT_4.1	125.0	1391	1	1.86E+05	4.25E+03	4.22E+03	2.28E+01	1.34E+00	1.73E-01	1.13E-02	1.78E-07
CT_4.2	20.0	1371	0.9967	1.86E+05	4.25E+03	4.22E+03	2.28E+01	1.34E+00	1.73E-01	1.13E-02	1.78E-07
CT_5	19.8	1351	1	1.86E+05	4.24E+03	4.22E+03	8.94E+00	1.34E+00	1.73E-01	1.13E-02	1.20E-09
CT_6.1	125.0	4086	1	1.86E+05	4.24E+03	4.22E+03	8.94E+00	1.34E+00	1.73E-01	1.13E-02	1.20E-09
CT_6.2	20.0	4066	0.9992	1.86E+05	4.24E+03	4.22E+03	8.94E+00	1.34E+00	1.73E-01	1.13E-02	1.20E-09
CT_7	19.8	4046	1	1.86E+05	4.23E+03	4.22E+03	5.38E+00	1.34E+00	1.73E-01	1.13E-02	3.66E-11
CT_Prod.Water1	19.7	451	0	1.46E+03	8.05E+01	1.96E-01	8.03E+01	1.61E-06	4.04E-08	2.62E-05	7.12E-05
CT_Prod.Water2	19.8	1351	0	2.53E+02	1.39E+01	9.96E-02	1.38E+01	8.81E-07	2.25E-08	1.03E-05	1.77E-07
CT_Prod.Water3	19.8	4046	0	6.73E+01	3.63E+00	7.14E-02	3.56E+00	8.33E-07	2.18E-08	2.54E-06	1.16E-09
DH_1.1	20.7	4046	0.9960	1.87E+05	4.24E+03	4.22E+03	5.93E+00	1.34E+00	1.73E-01	4.79E-02	7.97E+00
DH_1.2	15.0	4026	0.9956	1.87E+05	4.24E+03	4.22E+03	5.93E+00	1.34E+00	1.73E-01	4.79E-02	7.97E+00
DH_2	-10.1	2200	0.9949	1.87E+05	4.24E+03	4.22E+03	5.93E+00	1.34E+00	1.73E-01	4.79E-02	7.97E+00
CC_1	-10.1	2200	1	1.86E+05	4.22E+03	4.22E+03	3.97E-01	1.34E+00	1.73E-01	9.86E-05	1.44E-03
R_6	20.0	4046	0	5.07E+02	8.56E+00	0.00E+00	5.52E-01	0.00E+00	0.00E+00	3.66E-02	7.97E+00
R_1.1	-10.1	2200	0	9.43E+02	2.14E+01	7.86E+00	5.54E+00	2.62E-05	6.85E-06	4.78E-02	7.97E+00
CC_2.1	96.0	7152	1	1.86E+05	4.22E+03	4.22E+03	3.97E-01	1.34E+00	1.73E-01	9.86E-05	1.44E-03
CC_2.2	24.0	7132	0	1.86E+05	4.22E+03	4.22E+03	3.97E-01	1.34E+00	1.73E-01	9.86E-05	1.44E-03
CC_3	40.0	15000	0	1.86E+05	4.22E+03	4.22E+03	3.97E-01	1.34E+00	1.73E-01	9.86E-05	1.44E-03
R_1.2	0.0	110	0.3613	9.44E+02	2.14E+01	7.87E+00	5.53E+00	2.63E-05	6.86E-06	4.78E-02	7.97E+00
R_2	0.0	110	1	3.40E+02	7.74E+00	7.72E+00	1.84E-02	2.63E-05	6.86E-06	1.08E-05	7.13E-05
R_3	0.0	110	0	6.04E+02	1.37E+01	1.45E-01	5.52E+00	3.85E-09	2.39E-09	4.78E-02	7.97E+00
R_4	196.0	110	0	4.97E+02	8.06E+00	8.22E-30	9.03E-02	8.04E-30	8.03E-30	2.14E-02	7.95E+00
R_5.1	196.8	4066	0	4.97E+02	8.06E+00	8.22E-30	9.03E-02	8.04E-30	8.03E-30	2.14E-02	7.95E+00
R_5.2	20.0	4046	0	4.97E+02	8.06E+00	8.22E-30	9.03E-02	8.04E-30	8.03E-30	2.14E-02	7.95E+00
R_Prod.Water	105.0	110	1	1.07E+02	5.62E+00	1.45E-01	5.43E+00	3.85E-09	2.39E-09	2.64E-02	2.01E-02
R_Makeup	29.5	4046	0	1.06E+01	4.99E-01	0.00E+00	8.32E+00	0.00E+00	0.00E+00	9.27E-01	1.34E+00

Table 52: Stream data for Case C1, pressure-temperature swing with the use of a turbo-expander, for liquid transport

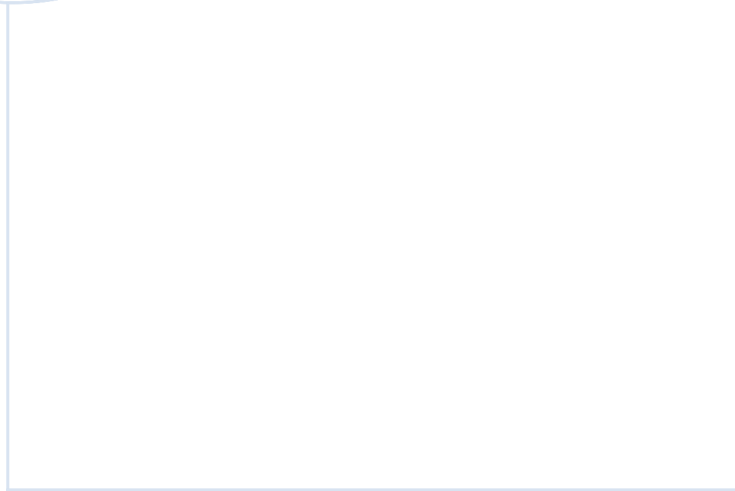
Stream	Temp. [C]	Pressure [kPa]	Vapor Fraction	Total mass flow [kg/h]	Total molar flow [kmol/h]	CO2 [kmol/h]	H2O [kmol/h]	N2 [kmol/h]	O2 [kmol/h]	MEA [kmol/h]	MEG [kmol/h]
CT_Feed	30.0	180	1	1.88E+05	4.32E+03	4.22E+03	1.03E+02	1.34E+00	1.73E-01	1.13E-02	0.00E+00
CT_RCY	41.4	180	1	3.66E+04	8.33E+02	8.32E+02	1.87E+00	1.21E-02	2.09E-03	1.05E-03	7.99E-03
CT_1	31.8	180	1	2.24E+05	5.16E+03	5.05E+03	1.05E+02	1.35E+00	1.75E-01	1.24E-02	7.99E-03
CT_2.1	125.0	481	1	2.24E+05	5.16E+03	5.05E+03	1.05E+02	1.35E+00	1.75E-01	1.24E-02	7.99E-03
CT_2.2	20.0	461	0.9849	2.24E+05	5.16E+03	5.05E+03	1.05E+02	1.35E+00	1.75E-01	1.24E-02	7.99E-03
CT_3	19.7	441	1	2.23E+05	5.08E+03	5.05E+03	2.78E+01	1.35E+00	1.75E-01	1.24E-02	2.52E-05
CT_4.1	125.0	1359	1	2.23E+05	5.08E+03	5.05E+03	2.78E+01	1.35E+00	1.75E-01	1.24E-02	2.52E-05
CT_4.2	20.0	1339	0.9967	2.23E+05	5.08E+03	5.05E+03	2.78E+01	1.35E+00	1.75E-01	1.24E-02	2.52E-05
CT_5	19.8	1319	1	2.22E+05	5.06E+03	5.05E+03	1.09E+01	1.35E+00	1.75E-01	1.24E-02	1.68E-07
CT_6.1	125.0	3992	1	2.22E+05	5.06E+03	5.05E+03	1.09E+01	1.35E+00	1.75E-01	1.24E-02	1.68E-07
CT_6.2	20.0	3972	0.9991	2.22E+05	5.06E+03	5.05E+03	1.09E+01	1.35E+00	1.75E-01	1.24E-02	1.68E-07
CT_7	19.8	3952	1	2.22E+05	5.06E+03	5.05E+03	6.42E+00	1.35E+00	1.75E-01	1.24E-02	4.75E-09
CT_Prod.Water1	19.7	441	0	1.40E+03	7.73E+01	1.84E-01	7.71E+01	1.28E-06	3.21E-08	2.26E-05	7.97E-03
CT_Prod.Water2	19.8	1319	0	3.10E+02	1.70E+01	1.19E-01	1.69E+01	8.87E-07	2.27E-08	1.14E-05	2.51E-05
CT_Prod.Water3	19.8	3952	0	8.42E+01	4.55E+00	8.77E-02	4.46E+00	8.53E-07	2.24E-08	3.00E-06	1.63E-07
DH.2.1	20.4	3952	0.9966	2.23E+05	5.06E+03	5.05E+03	6.97E+00	1.35E+00	1.75E-01	4.90E-02	7.97E+00
DH.2.2	6.1	3932	0.8825	2.23E+05	5.06E+03	5.05E+03	6.97E+00	1.35E+00	1.75E-01	4.90E-02	7.97E+00
DH.3	-15.0	2200	0.8333	2.23E+05	5.06E+03	5.05E+03	6.97E+00	1.35E+00	1.75E-01	4.90E-02	7.97E+00
CC.1	-15.0	2200	1	1.86E+05	4.22E+03	4.22E+03	1.29E-01	1.34E+00	1.73E-01	2.63E-06	5.32E-04
R.7	19.7	4129	0	5.07E+02	8.56E+00	5.07E+02	5.52E-01	0.00E+00	0.00E+00	3.66E-02	7.97E+00
R.1	-15.0	2200	0	3.71E+04	8.44E+02	8.29E+02	6.84E+00	1.21E-02	2.09E-03	4.90E-02	7.97E+00
CC.2.1	-26.9	1540	0.9705	1.86E+05	4.22E+03	4.22E+03	1.29E-01	1.34E+00	1.73E-01	2.63E-06	5.32E-04
CC.2.2	-30.0	1520	0	1.86E+05	4.22E+03	4.22E+03	1.29E-01	1.34E+00	1.73E-01	2.63E-06	5.32E-04
R.1.2	0.0	110	0.9844	3.72E+04	8.47E+02	8.32E+02	6.88E+00	1.21E-02	2.09E-03	4.90E-02	7.97E+00
R.2	0.0	110	1	3.66E+04	8.33E+02	8.32E+02	1.87E+00	1.21E-02	2.09E-03	1.05E-03	7.99E-03
R.3	0.0	110	0	5.94E+02	1.32E+01	1.44E-01	5.01E+00	1.61E-08	6.98E-09	4.80E-02	7.97E+00
R.4	195.6	110	0	4.97E+02	8.07E+00	1.29E-29	9.94E-02	3.17E-45	7.81E-30	2.42E-02	7.95E+00
R.5.1	196.4	4149	0	4.97E+02	8.07E+00	1.29E-29	9.94E-02	3.17E-45	7.81E-30	2.42E-02	7.95E+00
R.5.2	20.0	4129	0	4.97E+02	8.07E+00	1.29E-29	9.94E-02	3.17E-45	7.81E-30	2.42E-02	7.95E+00
R_Prod.Water	105.0	110	1	9.74E+01	5.10E+00	1.44E-01	4.91E+00	1.61E-08	6.98E-09	2.37E-02	1.85E-02
R_Makeup	20.0	4129	0	1.06E+01	4.92E-01	0.00E+00	4.53E-01	0.00E+00	0.00E+00	1.24E-02	2.71E-02

Table 53: Stream data for Case C1, pressure-temperature swing with the use of a turbo-expander, for dense phase transport

Stream	Temp. [C]	Pressure [kPa]	Vapor Fraction	Total mass flow [kg/h]	Total molar flow [kmol/h]	CO2 [kmol/h]	H2O [kmol/h]	N2' [kmol/h]	O2 [kmol/h]	MEA [kmol/h]	MEG [kmol/h]
CT_Feed	30.0	180	1	1.88E+05	4.32E+03	4.22E+03	1.03E+02	1.34E+00	1.73E-01	1.13E-02	0.00E+00
CT_RCY	41.4	180	1	3.40E+02	7.74E+00	7.72E+00	2.02E-02	2.25E-05	5.44E-06	1.32E-05	6.65E-05
CT_1	30.0	180	1	1.88E+05	4.33E+03	4.22E+03	1.03E+02	1.34E+00	1.73E-01	1.14E-02	6.65E-05
CT_2.1	120.0	467	1	1.88E+05	4.33E+03	4.22E+03	1.03E+02	1.34E+00	1.73E-01	1.14E-02	6.65E-05
CT_2.2	20.0	447	0.9816	1.88E+05	4.33E+03	4.22E+03	1.03E+02	1.34E+00	1.73E-01	1.14E-02	6.65E-05
CT_3	19.7	427	1	1.86E+05	4.25E+03	4.22E+03	2.39E+01	1.34E+00	1.73E-01	1.13E-02	1.76E-07
CT_4.1	120.0	1255	1	1.86E+05	4.25E+03	4.22E+03	2.39E+01	1.34E+00	1.73E-01	1.13E-02	1.76E-07
CT_4.2	20.0	1235	0.9966	1.86E+05	4.25E+03	4.22E+03	2.39E+01	1.34E+00	1.73E-01	1.13E-02	1.76E-07
CT_5	19.8	1215	1	1.86E+05	4.24E+03	4.22E+03	9.70E+00	1.34E+00	1.73E-01	1.13E-02	1.21E-09
CT_6.1	120.0	3510	1	1.86E+05	4.24E+03	4.22E+03	9.70E+00	1.34E+00	1.73E-01	1.13E-02	1.21E-09
CT_6.2	20.0	3490	0.9990	1.86E+05	4.24E+03	4.22E+03	9.70E+00	1.34E+00	1.73E-01	1.13E-02	1.21E-09
CT_7	19.8	3470	1	1.86E+05	4.23E+03	4.22E+03	5.42E+00	1.34E+00	1.73E-01	1.13E-02	2.62E-11
CT_Prod.Water1	19.7	427	0	1.43E+03	7.93E+01	1.83E-01	7.92E+01	1.50E-06	3.76E-08	2.46E-05	6.63E-05
CT_Prod.Water2	19.8	1215	0	2.60E+02	1.43E+01	2.60E+02	1.42E+01	8.08E-07	2.06E-08	9.98E-06	1.74E-07
CT_Prod.Water3	19.8	3470	0	8.05E+01	4.36E+00	7.52E-02	4.28E+00	8.17E-07	2.13E-08	3.57E-06	1.19E-09
DH_2.1	20.5	3470	0.9962	1.87E+05	4.24E+03	4.22E+03	5.97E+00	1.34E+00	1.73E-01	4.79E-02	7.97E+00
DH_2.2	17.8	3450	0.9961	1.87E+05	4.24E+03	4.22E+03	5.97E+00	1.34E+00	1.73E-01	4.79E-02	7.97E+00
DH_3	-10.1	2200	0.9949	1.87E+05	4.24E+03	4.22E+03	5.97E+00	1.34E+00	1.73E-01	4.79E-02	7.97E+00
CC_1	-10.1	2200	1	1.86E+05	4.22E+03	4.22E+03	3.98E-01	1.34E+00	1.73E-01	9.91E-05	1.44E-03
R_7	19.7	4129	0	5.07E+02	8.56E+00	0.00E+00	5.52E-01	0.00E+00	0.00E+00	3.66E-02	7.97E+00
R_1.1	-10.1	2200	0	9.44E+02	2.14E+01	7.86E+00	5.57E+00	2.62E-05	6.83E-06	4.78E-02	7.97E+00
CC_2.1	96.0	7152	1	1.86E+05	4.22E+03	4.22E+03	3.98E-01	1.34E+00	1.73E-01	9.91E-05	1.44E-03
CC_2.2	20.0	7132	0	1.86E+05	4.22E+03	4.22E+03	3.98E-01	1.34E+00	1.73E-01	9.91E-05	1.44E-03
CC_3.1	33.2	15020	0	1.86E+05	4.22E+03	4.22E+03	3.98E-01	1.34E+00	1.73E-01	9.91E-05	1.44E-03
CC_3.2	20.0	15000	0	1.86E+05	4.22E+03	4.22E+03	3.98E-01	1.34E+00	1.73E-01	9.91E-05	1.44E-03
R_1.2	0.0	110	0.3604	9.44E+02	2.14E+01	7.86E+00	5.57E+00	2.62E-05	6.83E-06	4.78E-02	7.97E+00
R_2	0.0	110	1	3.40E+02	7.73E+00	7.71E+00	1.85E-02	2.62E-05	6.83E-06	1.08E-05	7.11E-05
R_3	0.0	110	0	6.04E+02	1.37E+01	1.45E-01	5.55E+00	3.86E-09	2.38E-09	4.78E-02	7.97E+00
R_4	196.0	110	0	4.97E+02	8.06E+00	8.07E-30	9.10E-02	7.97E-30	4.46E-46	2.13E-02	7.95E+00
R_5.1	196.8	4149	0	4.97E+02	8.06E+00	8.07E-30	9.10E-02	7.97E-30	4.46E-46	2.13E-02	7.95E+00
R_5.2	20.0	4129	0	4.97E+02	8.06E+00	8.07E-30	9.10E-02	7.97E-30	4.46E-46	2.13E-02	7.95E+00
R_Prod.Water	105.0	110	1	1.08E+02	5.65E+00	1.45E-01	5.46E+00	3.86E-09	2.38E-09	2.66E-02	2.02E-02
R_Makeup	20.0	4129	0	1.06E+01	4.92E-01	0.00E+00	4.53E-01	0.00E+00	0.00E+00	1.24E-02	2.71E-02

Table 54: Stream data for Case C1, pressure-temperature swing with the use of a turbo-expander, for supercritical transport

Stream	Temp. [C]	Pressure [kPa]	Vapor Fraction	Total mass flow [kg/h]	Total molar flow [kmol/h]	CO2 [kmol/h]	H2O [kmol/h]	N2' [kmol/h]	O2 [kmol/h]	MEA [kmol/h]	MEG [kmol/h]
CT_Feed	30.0	180	1	1.88E+05	4.32E+03	4.22E+03	1.03E+02	1.34E+00	1.73E-01	1.13E-02	0.00E+00
CT_RCY	41.4	180	1	3.40E+02	7.74E+00	7.72E+00	2.02E-02	2.25E-05	5.44E-06	1.32E-05	6.65E-05
CT_1	30.0	180	1	1.88E+05	4.33E+03	4.22E+03	1.03E+02	1.34E+00	1.73E-01	1.14E-02	6.65E-05
CT_2.1	120.0	467	1	1.88E+05	4.33E+03	4.22E+03	1.03E+02	1.34E+00	1.73E-01	1.14E-02	6.65E-05
CT_2.2	20.0	447	0.9816	1.88E+05	4.33E+03	4.22E+03	1.03E+02	1.34E+00	1.73E-01	1.14E-02	6.65E-05
CT_3	19.7	427	1	1.86E+05	4.25E+03	4.22E+03	2.39E+01	1.34E+00	1.73E-01	1.13E-02	1.76E-07
CT_4.1	120.0	1255	1	1.86E+05	4.25E+03	4.22E+03	2.39E+01	1.34E+00	1.73E-01	1.13E-02	1.76E-07
CT_4.2	20.0	1235	0.9966	1.86E+05	4.25E+03	4.22E+03	2.39E+01	1.34E+00	1.73E-01	1.13E-02	1.76E-07
CT_5	19.8	1215	1	1.86E+05	4.24E+03	4.22E+03	9.70E+00	1.34E+00	1.73E-01	1.13E-02	1.76E-07
CT_6.1	120.0	3510	1	1.86E+05	4.24E+03	4.22E+03	9.70E+00	1.34E+00	1.73E-01	1.13E-02	1.21E-09
CT_6.2	20.0	3490	0.9990	1.86E+05	4.24E+03	4.22E+03	9.70E+00	1.34E+00	1.73E-01	1.13E-02	1.21E-09
CT_7	19.8	3470	1	1.86E+05	4.23E+03	4.22E+03	5.42E+00	1.34E+00	1.73E-01	1.13E-02	2.62E-11
CT_Prod.Water1	19.7	427	0	1.43E+03	7.93E+01	1.83E-01	7.92E+01	1.50E-06	3.76E-08	2.46E-05	6.63E-05
CT_Prod.Water2	19.8	1215	0	2.60E+02	1.43E+01	2.60E-02	1.42E+01	8.08E-07	2.06E-08	9.98E-06	1.74E-07
CT_Prod.Water3	19.8	3470	0	8.05E+01	4.36E+00	7.52E-02	4.28E+00	8.17E-07	2.13E-08	3.57E-06	1.19E-09
DH.2.1	20.5	3470	0.9962	1.87E+05	4.24E+03	4.22E+03	5.97E+00	1.34E+00	1.73E-01	4.79E-02	7.97E+00
DH.2.2	17.8	3450	0.9961	1.87E+05	4.24E+03	4.22E+03	5.97E+00	1.34E+00	1.73E-01	4.79E-02	7.97E+00
DH.3	-10.1	2200	0.9949	1.87E+05	4.24E+03	4.22E+03	5.97E+00	1.34E+00	1.73E-01	4.79E-02	7.97E+00
CC.1	-10.1	2200	1	1.86E+05	4.22E+03	4.22E+03	3.98E-01	1.34E+00	1.73E-01	9.91E-05	1.44E-03
R.7	19.7	4129	0	5.07E+02	8.56E+00	0.00E+00	5.52E-01	0.00E+00	0.00E+00	3.66E-02	7.97E+00
R.1.1	-10.1	2200	0	9.44E+02	2.14E+01	7.86E+00	5.57E+00	2.62E-05	6.83E-06	4.78E-02	7.97E+00
CC.2.1	96.0	7152	1	1.86E+05	4.22E+03	4.22E+03	3.98E-01	1.34E+00	1.73E-01	9.91E-05	1.44E-03
CC.2.2	24.0	7132	0	1.86E+05	4.22E+03	4.22E+03	3.98E-01	1.34E+00	1.73E-01	9.91E-05	1.44E-03
CC.3.1	40.0	15000	0	1.86E+05	4.22E+03	4.22E+03	3.98E-01	1.34E+00	1.73E-01	9.91E-05	1.44E-03
R.1.2	0.0	110	0.3604	9.44E+02	2.14E+01	7.86E+00	5.57E+00	2.62E-05	6.83E-06	4.78E-02	7.97E+00
R.2	0.0	110	1	3.40E+02	7.73E+00	7.71E+00	1.85E-02	2.62E-05	6.83E-06	1.08E-05	7.11E-05
R.4	0.0	110	0	6.04E+02	1.37E+01	1.45E-01	5.55E+00	3.86E-09	2.38E-09	4.78E-02	7.97E+00
R.5	196.0	110	0	4.97E+02	8.06E+00	8.07E-30	9.10E-02	7.97E-30	4.46E-46	2.13E-02	7.95E+00
R.6.1	196.8	4149	0	4.97E+02	8.06E+00	8.07E-30	9.10E-02	7.97E-30	4.46E-46	2.13E-02	7.95E+00
R.6.2	20.0	4129	0	4.97E+02	8.06E+00	8.07E-30	9.10E-02	7.97E-30	4.46E-46	2.13E-02	7.95E+00
R_Prod.Water	105.0	110	1	1.08E+02	5.65E+00	1.45E-01	5.46E+00	3.86E-09	2.38E-09	2.66E-02	2.02E-02



 **NTNU**

Norwegian University of
Science and Technology